ACTINIDE CHALCOGENIDO AND CHALCOGENOLATE COMPOUNDS

By

MARISSA RINGGOLD

A dissertation submitted to the

School of Graduate Studies

Rutgers, the State University of New Jersey

In partial fulfillment of the requirements

for the degree of

Doctor of Philosophy

Graduate Program in Chemistry

Written under the direction of

John G. Brennan

And approved by

_____

_____

_____

_____

New Brunswick, New Jersey

January, 2019

ABSTRACT OF THE DISSERTATION

Actinide Chalcogenido and Chalcogenolate Compounds

By MARISSA RINGGOLD

Disseration Director:

John G. Brennan

Actinide chemistry, specifically thorium and uranium chalcogenolate and chalcogenido complexes are relatively unexplored. Traditionally in literature they contain sterically hindered environments or are synthesized under aqueous conditions. However, it has been discovered that thorium metal reductively inserts into the E-E bond of REER (R= Ph, C_6F_5; E = S, Se) to from stable chalcogenolate compounds whose size is determined by the identity of the neutral donor ligand or additional chalcogen in air-free, water-free conditions without the use of large bulky ligands.

Thorium cubanes $(py)_8Th_4(\mu_3\text{-}E')_4(\mu_2\text{-}EPh)_4(\eta\text{-}EPh)_4$ (E, E′ = S, Se) were prepared from ligand-based redox reactions of elemental E′ with $Th(EPh)_4$. Products with all four possible E/E′ combinations (E,E′ = S,S; Se,Se; S,Se; Se,S) were isolated and structurally characterized, ligand exchange reactions were explored, and the heterochalcogen compounds $(py)_8Th_4(\mu_3\text{-}S)_4(\mu_2\text{-}SePh)_4(\eta\text{-}SePh)_4$ and $(py)_8Th_4(\mu_3\text{-}Se)_4(\mu_2\text{-}SPh)_4(\eta\text{-}SPh)_4$ were heated to deliver solid solutions of ThS_xSe_{2-x}. NMR spectroscopy indicated that the structure of $(py)_8Th_4(\mu_3\text{-}Se)_4(\mu_2\text{-}SePh)_4(\eta\text{-}SePh)_4$ is static in pyridine solution, with no exchange between bridging and terminal PhE^- ligands on

the NMR time scale. A computational analysis of ^{77}Se NMR shifts provides insight into the solution structure of both clusters and monomeric chalcogenolates.

Thorium chalcogenolates $Th(ER)_4$ react with 2,2'-bipyridine (bipy) to form complexes with the stoichiometry $(bipy)_2Th(ER)_4$ (E = S, Se; R = Ph, C_6F_5). All four compounds have been isolated and characterized by spectroscopic methods and low-temperature single crystal x-ray diffraction. Two of the products, $(bipy)_2Th(SC_6F_5)_4$ and $(bipy)_2Th(SeC_6F_5)_4$[1], crystallize with lattice solvent, $(bipy)_2Th(SPh)_4$ crystallizes with no lattice solvent, and the selenolate $(bipy)_2Th(SePh)_4$ crystallizes in two phases, with and without lattice solvent. In all four compounds the available volume for coordination bounded by the two bipy ligands is large enough to allow significant conformational flexibility of thiolate or selenolate ligands. ^{77}Se NMR confirms that the structures of the selenolate products are the same in pyridine solution and in the solid state. Attempts to prepare analogous derivatives with 2,2′:6′,2″-terpyridine (terpy) were successful only in the isolation of $(terpy)(py)Th(SPh)_4$, the first terpy compound of thorium. These materials are thermochroic, with color attributed to ligand-to-ligand charge transfer excitations.

In addition, heterometallic compounds with both thorium and uranium have been explored. Four clusters $(py)_8Th_4[Hg(EPh)_2]_4(\mu_3\text{-}E')_4(\mu_2\text{-}EPh)_4(\eta\text{-}EPh)_4$, $(py)_8U_4[Hg(EPh_2)]_4(\mu_3\text{-}E')_4(\mu_2\text{-}EPh)_4(\eta\text{-}EPh)_4$ (E' = S, Se; E = Se) and three cation anion pairs $[U_8S_{13}I_3py_{17}][HgI_4][HgI_3py]$, $[ThF_2bipy_2py_3][Ag_4SePh_6]$, $[Th_8S_{13}I_4py_{18}][HgI_4]$ have been synthesized, isolated, and structurally characterized. These compounds integrate

[1] Compounds $(bipy)_2Th(SeC_6F_5)_4$ and $(bipy)_2Th(SC_6F_5)_4$ were made and characterized fully by Matthew Stuber and Wen Wu respectively.

mercury as an external ligand or counter ion instead of a bridging moiety inside the inner core structure as seen in previous lanthanide compounds. 100% occupancy of the mercury moiety in the cubane clusters is not consistent or easily achieved, yet all these compounds are of significant interest when compared to other heterometallic compounds.

Acknowledgements

First and foremost, I want to thank my research advisor Professor John G. Brennan. Your passion and excitement about research is contagious. Thank you for always patiently listening to my research ideas. Being able to creatively approach science and have you give valuable expertise and support was a great fit for my time in graduate school. I felt as though this was the lab I was meant to be in and was grateful for the opportunity to succeed.

Special thanks to my thesis committee Professor Alan Goldman and Professor Martha Greenblatt for their constructive critiques and helpful insights.

Special thanks to Dr. Thomas Emge who collected, processed, and interpreted all my X-ray crystallographic data, then taught me how to do the same, albeit not as well. Thanks so much for your patience and dedication, without you I would not have anything to write about.

Special thanks to Dr. Anna Y. Kornienko for all the support both in and out of lab. You were a constant sounding board for all questions both scientific and professional. You challenged me to work hard, think realistically about my goals, and then execute them.

Thank you to my labs mates for being a source of support and sometimes of frustration. I appreciate the lunches, interesting conversations, and crazy antics. You all helped make this experience enjoyable.

My first research Professor Timothy B. Clark helped start me down path that ultimately led here. Thank you so much for your guidance and support. You were a great

mentor who genuinely cared not just about my research but me as a person, always looking out for my best interest.

I would also like to thank various teachers who impacted me along the way. My high school chemistry teacher Deidre Walker for showing me how exciting and challenging chemistry could be. My middle school English teacher Shalee Wells Okelberry for encouraging me to pick a future career that would allow me to fully use and develop my intellectual prowess.

Lastly but most importantly thank you so much to my family and friends. I could not have done this without your faith and support. On those hard days when nothing worked, and I felt alone, I always had you to fall back on. Special thanks to my family because I am who I am today because of the foundations you built up in me. Thank you so much. I love you.

Dedication

To the sacrifices my family made for me to be where I am today. I do this for and because of you. Thank you.

Table of Contents

List of Tables

List of Illustrations

List of Abbreviations

An	Actinide
Ln	Lanthanide
Bipy	2,2'-bipyridine
Terpy	2,2':6'2"-terpyridine
TMEDA	N,N,N',N' tetramethyethylenediamine
Py	Pyridine
THF	Tetrahydrofuran
Se	Selenium
S	Sulfur
Te	Tellurium
E	Se, S or Te
NMR	Nuclear magnetic resonance spectroscopy
SEM	Scanning Electron Microscopy
PXRD	Powder X-ray Diffraction

Parts of the thesis have been previously published as follows:

Chapter 1 of the thesis has been published as:

> Ringgold, M.; Rehe, D.; Hrobarik, P.; Kornienko, A.Y.; Emge, T.J.; Brennan, J. G.; Thorium Cubanes–Synthesis, Solid-State and Solution Structures, Thermolysis, and Chalcogen Exchange Reactions. *Inorganic Chemistry*, **2018**, 57, 7129.

Chapter 2 of the thesis has been published as:

> Ringgold, M.; Wu, W.; Stuber, M.; Kornienko, A. Y.; Emge, T. J.; Brennan J. G.; Monomeric Thorium Chalcogenolates with Bipyridine and Terpyridine Ligands. *Dalton Transactions,* **2018**, 47,14652.

Introduction

Actinide (An; An = Th, U) chemistry is one of the relatively unexplored fundamental challenges left in inorganic chemistry. Access to unique physical and chemical properties can be realized due to the complicated nature of participating bonding orbitals. Specifically, the small energy difference between the 5f and 6d orbitals along with the partial shielding of these orbitals by the previously filled s and p orbitals contributes to these possible characteristics. Although lanthanide chemistry would seemingly give some insight into predicting An chemistry, the parallels are not as apparent as previously hypothesized. Unlike their lanthanide (Ln) counter parts which only have ionic bonds due to overshadowing of 4f by 5s and 5p, the substantial number of valence atomic orbitals of similar radial distribution and energy (5f, 6p, 6d, 7s, 7p) in An provides the possibility for covalency and thus affords different possibilities for reactivity and bonding (Figure 1). Another factor that influences which orbitals are accessible for bonding is relativistic effect. As nuclei get heavier, attractions increase, and there is a relative stabilization and contraction of both s and p orbitals which forces the 5f orbitals to jut out more than the 4f orbitals do (Figure 2). Furthermore, there is still no firm understanding of the relative contributions from covalent and ionic bonding to complex stability. It has been proven that the identity of the neutral donor ligand, added chalcogenolate, and solvent can affect the final crystal structure for both Ln and An. Monitoring these changes in cluster properties as a function of size will give insight into how these characteristics change.

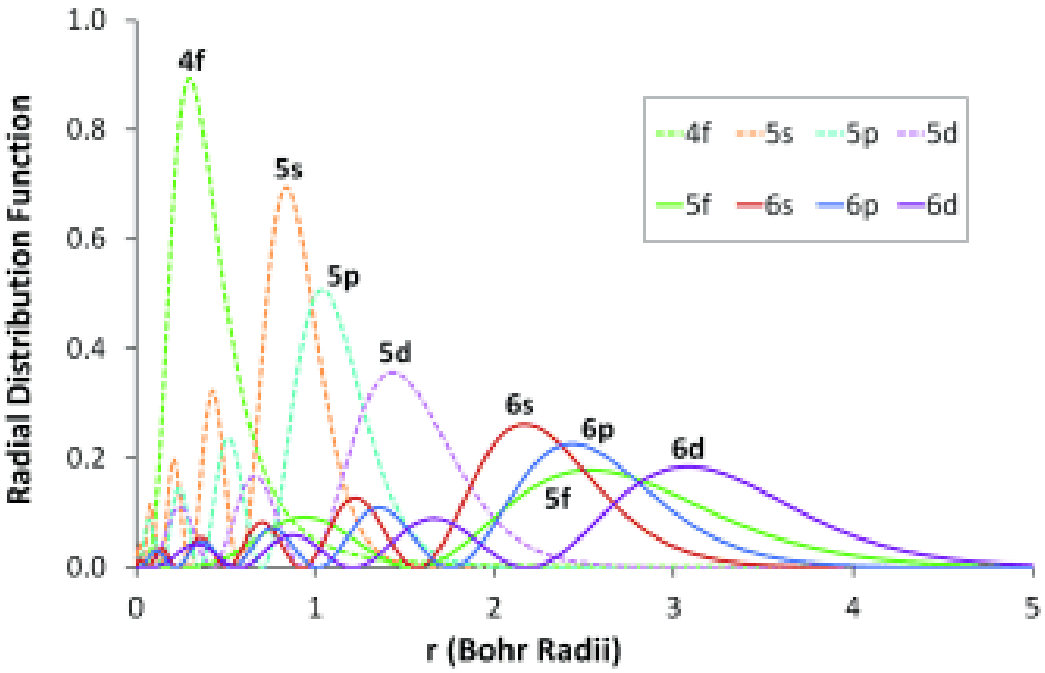

Figure 1: Radial distribution function of atomic orbitals.[1]

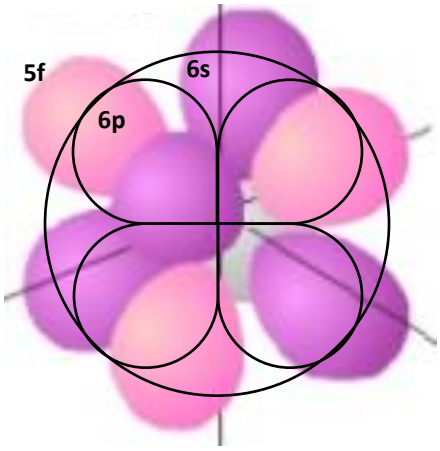

Figure 2: Visual representation of S and P orbital contraction due to relativistic effect.

Transition metal and lanthanide compounds have been given considerably more attention than their actinide counterparts. Actinide complexes with softer chalcogenolate ligands are rarely seen in the literature. However, An chalcogenolates have been isolated with sterically hindered and extremely bulky stabilizing ligands.[2–8] Th in particular, is

most often seen with large sterically bulky ligands like $ECPh_3$ (E=S, O) and K(18-crown-6) ligands,[9] or tetradentate dianionic diamine bis(phenolate) ligands.[10] U has a much more extensive presence in the literature comprised of various complexes and compounds. Polychalcogenido-bridged uranium complexes with elemental chalcogen have also been presented in the literature.[11] These complexes take advantage of bulky chelating N-anchored ligands substituted with adamantyl groups as a way to investigate different pathways to U(IV) with magnetic properties. Though each of these studies was helpful in elucidating relative orbital contribution and are a few of the complexes published, they all fail to provide insight into bonding without sterically bulky ligands. Sterically hindered stabilizing groups greatly decrease the solubility and inevitably create a solid substance, following the usual trend in this chemistry to use ancillary ligands with many more examples available.[12–19]

When looking to synthesize larger clusters, a simple monomer moiety can help build the initial framework. The bonding character of the metal-ligand bond gives basic information about covalent vs iconic character, preferred coordination, and steric restrictions. Many examples are prevalent in the literature for both U and Th monomers, the only caveat being that they contain large bulky ligands that help stabilize the complex thus making it easier to isolate. One notable example of this is the heteroleptic An(IV) halide complexes, [An(salan-t Bu_2)X_2], which provide versatile precursors for the synthesis of robust alkyl complexes and can yield CO insertion products.[10] In addition to the tradition bulky ligands, actinides can also be utilized with PNP moieties demonstrating An ability to be stabilized by multidentate ligands. PNP U(III) 7-coordinate compounds with *pseudo*-meridional and *pseudo*-facial geometries were to

maintain hemilabile character both in the solid-state and in solution.[20] Although these large moieties were used to stabilize structures and decrease solubility for easy isolation, their steric bulk allows for in-depth analysis of the remaining coordination sites. This is elegantly seen in the NMR analysis of covalency in $[K(18\text{-crown-}6)][Th(\eta^2\text{-}E_2)(NR_2)_3]$ (E = Se, **2**; E = Te, **3**), respectively. The orbitals used in bonding where explored with DFT studies and Se/Te NMR to reveal the shortest An-E bonds.[9] Though a multitude of examples exist, these three monomers displayed key insights that were applied to the research described forthwith.

Actinide clusters have been harder to achieve than their main element counterparts. The tendency of oxo ligands to generate soluble oxo compounds instead of oxide particles like in $[UO_2(S_2CN\text{-}iPr_2)_2(SS)^{2+}]$[21] and a uranyl thiolate[21] complicates cluster synthesis in the case of U^{6+}. There are even examples of dimers with bridging carbon monoxide molecules that employ N-heterocyclic carbenes in order to stabilize the structure.[22] A plethora of other examples with U clusters are present from aryloxides, to phosphines, to trisaminomethylamines and much more, all mainly with the use of ancillary ligands.[1] There are even examples of U, Th and Pu with oxide, peroxide and hydroxide bridges ranging from 4-38 An cations with varying oxidation states.[23] One of the most notable examples being that sizeable $U_{120}Ox_{90}$ (Ox = oxalate). The shell consists of 12 five-membered rings of uranyl diperoxide hexagonal bipyramids that share vertexes, upon dissolution in water the 60 uranyl polyhedra that form the shell structure detach from the cluster leaving a $U_{60}Ox_{30}$ core.

Additionally, significant insight has been discovered through in-depth experimental treatment of many chalcogenido complexes. For example, the first reported

Th-Se resonance was yielded from a homoleptic soft-donor actinide compound. Through a combination of DFT, NBO and QTAIM more covalency was found in An-Se than an An-S bonds.[24] Ancillary ligand K(18-crown-6) installed by reductive deprotection yields oxo and sulfide complexes [K(18- crown-6)][Th(O)$(NR_2)_3$] and [K(18-crown-6)][Th(S)$(NR_2)_3$] respectively. The in-depth exploration of metal-ligand bonding via quantum chemical indicates that the M–E interactions have triple bond character and the M–N have double bond character each polarized away from the metal.[25] Furthermore, isostructural compounds M[$N(EPR_2)_2]_3$ (M = U, Pu, La, Ce; E = S, Se, Te; R = Ph, *i*Pr, H) is one rare examples U-Se/Te bonds reported in the literature.[26] DFT calculations and molecular orbital overlap show consistency in theory and experiment. Additionally, the covalency differences between the d-orbital participation in M-E bonds and the f-orbital participation of Ln-E and An-E was emphasized. Lastly, the most analogous structure to the chemistry discussed in this thesis is the $[U(py)_2(SePh)(\mu_3\text{-}Se)(\mu_2\text{-}SePh)]_4 \cdot 4py$.[27] The An(IV) cluster with bridging chalcogenido forming a distorted cubane core and bridging and terminal chalcogenolate ligands.

The electronics of these compounds are just as interesting as the bonding and physical properties. Though these complexes are usually colorless, since Th^{4+} has a noble gas electron configuration of [Rn] and thus no electrons to participate in excitation, a different ligand-ligand charge transfer could expose a range of colored Th compounds. Color is a result of electronic transitions between non-degenerate orbitals whose energy corresponds to the energy of the visible spectrum 369 – 769 nm. If the energy of this separation does not fall within the visible range no color will be observed. However, for ligand-ligand charge transfer the electron is no longer required to stay on the metal or E

as it does with ligand-metal or metal-ligand charge transfer. With empty π* orbitals and more of them for increasingly multidentate ligands the range of possibilities is greatly increased. This increase in possible transitions leads to a possibility in the shift of the visible maximum. There is precedence for this ligand-ligand charge transfer in the literature,[28–34] but there is also a question of mixing of the metal orbitals. All of which adds to the complicated nature of An chemistry.

In order to examine bonding, it is desirable to prepare homoleptic complexes without the steric influences of bulky stabilizing substituents.[35] It was clearly shown that oxidation of elemental lanthanides is a viable synthetic route to unsupported complexes containing only chalcogenolate anions and solvent molecules bound to the lanthanide ion.[36–40] This ideal was applied to and found to still hold true with An. Upon targeting chalcogenolate clusters three categories of products have emerged that will be discussed in detail in this thesis. Chapter one deals with the synthesis and structure of Th cubane clusters and their subsequent NMR studies and thermolysis. Chapter two presents bipyridine (2,2'-bipyidine = bipy) and terpyridine (2,2':6'2"-terpyridine = terpy) clusters showing the intricacies of multidentate ligands. Lastly, chapter three explores heterometallic mercury cubanes with both uranium and thorium. Each of these with a basis previously established in literature, but with results unseen until now.

Chapter 1

Synthesis, Solid-State and Solution Structures, Thermolysis, and Chalcogen Exchange Reactions of Thorium Cubane Clusters

Introduction

Actinide (An) cluster chemistry[23,27,41–62] is a potentially rich field, motivated by the unique chemical[19,63–74] and physical[75–89] properties of the actinide elements and the possibility of harnessing multiple metal centers to afford unique cooperative reactions. While the possibility of cooperativity exists, rationally achieving this goal requires a more detailed understanding of fundamental physical properties of f-element compounds, as well as a deeper appreciation of how polynuclear actinide compounds behave in solution. Oxide-based actinide cluster chemistry[51,56–60] is well-established, but related compounds with less electronegative chalcogenido ligands[27,41–44,90] are relatively unexplored. Given that actinide−chalcogenide bonds are ideal subjects for probing covalency and the nature of the actinide−ligand bond, there is a strong fundamental motivation for developing the chemistry of actinide molecules and clusters with chalcogenido ligands.

Thorium has numerous intrinsic properties that make this metal attractive for studying the chemical properties of actinide clusters. Most importantly, Th(IV) is diamagnetic, and so NMR spectroscopy can be used to explore structure and bonding,[9,91–99] ligand dynamics,[24,92,100–102] and chemical reactivity.[9,94,103–106] In addition, the lack of thorium redox activity, as evidenced by the paucity of well-defined Th(III) compounds,[107–110] simplifies reactivity and minimizes the tendency of compounds to undergo undesirable side reactions.

Compounds of thorium with chalcogen-based anions[14,90,103,111–115] are limited. In early work, sterically demanding ancillary ligands[14,113,114] were used to kinetically stabilize coordination complexes, leading to isolation of the first discrete compounds with

An−E bonds. More recently, several stable molecular thorium chalcogenolates have been prepared,[24,94,103,111] showing that steric saturation is not a prerequisite to form stable products. Of these molecular compounds, the tetrachalcogenolates $Th(EPh)_4$ (E = S, Se)[111] are convenient starting materials for the synthesis of nanoscale thorium clusters using either ligand based redox chemistry or metathesis reactions, as evidenced by a description of the first thorium cubane compounds $(py)_8Th_4(\mu_3\text{-}E)_4(\mu_2\text{-}EPh)_4(\eta\text{-}E'C_6F_5)_4$ (E,E′ = S, Se).[41] This work was limited to the synthesis of compounds with the same chalcogen atom in both μ_3-E and μ_2-EPh moieties, otherwise chalcogen exchange processes between E and EPh sites led to products with random distributions of chalcogen atoms.

The present work explores actinide cubane chemistry in detail, showing that all possible combinations of E′/EPh ligands (E′, E = S or Se) in $(py)_8Th_4(\mu_3\text{-}E')_4(\mu_2\text{-}EPh)_4(\eta\text{-}EPh)_4$ can be realized experimentally and finding that thermal decomposition of heterochalcogen compounds leads to the formation of a ThS_xSe_{2-x} alloy. Cluster reactivity is explored to demonstrate that both PhE^- and E^{2-} ligands will undergo ligand-based redox reactions to form products with more electronegative ligands. Solution ^{77}Se NMR data provide insight into the dynamic behavior of these clusters, and a computational analysis of ^{77}Se NMR shifts reveals that solid-state structures are maintained in solution. All computational details can be found at 10.1021/acs.inorgchem.8b00836.

Figure 3. Thermal ellipsoid diagram of $(py)_8Th_4(\mu_3\text{-}S)_4(\mu_2\text{-}SPh)_4(\eta\text{-}SPh)_4$ (**1**) with the H atoms removed for clarity and ellipsoids at the 50% probability level. The view direction for Figures 3 – 6 is along the 4bar or pseudo 4bar axis (see text). Significant bond-length averages are given in Table 2.

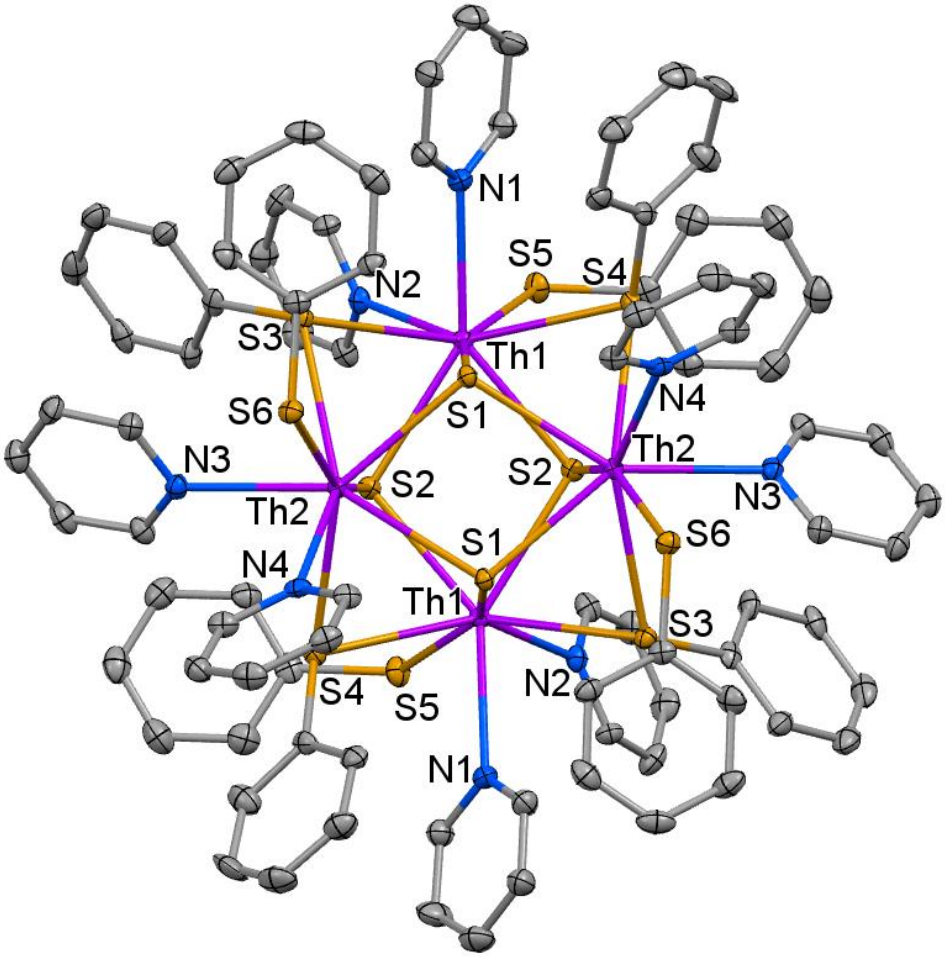

Figure 4. Thermal ellipsoid diagram of the first of two molecules in crystals of $(py)_8Th_4(\mu_3\text{-}Se)_4(\mu_2\text{-}SePh)_4(\eta\text{-}SePh)_4$ (**2**) with the H atoms removed for clarity and ellipsoids at the 50% probability level. The second unique molecule in compound **2** differs from the first only by the minor rotations of py and EPh ligands. Significant bond-length averages are given in Table 2.

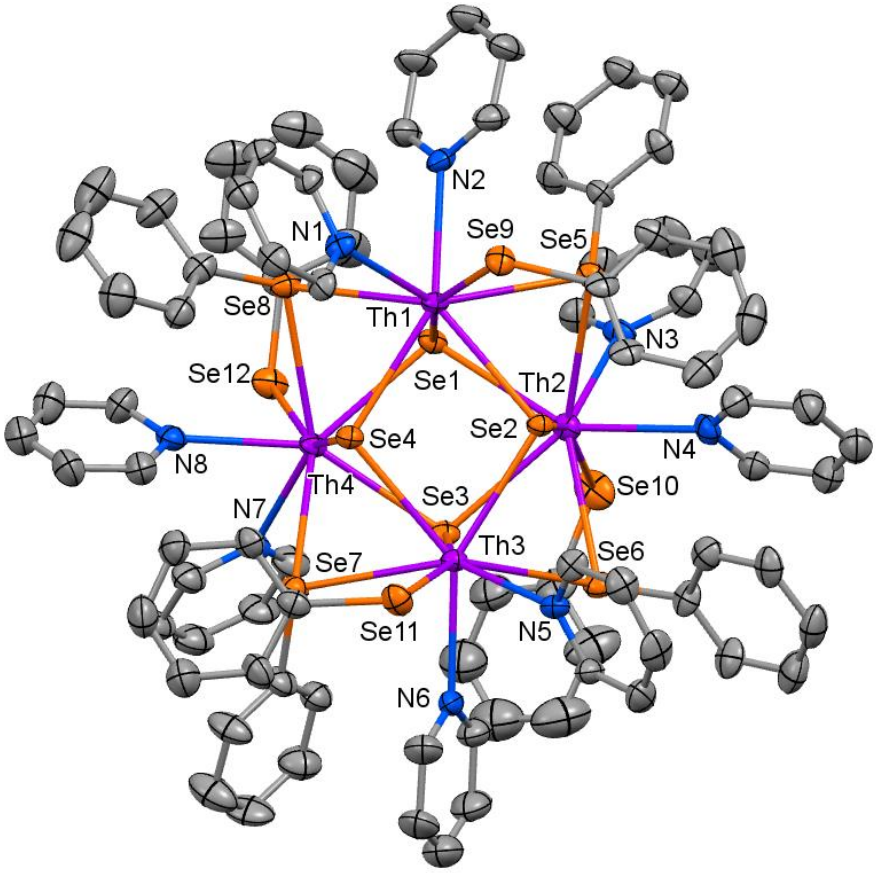

Figure 5. Thermal ellipsoid diagram of $(py)_8Th_4(\mu_3\text{-}S)_4(\mu_2\text{-}SePh)_4(\eta\text{-}SePh)_4$ (**3**) with the H atoms removed for clarity and ellipsoids at the 50% probability level. Significant bond-length averages are given in Table 2.

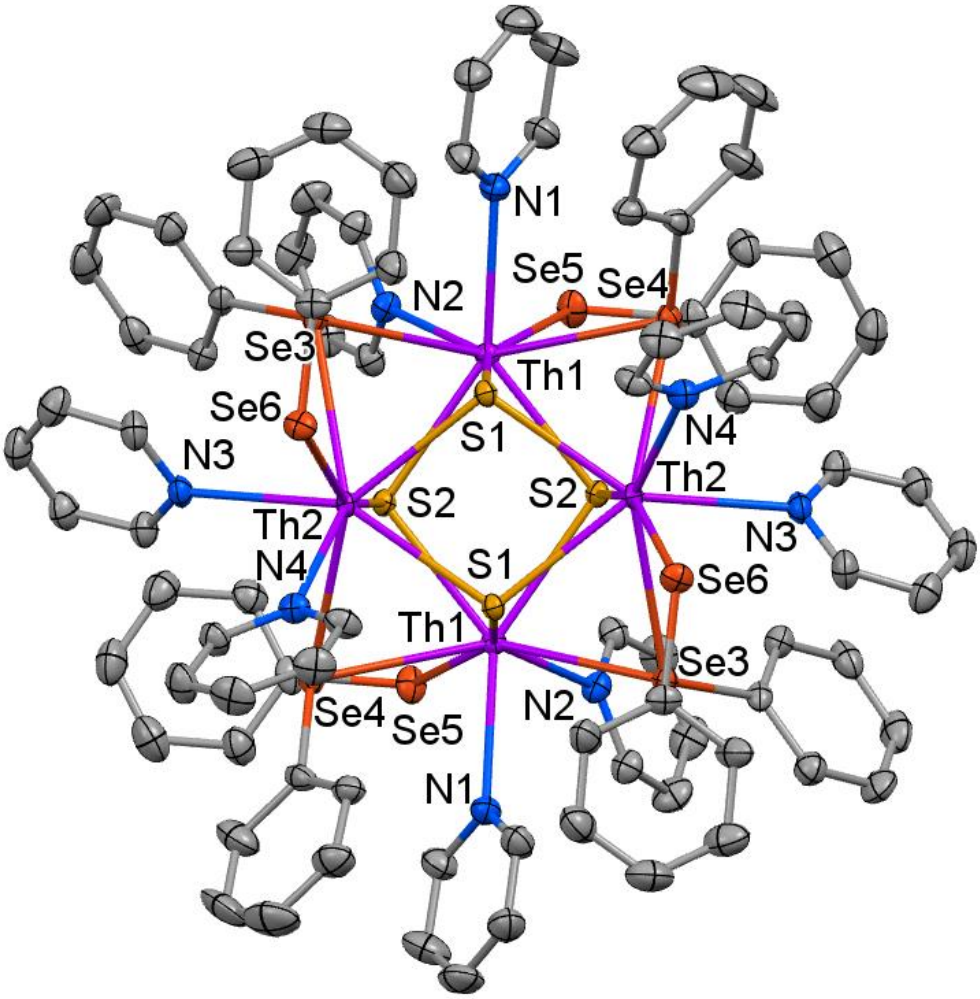

Figure 6. Thermal ellipsoid diagram of $(py)_8Th_4(\mu_3\text{-}Se)_4(\mu_2\text{-}SPh)_4(\eta\text{-}SPh)_4$ (**4**) with the H atoms removed for clarity and ellipsoids at the 30% probability level. There is only one crystallographically independent set of $(py)_2ThSe(SPh)_2$ atoms. Significant bond-length averages are given in Table 2.

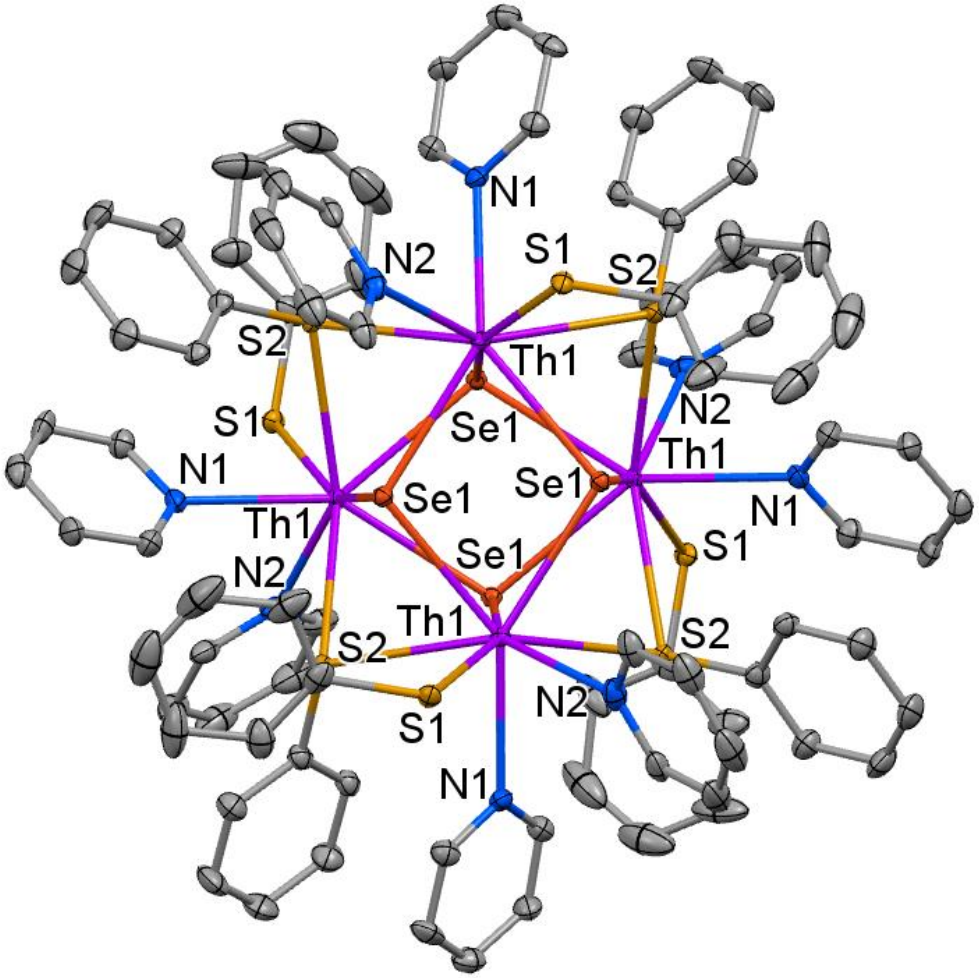

Figure 7. Generalized side and top views of the common core $Th_4E_{12}N_8$ region for thorium cubanes **1 – 4**. The view directions are normal to the square-like and rhomboid-like faces, respectively, for the unique side and top views.

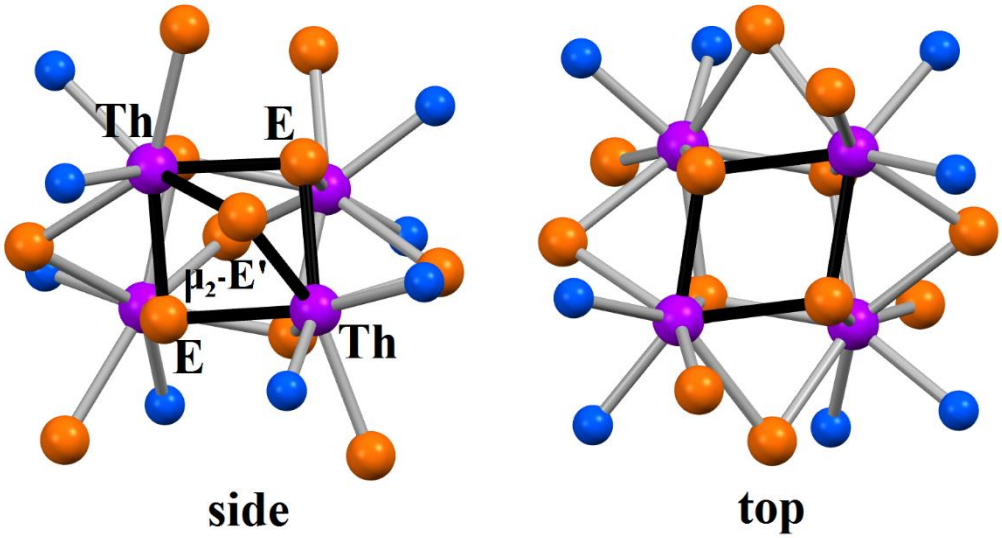

Results and Discussion

In situ prepared $Th(EPh)_4$ (E = S, Se)[111] undergoes ligand based redox reactions with elemental E′ (E′ = S, Se) in pyridine. Elemental E′ is reduced to E'^{2-}, and the PhE^- from $Th(EPh)_4$ is oxidized to PhEEPh, leading to the formation of $(py)_8Th_4(\mu_3\text{-}S)_4(\mu_2\text{-}SPh)_4(\eta\text{-}SPh)_4$ (**1**), $(py)_8Th_4(\mu_3\text{-}Se)4(\mu_2\text{-}SePh)4(\eta\text{-}SePh)_4$ (**2**), and $(py)_8Th_4(\mu_3\text{-}S)_4(\mu_2\text{-}SePh)_4(\eta\text{-}SePh)_4$ (**3**) (Scheme 1). Elemental mercury expedites the reaction either by forming a reactive Th/Hg amalgam or by insertion of Hg into the E−E bond, followed by transmetalation with elemental Th. If Hg contamination of Th waste is problematic, these reactions can be reproduced without Hg, but the rates will be slower and dependent on the level of Th surface oxidation.

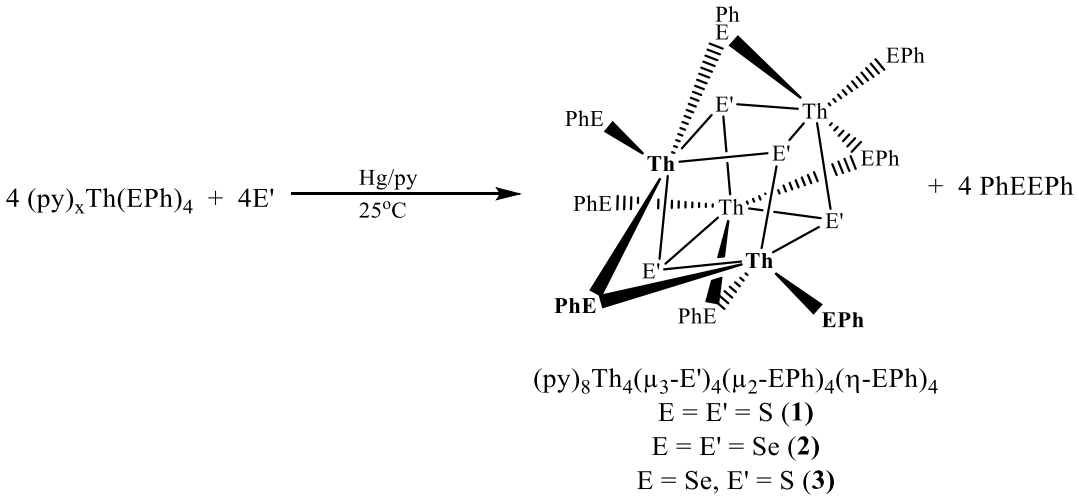

$(py)_8Th_4(\mu_3\text{-}E')_4(\mu_2\text{-}EPh)_4(\eta\text{-}EPh)_4$
E = E' = S (**1**)
E = E' = Se (**2**)
E = Se, E' = S (**3**)

Scheme 1: Synthesis of thorium cubanes **1-3.**

While E′ is reduced by PhE^- when the electronegativity of E′ is equal to or greater than the electronegativity of E, the reaction does not proceed when E′ is less electronegative than E. To establish the synthetic feasibility of all possible E/E′ combinations, the final cubane target $(py)_8Th_4(\mu_3\text{-}Se)_4(\mu_2\text{-}SPh)_4(\eta\text{-}SPh)_4$ (**4**) was approached in two ways. First, Th metal was used to reduce a mixture of PhSSPh and PhSeSePh, and elemental Se was then added to oxidize the $PhSe^-$ ligand (Scheme 2), and second, the selenido cubane **1** can be prepared in situ and reacted further with PhSSPh, resulting in displacement of the surface PhSe moieties with PhS (Scheme 3).

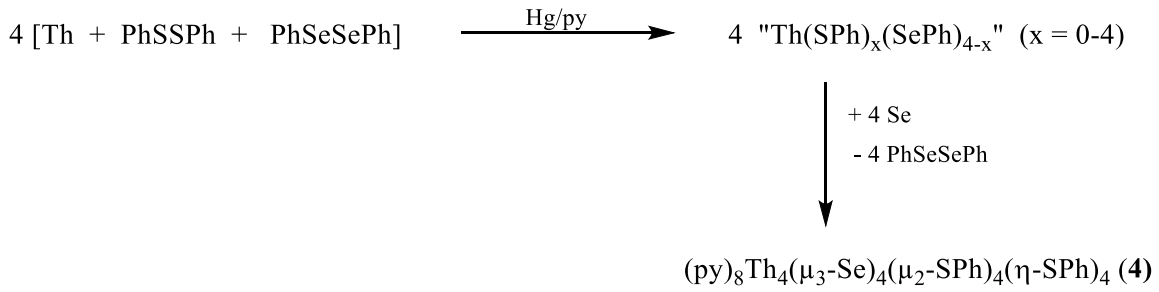

Scheme 2: Synthesis of thiolate-capped selenido cubane 4 from heterochalcogenolate starting materials.

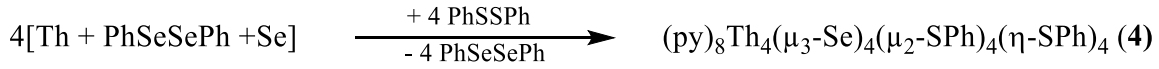

Scheme 3: Ligand exchange on cluster surface for form compound 4.

Compounds **1**−**4** were characterized by spectroscopic methods and by low-temperature single-crystal X-ray diffraction, with POVRAY diagrams for **1**−**4** given in Figures 3−6, respectively. Unlike the recently described $Th_4(\mu_3\text{-}E)_4(\mu_2\text{-}EPh)_4(\eta\text{-}E'C_6F_5)_4$ cubanes[41] with fluorinated chalcogenolate ligands that crystallize only in the tetragonal I4- cell, or in lanthanide chemistry, where surface ER ligands can have a dramatic impact on cluster structure,[37,116] compounds **1**−**4** crystallize in a number of lower symmetry unit cells, with all having the same basic structure. PXRD data for bulk isolated products show that it is possible to have more than one crystalline phase present for **2**, but the P21/n phase listed in Table S1 is reproducibly the dominant phase. Upon the basis of PXRD measurements on bulk samples of compounds **1**, **3**, and **4**, the only phase present is the corresponding phase.

All four structures contain the same $(py)_8Th_4(\mu_3\text{-}E)_4(\mu_2\text{-}E'Ph)_4(\eta\text{-}E'Ph)_4$ tetrameric core, with different numbers and orientations of lattice pyridine molecules. Cluster cores as shown in Figure 7 are defined by a significantly distorted Th_4E_4 cube, with the four equivalent "side" Th_2E_2 square faces containing μ_2-EPh ligands that bridge the two Th atoms on each side face. Unlike the slightly distorted Th_2E_2 squares on the sides, the "top" and "bottom" Th_2E_2 faces are highly distorted rhomboids, as shown in Figure 7. Comparisons of key interatomic geometries in **1**−**4** are given in Table 1.

Table 1. Ranges of selected distances (Å), angles and torsions (degrees) in X-ray structures of **1** – **4**.

	E,E'=S, S	*E,E'=Se, Se*	*E,E'=S, Se*	*E,E'=Se, S*
distance	**1**	**2**	**3**	**4**
Th–N	2.628—2.691(5) [a]	2.633—2.697(9)	2.630—2.709(3)	2.651—2.697(<
Th–μ_3E *(side)*	2.763—2.772(2)	2.894—2.913(1)	2.760—2.778(1)	2.909(<1)
Th–μ_3E *(top)*	2.786—2.854(2)	2.923—2.973(1)	2.798—2.849(1)	2.943—2.952(1
Th–μ_2E'Ph	2.990—3.046(2)	3.069—3.150(1)	3.107—3.164(1)	2.970—3.020(1
Th–ηE'Ph	2.860—2.876(2)	2.970—3.015(1)	2.986—3.000(<1)	2.884(1)
Th···Th' *(side)*	4.011—4.024(<1)	4.139—4.164(<1)	4.037—4.051(<1)	4.116(<1)
Th···Th" *(top)*	4.522—4.525(<1)	4.652—4.722(<1)	4.508—4.517(<1)	4.708(<1)
bond angle	**1**	**2**	**3**	**4**
Th–μ_3E–Th *(si*	91.2—92.6(<1)	89.21—90.54(3)	92.06—93.17(3)	89.22—89.39(1
Th–μ_3E–Th *(to*	106.7—106.7(<1)	104.75—107.33(3)	106.15—106.23(3)	105.98(2)
Th–μ_2E'–Th *(s*	83.3—84.2(<1)	83.15—84.12(3)	80.15—80.93(1)	86.81(3)
Th–μ_2E'–C	117.1—119.8(2)	112.4—118.8(4)	113.7—117.4(1)	117.5—118.4(2
Th–ηE'–C	114.3—115.6(2)	112.0—114.0(4)	112.8—114.0(1)	113.8(2)

torsion angle [b]	**1**	**2**	**3**	**4**
Th–μ_2E'–C–C	44—53	42—59	37—49	48
μ3E−Th−ηE′−C	46—47	25—53	45—48	39
Th···Th−N−C	4—5, 102—106	1—14, 92—99	2—8, 104—107	0, 93
μ3E···μ2E′−C−	1.8, 5.3	0.4—9.8, 0.1—5.4	1., 8.7	3.1
intramolecular[c]	**1**	**2**	**3**	**4**
C_β(ηE')···μ_3E	3.51, 3.53	3.38-3.70, 3.42-3.47	3.65, 3.64	3.59
C_β(μ^2E')···μ_3E	3.64, 3.66	3.73-3.86, 3.77-3.79	3.72, 3.73	3.73
cen(ηE'-Ph)···core	6.39, 6.46	6.14-6.48, 6.19-6.44	6.54, 6.58	6.41
cen(η_2E'-Ph)···cor	6.43, 6.44	6.61-6.66, 6.61-6.63	6.56, 6.59	6.48

[a] Average ESD for values contributing to the range are given in parentheses.

[b] Absolute values are used here and all ESDs are less than 1.0°. For Th-Th-N-C, both Th atoms are on the same "side", as defined in Figure 7 and the two ranges separated by a comma correspond to the two py bonded to Th atoms. For compound **2**, ranges for both unique molecules are given.

[c] These intramolecular distances relate to the conformation of the rotatable E'-Ph group and the distance between the centroids of its phenyl ring and the centroid of the "core" $Th_4E_4E'_8N_4$ region.

Table 2. Selected H···E contact geometries in **1** – **4**. [a]

Intramolecular	**1**	**2**	**3**	**4**
H(μ_2E')···μ_3E	*2.82, 2.84*	*2.72, 2.96*	*2.88, 2.89*	*2.89*
		3.01, 2.94		
H(py2)···μ_3E	3.09, 2.98	3.39, 3.33	3.12, 3.01	3.17
		3.39, 3.37		
H(py1)···μ_3E	3.24, 3.52	3.41, 3.16	3.26, 3.48	3.43
		3.23, 3.33		
H(ηE')···μ_3E	3.04, 3.08	3.88, *2.98*	3.19, 3.21	3.33
		3.74, 3.16		
H(py1)···μ_2E'	*2.69, 2.74*	*2.85, 2.78*	*2.80, 2.80*	*2.66*
		2.88, 2.84		
H(py1)···ηE'	*2.89, 2.91*	*3.07, 2.97*	*2.98, 2.98*	*2.93*
		2.95, 2.90		
H(py2)···ηE'	3.36, 3.20	*3.05, 3.05*	3.33, 3.21	3.19
		3.12, 3.15		

Intermolecular	**1**	**2**	**3**	**4**
H(py)···ηE'	*2.92, 2.88*	*3.07, 2.97*	*2.96, 2.95*	*3.01*, 3.41
H(μ_2E')···ηE'	> 3.6	3.13, 3.12	> 3.6	3.54
solvent···ηE'	3.03, 3.16	3.21, 3.11	3.15	> 3.6

[a] Italicized values are those less than the van der Waals radii sum (Bondi), 2.8 Å for H···N, 3.0 Å for H···S, and 3.1 Å for H···Se. All H atoms are at calculated positions for sp^2 geometry and C-H distance of 0.95 Å (SHELXL). Average ESDs are 0.01 – 0.02 Å for distances and 0.05 – 0.10° for angles. Note that, due to molecular site symmetry, there are two, four, two, and one unique values for named contacts for compounds **1**, **2**, **3**, and **4**, respectively.

Individual bond distances are all consistent with prior literature, with narrow ranges of Th−N,[41,111,113,117,118] Th−E,[41,119,1201j,40] or Th−EPh[41,103,111,113,118] and values that reflect the atomic sizes,[121,122] as shown in Table 1. A very good agreement of the X-ray determined Th−E/Th−E′ bond lengths with those optimized at the DFT (PBE0-D3(BJ)/ECP/def2-TZVP) level (cf. Table 2 and Table 3) is observed.

The close intramolecular H atom contact distances in **1**−**4** as given in Table 2 were a measure not only of possible weak H-bonding interactions but also of the conformational flexibility of μ-E′Ph, η-E′Ph, and py ligands. The magnitude and consistency of these values, as well as those of the torsion angles about Th−N and Th−E′, indicate that there is limited flexibility in the ligands for any one of these compounds. Additionally, to locate significant conformational variations on going from **1** to **4**, molecular overlay calculations (CCDC Mercury) were performed, and the largest deviations were clearly located about the terminal E′Ph groups, as depicted in Figure 8 and listed in Table 4.

Cubanes **1**−**4** and the recently described Th clusters with fluorinated chalcogenolates[41] afford an opportunity to establish the impact of ring fluorination on the Th−E bond length for thiolate and selenolate ligands. Both Th−S and Th−Se bond lengths are elongated when the aromatic ring is fluorinated. For thiolates, the terminal Th−S(C_6F_5) bonds [2.904(2) Å in $(py)_8Th_4S_4(SPh)_4(SC_6F_5)_4$ and 2.899(2) Å in $(py)_8Th_4Se_4(SePh)_4(SC_6F_5)_4$][41] are longer than the terminal Th−S(Ph) bonds in the present work [2.860−2.876(1) Å in **1** and 2.884(1) Å in **4**] by∼0.03 Å. Similarly for selenolates, the terminal Th−Se(C6F5) bonds [3.020(1) Å in $(py)_8Th_4Se_4(SePh)_4(SeC_6F_5)_4$ and 3.030(1) Å in $(py)_8Th_4S_4(SPh)_4(SeC_6F_5)_4$][41] are also

longer than the terminal Th−Se(Ph) bonds in **2** and **3** [2.989−3.005(1) Å in **2** and 2.986−3.000(1) Å in **3**] by∼0.03 Å. This lengthening is consistent with the polarizing ability of the fluorine substituents, namely, the withdrawal of negative charge from the chalcogen atom E in the EC_6F_5 group resulting in less electrostatic attraction and covalent bonding between Th and E. This polarization effect is reflected in the atomic partial charges and delocalization indices given in Table 3. A similar impact on M−E bond lengths was noted in analogous lanthanide systems.[36,123]

Table 3. DFT optimized Th-E bond-lengths (in Å), QTAIM delocalization indices, DI(Th-E), as a measure of the Th-E bond covalency, and CM5 atomic charges at thorium and chalcogen centers in selected systems [a,b]

	Th-E bond-lengths			DI(Th-E)			CM5 atomic charges			
Compound	Th–μ_3E	Th–μ_2E	Th–ηE	Th–μ_3E	Th–μ_2E	Th–ηE	Th	μ_3E	μ_2E	ηE
$(py)_8Th_4(\mu_3\text{-}S)_4(\mu_2\text{-}SPh)_4(\eta\text{-}SPh)_4$ (**1**)	2.786	2.987	2.836	0.531	0.338	0.519	0.626	-0.403	-0.182	-0.277
$(py)_8Th_4(\mu_3\text{-}Se)_4(\mu_2\text{-}SePh)_4(\eta\text{-}SePh)_4$ (**2**)	2.922	3.114	2.974	0.532	0.352	0.529	0.666	-0.428	-0.240	-0.338
$(py)_8Th_4(\mu_3\text{-}S)_4(\mu_2\text{-}SePh)_4(\eta\text{-}SePh)_4$ (**3**)	2.791	3.109	2.982	0.533	0.344	0.516	0.662	-0.372	-0.261	-0.338
$(py)_8Th_4(\mu_3\text{-}Se)_4(\mu_2\text{-}SPh)_4(\eta\text{-}SPh)_4$ (**4**)	2.920	2.995	2.827	0.528	0.337	0.529	0.635	-0.462	-0.163	-0.279
$(py)_8Th_4(\mu_3\text{-}Se)_4(\mu_2\text{-}SePh)_4(\eta\text{-}SeC_6F_5)_4$	2.934	3.093	3.008	0.525	0.366	0.488	0.558	-0.316	-0.248	-0.308
$(py)_8Th_4(\mu_3\text{-}Se)_4(\mu_2\text{-}SePh)_4(\eta\text{-}SC_6F_5)_4$	2.934	3.095	2.870	0.523	0.363	0.484	0.546	-0.323	-0.252	-0.253
$Th_4(\mu_3\text{-}Se)_4(\mu_2\text{-}SePh)_4(\eta\text{-}SePh)_4$	2.871	3.040	2.943	0.565	0.445	0.712	0.627	-0.402	-0.214	-0.256
(*fully desolvated cluster of* **2**)										
$(py)_3Th(SeC_6F_5)_4$			2.920			0.589	0.759			-0.269
$(py)_4Th(SeC_6F_5)_4$			2.980			0.511	0.790			-0.287
$(py)_3Th(SePh)_4$			2.915			0.600	0.757			-0.310
$(py)_4Th(SePh)_4$			2.967			0.530	0.775			-0.321
Ph_2Se										-0.038
$(C_6F_5)_2Se$										+0.028

[a] PBE0-D3(BJ)/ECP/def2-TZVP results (cf. Computational details); [b] Only averaged values over chemically equivalent atoms/bonds are given here.

A comparison of Th−ligand and U−ligand bond lengths is also possible. A related uranium cubane, $(py)_8U_4(\mu_3\text{-}Se)_4(\mu_2SePh)_4(\eta\text{-}SePh)_4$, has been described,[27] crystallizing in the monoclinic space group C2/c as observed for **1**, **2**, and **3**, but not for **4**. The $P2_1/n$ phase of **2** was the most commonly produced form, and its crystal structure results were the most precisely determined of the four phases observed for **2**. While the U_4Se_4 cluster[27] and the fully characterized $P2_1/n$ phase of **2** presented here are not isostructural, they are isomorphous, and so a comparison of average bond lengths is appropriate. There is a significant difference in the ionic radii of eight-coordinate Th(IV) and U(IV), with the uranium ion smaller by 0.05 Å,[122] and this difference should be reflected systematically in all metal−ligand interatomic separations. These expected differences are observed: the average differences between Th−L and U−L bond lengths (Δ) are all within 0.02 Å of that predicted by using appropriate ionic radii[122] for all four ligands: An−N(py) (Th, 2.671 Å; U−N; 2.619 Å, ΔTh−U = 0.052 Å), An−Se2− (Th, 2.940 Å; U, 2.868 Å; ΔTh−U = 0.072 Å), terminal An−Se(Ph) (Th, 2.994 Å; U, 2.927 Å; ΔTh−U = 0.067 Å), and bridging An−Se(Ph) (Th, 3.108 Å; U, 3.061 Å; ΔTh−U = 0.047 Å).

Figure 8. Molecular overlay of compounds **1** (red) and **2** (blue) using the "calculate overlap" feature in CCDC graphics program Mercury. The Th, Se, S and N atoms are colored cyan, gold, yellow, and blue, respectively. View highlights region of largest deviation, namely, rotated terminal E'Ph groups and accompanying py nearest to the E'Ph. Relevant conformational angles and interatomic distances are in Table 3.

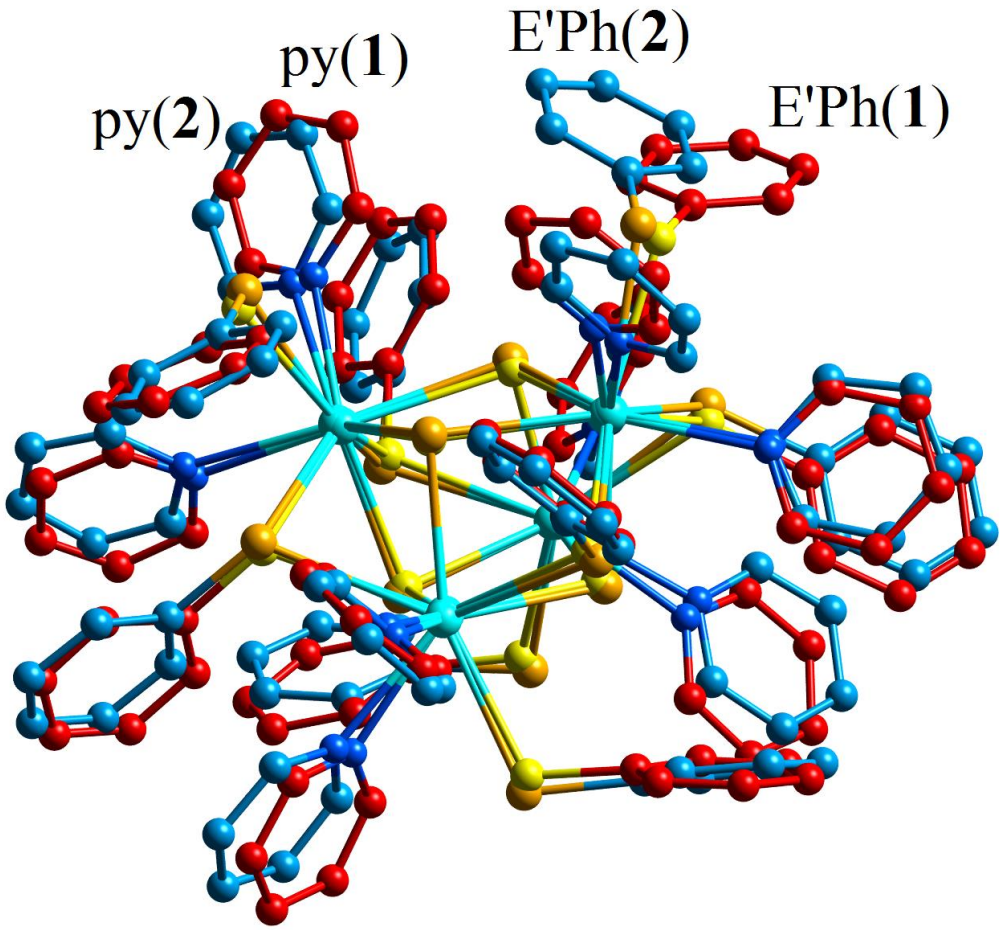

^{77}Se NMR and Solution Structure. Both ^{1}H and ^{77}Se NMR spectroscopy can be used to probe solution structure, with ^{77}Se data being particularly useful because of the large chemical shift dispersion of this spin-half (I = 1/2) nucleus. The ^{77}Se NMR shifts for the mononuclear, tetraselenolate compounds $(py)_nTh(SeAr)_4$ (Ar = Ph, C_6F_5; n = 3 or 4), the Se-containing thorium cubanes, and selected, purely organic arylselenides are summarized in Table 5. The data show an excellent match between experimental and DFT-calculated data (R2 = 0.996; root-mean-square deviation (RMSD) = 15 ppm),

allowing for a reliable computer-aided signal assignment and structure elucidation. In addition, ^{77}Se shifts in Th−Se species are very sensitive to subtle structural changes, allowing us to establish the number of metal-coordinated solvent molecules in solution. This sensitivity is evident, for example, for the $(py)_nTh(SeAr)_4$ (Ar = Ph, C_6F_5) series, where complexes with four pyridines coordinated directly to thorium center are predicted to display ^{77}Se resonances shifted upfield by ca. 80− 90 ppm as compared to their $(py)_3Th(SeAr)_4$ congeners (cf. Table 5). The shielding upon additional solvent coordination could be primarily ascribed to a Th−Se bond elongation (reduced Th−Se bond covalency) and electron-density accumulation at the chalcogen centers (cf. Table 4). The experimental and computed ^{77}Se shifts for mononuclear complexes in pyridine-d5 confirm thus the different Th coordination-environment for systems with SePh (n = 3) and SeC_6F_5 (n = 4) ligands in solution, consistent with their solid-state structures.

Table 4. Short H···H distances (Å) for the closest py···E'Ph interactions in **1 – 4** (see Figure 8). [a]

	1	**2**	**3**	**4**
H(μ_2E')···H(py) outer	2.60, 2.45	2.68, 3.54, 2.52, 2.61 2.93, 2.97, 2.64, 2.56	2.74, 2.64	2.61
H(μ_2E')···H(py) inner	2.77, 2.69	2.56, 2.62, 3.28, 2.80 2.60, 2.78, 3.05, 2.69	2.66, 2.65	3.08

[a] There are up to four instances of these py···E'Ph contacts per $Th_4(\mu_3\text{-}E)_4(\mu_2\text{-}EPh)_4(\eta\text{-}E'Ph)_4$ compound, namely, one for each unique terminal E'Ph ligand. The closest py ligand is bonded to the same Th atom as the E'Ph, ESDs are 0.01 – 0.02 Å. The terms "outer" and "inner" refer to the relative position of the contact with respect to the molecular centroid for the C(2) *versus* C(6) atom of the E'Ph ring.

Measurements of selenido clusters are equally informative. Solution ^{77}Se NMR analysis of cubane **2** shows three ^{77}Se resonances at 928 ppm (μ3-Se), 460 ppm (μ_2-SePh), and 573 ppm (η-SePh) that are assigned by comparison with both the Se^{2-} (904 ppm) and μ_2-SePh (479 ppm) resonances in $(py)_4Th_4(\mu_3\text{-}Se)_4(\mu_2\text{-}SePh)_4(\eta\text{-}SC_6F_5)_4$[41] and the resonance at 659 ppm for the terminally bound SePh in $(py)_3Th(SePh)_4$. The ^{77}Se NMR shifts computed for fully desolvated Th cubanes are generally more deshielded than those in pyridine coordinated clusters (cf. Table 5), more so for "in-cube", μ3-Se, and terminal, η-Se, selenium atoms (>140 ppm), while somewhat smaller deshielding (∼40−70 ppm) is observed for bridging, μ_2-SeAr, ligands. An excellent match between experimental and DFT-computed ^{77}Se shifts for pyridine coordinated Th cubanes supports thus the maintenance of the tetrametallic Th_4E_4 structures (coordinated by two pyridine molecules at each Th center) in solution, with no exchange between bridging and terminal SePh sites on the NMR time scale. Cubane **4** is also static in solution, with two sets of SPh resonances observed in the ^{1}H NMR spectrum at 25 °C.

Table 5. Summary of experimental and DFT computed ^{77}Se NMR shifts (in ppm *vs.* Me_2Se) for selected systems [a]

Compound	Calcd. δ(^{77}Se)			Expt. δ(^{77}Se)		
	μ$_3$-Se	μ$_2$-SePh	η-SeAr[b]	μ$_3$-Se	μ$_2$-SePh	η-SeAr[b]
$Th_4Se_4(\mu_2\text{-}SePh)_4(\eta\text{-}SePh)_4$ (*fully desolvated cluster of* **2**)	1150	552	806	-	-	-
$(py)_8Th_4Se_4(\mu_2\text{-}SePh)_4(\eta\text{-}SePh)_4$ (**2**)	951	485	545	928	460	573
$(py)_8Th_4Se_4(\mu_2\text{-}SePh)_4(\eta\text{-}SeC_6F_5)_4$[41]	904	477	343	915	480	369
$(py)_8Th_4Se_4(\mu_2\text{-}SePh)_4(\eta\text{-}SC_6F_5)_4$[41]	890	478	-	904	479	-
$(py)_3Th(SeC_6F_5)_4$			490			-
$(py)_4Th(SeC_6F_5)_4$[111]			402			400

$(py)_3Th(SePh)_4$[111]	644	659
$(py)_4Th(SePh)_4$	565	-
PhSSePh[124]	517	520
PhSeSePh[125]	469	456
Ph_2Se[125]	415	402
C_6F_5SePh[125]	274	265
$(C_6F_5)_2Se$[125]	98	110
PhSeH[125]	155	152

[a] NMR shifts computed at the 2c-ZORA(SO)/PBE0-40HF/TZ2P/DZP level using a COSMO solvation model (cf. Computational details); [b] Ar = Ph or C_6F_5; [c]

It is noted further that, although the ^{77}Se shifts for "in-cube" μ_3-Se atoms are close to that measured for [K(18-crown6)][Th(Se)$(NR_2)_3$][$\delta(^{77}Se)$ = 992 ppm in pyridine-d5], which contains a highly polarized triple Th−Se bond [d(Th−Se) = 2.653 Å; DI(Th−Se) = 1.266] (DI = delocalization index),[9] both NLMO and QTAIM analyses show strongly polarized single Th−E bonds in compounds **1**−**4** (cf. Table 4; note that the DI integrates the electron density in the bonding region between two atoms in question and is closely related to the covalent bond order, reduced by bond polarity; that is, DI = 1.0 for a "pure" covalent single bond, and DI = 2.0 for a pure covalent double bond, but DI = 0.0 for a pure ionic bond). This is also reflected in notably longer Th−Se distances, which vary from 2.894 to 2.973 Å (cf. Table 1). Despite much smaller Th− E bond covalency, the strong ^{77}Se deshielding of the μ_3-Se^{2-} ligand atoms can be attributed to the presence of multiple adjacent Th(IV) centers. These form low-lying unoccupied MO orbitals, composed largely from Th(6d) atomic orbitals (with a minor Se(4p) contribution), and are magnetically coupled with suitable occupied MOs with a predominant Se(4p) character. The latter are energetically higher for μ_3-Se-centered MOs than for those localized at μ_2-Se or η-Se, that leads to lower excitation energies (ΔE) appearing in the denominator of the Ramsey formula and thus larger paramagnetic shielding for μ_3-Se^{2-} atoms. The diamagnetic and spin−orbit shielding contributions are comparable with those in mononuclear Th−Se compounds, and the trends in NMR shifts are dictated solely by σp shielding, consistent with previous findings.[9] In passing that more extreme deshielding for the μ_3-Se^{2-} ligand, with $\delta(^{77}Se)$ = +2006 ppm, was found for a titanium(IV) selenido cluster, $[(\eta\text{-}C_5H_5)Ti]_4(\mu_2\text{-}Se)_3(\mu_3Se)_3$.[126]

Generally, upfield ^{77}Se shifts for SeC_6F_5-containing compounds as compared to their nonfluorinated SePh congeners were also found for some organoselenides (see Table 5), although the former possesses more positive charge at the Se center (cf. Table 3). This somewhat counterintuitive behavior can be ascribed to a less efficient π-conjugation of the Se electron lone pairs with the perfluorinated aryl group(s), as evident, for example, from the more acute C−Se−C bond angle, the larger selenium lone-pair occupancy, and/or notably smaller participation of Se(4p) in the HOMO−5 orbital (with the most dominant contribution to the σp (^{77}Se); HOMO = highest occupied molecular orbital) when comparing $(C_6F_5)_2Se$ with Ph_2Se. The expected ^{77}Se deshielding upon introducing electronegative fluorine substituents is, however, observed when comparing organoselenium compounds with Se-bound fluorinated and nonfluorinated alkyl groups.[125,127]

Cluster Reactivity. Ligand-based redox chemistry outlined in Scheme 3 was confirmed synthetically in a preparative scale reaction of cluster **2** with PhSSPh. The reaction (Scheme 4) was conducted at 25 °C using stoichiometric amount of PhSSPh, and the resulting colorless crystals were verified by single-crystal X-ray diffraction as the mixed chalcogenide compound **4**.

Scheme 4

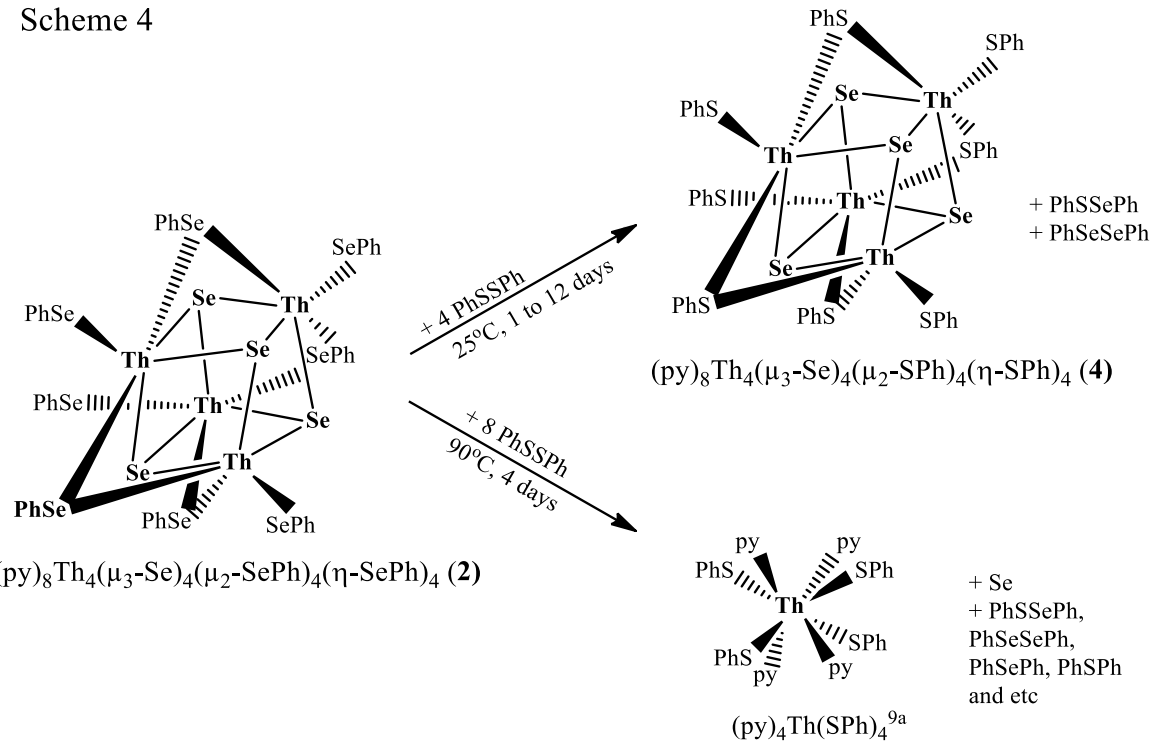

$(py)_8Th_4(\mu_3\text{-}Se)_4(\mu_2\text{-}SePh)_4(\eta\text{-}SePh)_4$ (**2**)

$(py)_8Th_4(\mu_3\text{-}Se)_4(\mu_2\text{-}SPh)_4(\eta\text{-}SPh)_4$ (**4**)

$(py)_4Th(SPh)_4$[9a]

Scheme 4: Reactivity of all-selenium compound 2 with diphenyl disulfide under different conditions.

This chalcogenolate exchange reaction is clearly driven by electrostatic forces, and the system affords an opportunity to also evaluate the reversibility of the E/EPh redox reactions in Schemes 1 and 2. In an attempt to explore the complete replacement of Se by S in the Se/SePh cluster, 2 was mixed with PhSSPh (1:8) at elevated temperatures. Surprisingly, there was no evidence for the formation of **1** or **4**, but instead (Scheme 4) monometallic $(py)_4Th(SPh)_4$[111] was isolated in high yield, with PXRD characterization indicating that this was the only crystalline product formed. The remarkable range of organic products observed is consistent with earlier work on solution speciation of

$R_2E_2/R'_2E'_2$ mixtures.[124] While it has previously been shown that larger chalcogenido clusters can be fragmented[128] under appropriate conditions, this is the first time that the reversibility of these ligand-based $E/PhE^-/E^{2-}$/ PhEEPh redox reactions has been demonstrated. This reactivity is consistent with previous work showing that M(SPh)x react with S but not Se.

Thermolysis. Molecular thermolysis[40,111,129–133] is potentially useful as a low-temperature approach to the synthesis of metastable solid-state materials, and the heterochalcogen compounds **3** and **4** present a unique opportunity to explore the low temperature preparation of ternary solid-state materials. Thermolyses of **3** and **4** were performed at the same temperature conditions as for previously reported[111] monomeric $Th(EPh)_4$ compounds (Scheme 5). The PXRD analyses revealed that the products do not contain a mixture of previously reported ThS_2[134] and $ThSe_2$[135] solid-state materials, but, instead, a new ThS_xSe_{2-x} alloy phase is observed. The crystallinity of the thermolysis product from **3** differed slightly from that of the product from **4**, suggestive of different cooling rates for the two thermolysis runs, rather than significantly different S/Se ratios.

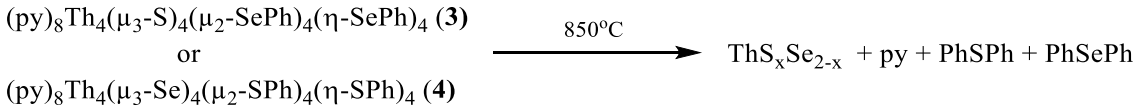

Scheme 5: Thermolysis of the heterochalcogen compounds 3 and 4.

According to scanning electron microscopy (SEM), the resulting powders of the thermal residuals for compounds **3** and **4** have different surface morphologies (Figure 9). Both in any system where chalcogen exchange reactions are possible, aryl migration could favor the elimination of PhSPh over PhSePh, with the consequent formation of a Se-rich solid-state product.

Figure 9. SEM images of thermolysis products (in 100 nm scale) for (a) compound **3**, and (b) compound **4**.

(a) **(b)**

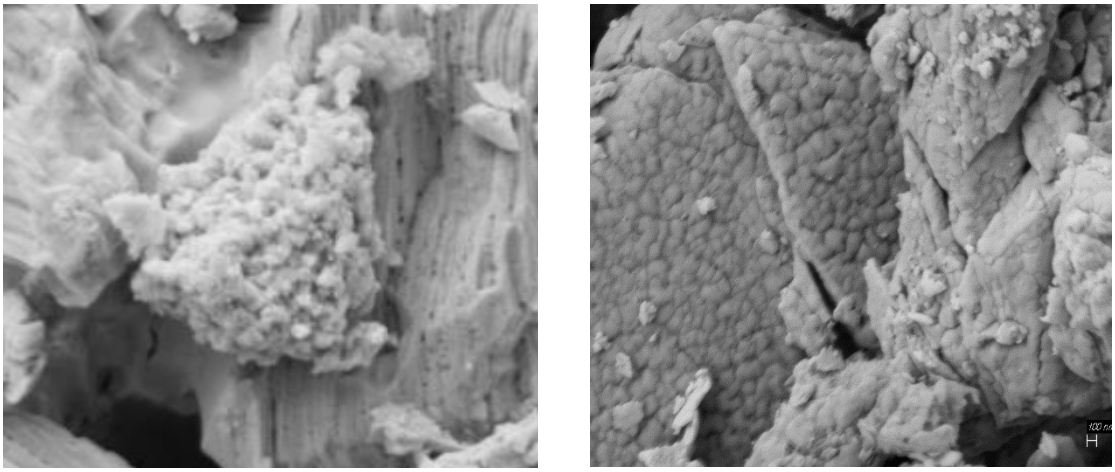

Conclusion

A family of $(py)_8Th_4(\mu_3\text{-}E')_4(\mu_2\text{-}EPh)_4(\eta\text{-}EPh)_4$ (E, E′ = S, Se) cubane clusters were prepared for all combinations of E, E′ = S, Se, using ligand-based redox reactions in which PhE anions reduce elemental E or when PhS^- reduces PhSeSePh. These clusters crystallize in a variety of unit cells, always with the same basic core structure. NMR measurements indicate that solid state structure is maintained in solution and that the cluster surface EPh ligands are static on an NMR time scale. The selenido compounds are all unstable with respect to reactions that replace Th−Se bonds with Th−S bonds. Measured and calculated ^{77}Se NMR shifts are in a good agreement and confirm the Th coordination numbers in solution. Thermolysis of the heterochalcogen compounds suggests the formation of a ThS_xSe_{2-x} alloy.

Experimental Conditions

Reaction of Compound 2 with PhSSPh (Scheme 4). Crystalline **2** (1.31 g, 0.42 mmol) and PhSSPh (0.550 g, 2.52 mmol) were combined in 30 mL of pyridine and stirred for 12 d at 25 °C. The solution was filtered to remove a trace amount of yellow powder, concentrated to ca. 14 mL, and layered with hexane (28 mL) to give colorless crystals (0.32 g, 27%), which were identified as **4** by single-crystal X-ray diffraction.

NMR Scale. Crystalline 2 (0.110 g, 0.03 mmol) was mixed with PhSSPh (0.039 g, 0.0.18 mmol) in 0.8 mL of pyridine-d5. The mixture was stirred for ~1 min and then allowed to settle at 25 °C for 45 min. ^{77}Se NMR spectrum was collected within the first 12 h and contained resonances at 520 (s, PhSSePh)[124] and 456 (s, PhSeSePh)[136] ppm. After 6 d, yellow crystals had formed in the NMR tube. These were identified as PhSeSePh[137] by X-ray diffraction. GC-MS of the solution revealed a number of products including PhSeSeSeSPh (*m/z*, 424), PhSSSSePh (*m/z*, 330), PhSSPh (*m/z*, 218), PhSePh (*m/z*, 234), and PhSPh (*m/z*, 186).

Reaction of 2 with Excess PhSSPh (Scheme 4). Crystalline **2** (1.56 g, 0.50 mmol) and PhSSPh (0.873 g, 4.00 mmol) were combined in 40 mL of pyridine and stirred for 4 d at 90 °C. The deep yellow solution was filtered from a small amount of yellow powder, concentrated to ca. 26 mL, and layered with hexane (14 mL) to give colorless crystals (0.65 g, 69%) that were identified as $(py)_4Th(SPh)_4$[111] by single-crystal X-ray diffraction. The purity of the final monomeric product was verified by comparing experimental and calculated PXRD of the bulk materials. The residue of the deep yellow solution was analyzed by GC-MS to reveal the presence of PhSSePh (*m/z*, 266), PhSSPh (*m/z*, 218), PhSeSePh (*m/z*, 314), PhSePh (*m/z*, 234), and PhSPh (*m/z*, 186).

Thermolysis (Scheme 5). Ground samples of **3** or **4** (∼20 mg) were placed in a quartz thermolysis tube under nitrogen atmosphere that was evacuated and purged with argon three times, sealed under vacuum, and placed into a model 847 Lindberg tube furnace. The initially empty "cold" end of the glass tube was held at −196 °C by immersion in liquid nitrogen. The samples were heated to 850 °C at a ramp rate of 10 °C/min and then held at 850 °C for 6 h, at which time it was cooled to 25 °C at a rate of 3.5 °C/min. The gray-black powder that was formed at the sample end of the quartz tube was placed on Kapton tape and identified by PXRD as a solid-state mixture, or alloy, of isomorphic ThS_2 and $ThSe_2$, namely, ThS_xSe_{2-x}, with approximately equal amounts of Se and S based upon the resulting unit cell dimensions from whole pattern fitting routine (JADE7) after using as starting point either the ThS_2 phase[14,111–115] (Pmnb (62), Z = 4, PDF No. 751967), or the $ThSe_2$ phase[138] (Pmnb (62), Z = 4, PDF No. 74-0978). However, the nearly equal amounts of Se and S determined from the calculated unit cell alone may not be accurate due to the considerable asymmetrical broadening of peaks as a result of low-dimensional and restacking effects of the crystal packing on the nano scale, similar to those observed for MoS_2,[139] TaS_2,[140] and NbS_2.[141] GC-MS analysis of the volatile products identified py (*m/z* 79), SPh2 (*m/z* 186), and $SePh_2$ (*m/z* 234).

Scanning Electron Microscopy (SEM). Field-emission scanning electron microscopy (FE-SEM, ZEISS Sigma) and energy-dispersive X-ray spectroscopy (EDS, silicon drift detector from Oxford Instruments) were employed to observe the morphological characteristics of the pyrolysis materials. Imaging and EDS were completed using 5 and 15 keV electron beam voltages correspondently. All samples were

covered with 20 nm Au coating using rotary-pumped sputter coating system (EMS150R, Electron Microscopy Sciences) and placed on carbon adhesive tapes with specimen holders (Ted Pella).

Powder X-ray Diffraction (PXRD). PXRD data for compounds **1**−**4** were obtained with a Bruker Vantec-500 area detector and a Bruker FR571 rotating-anode X-ray generator operating at 40 kV and 50 mA and equipped with a three-circle Azlan goniometer. The system used 0.5 mm pinhole collimation and a Rigaku Osmic parallel-mode (e.g., primary beam dispersion less than 0.016° in 2θ) mirror monochromator (Cu Kα; λ = 1.5418 Å). Data were collected at 20 °C with a sample-to-detector distance of ∼26 cm. Spatial calibration and flood-field correction for the area detector were performed prior to data collection. The 2048 × 2048-pixel images were collected at the fixed detector (2θ) angles of 0 and 15° for ∼10 min with ω fixed and continuous rotation in ϕ (capillary axis) of ∼2° per min. For the intensity versus 2θ plots,[142] background levels, modeled as amorphous scattering from air, capillary, and sample, were subtracted, and integrations in χ (Bruker GADDS)[143] were performed. No other corrections to the PXRD data were made. PXRD of bulk samples were compared with the calculated diffraction pattern of the respective compound. To account for the temperature difference in the PXRD (T = 293 K) and single-crystal (T = 153 K) patterns, a wavelength of 1.51 Å was used for the calculated PXRD patterns. Also, it appeared that the intensity and d-spacings of low-angle PXRD data were much less affected by evaporation of lattice solvent. Thus, the 4° <2 θ < 12 ° PXRD data provided an excellent region for the phase verification performed here. Diagrams of the PXRD data are available in the Supporting Information[144].

Single-Crystal X-ray Structure Determination. Data for 1−16 were collected on a Bruker Smart APEX CCD diffractometer with graphite monochromatized Mo Kα radiation (λ = 0.71073 Å) at 100 or 120 K.[145] All experimental details can be found in the published paper.[144] Thermal ellipsoid diagrams for **1**−**4** are shown in Figures 3−6, respectively.

Chapter 2

Monomeric Thorium Chalcogenolates with Bipyridine and Terpyridine Ligands

Compounds $(bipy)_2Th(SeC_6F_5)_4$ and $(bipy)_2Th(SC_6F_5)_4$ were synthesized and characterized fully by Matthew Stuber and Wen Wu respectively.

Introduction

The actinide elements continue to represent one of the great challenges in inorganic chemistry because of the complicated nature of the valence 5f orbitals and the variable influence of covalent/ionic bonding in actinide systems. Interest in probing the importance of covalent bonding has inspired recent efforts to develop the chemistry of actinides with relatively electropositive chalcogen based anions (i.e. ER^-, E^{2-}; E = S, Se, Te; R = organic) because of the intrinsic nature of these ligands form covalent bonds with metals.[146,147] A firm understanding of the fundamental chemical and physical properties of molecules with actinide-chalcogen bonds is also important because it provides the necessary foundation for understanding size dependent chemical and physical properties of actinide systems.

2,2'-Bipyridine (bipy) has been used extensively in actinide chemistry,[148–157] because chelating ligands impart thermal stability, and because the extended π* orbitals are a potential reservoir for electrons in transition states[158–160] or in ground states, as a bipy radical anion.[107,151,161–169] Compounds of uranium with bipyridine dominate the actinide literature, with an extensive array of halide[10,63,158,162–165,170–182] and carboxylates derivatives,[183–189] but less conventional compounds such as the remarkable uranium imido bipy complexes also exist.[158,159,163,170,172,182,190–192] Products in which bipy is anionic are also well established, i.e. $U(bipy)_4$[161] and a series of actinide metallocenes.[113,165,193,194]

Thorium compounds are potential sources of insight into the electronic properties of actinide compounds because the electronically silent nature of the Th(IV) ion (no $f^n \rightarrow f^{n-1}d^1$ promotion, LM or ML charge transfer) simplifies the assignment of ligand

based electronic transitions. While there are a number of Th compounds with bipy ligands[10,107,113,165–167,193] and a number of instances where pairs of bidentate ligands have been used to give stable 8 coordinate bis-chelate ligand compounds,[162,168,175–178,182,195–202] there are no examples of thorium compounds with two bipy ligands.

This work outlines the synthesis and characterization of bipyridine complexes of thorium chalcogenolates $Th(ER)_4$. In order to probe the origin of the color in these compounds, analogous chemistry with 2,2′,6′,2″-terpyridine (terpy) was also explored.

Results and Discussion

Thorium metal reacts with RE-ER (E = S, Se; R = Ph, C_6F_5) to reductively cleave the E-E bond and form Th(IV) chalcogenolates that react with bipy to form bis-bipy chelate compounds $(bipy)_2Th(EPh)_4$ (Scheme 6) and $(bipy)_2Th(EC_6F_5)_4$ (Scheme 7). This is an attractive synthetic approach due to the minimal number of reagents involved, the relatively high yields, and the ease with which intended products can be isolated, because there are no solid-state byproducts. Addition of catalytic mercury is not required but reduces the amount of time required for all the Th metal to be consumed.

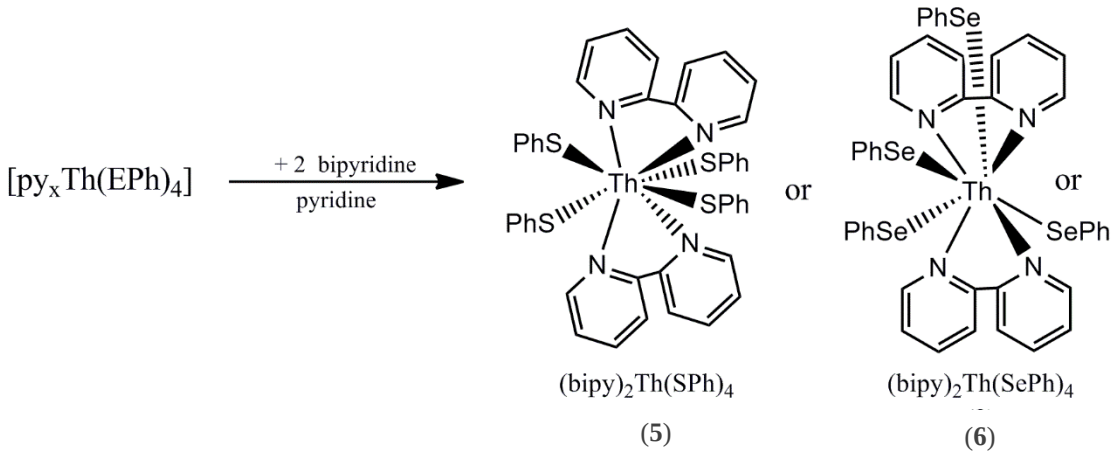

Scheme 6. Synthesis of bis-bipyridine thorium(IV) chalcogenolate complexes by displacement of pyridine with bipy.

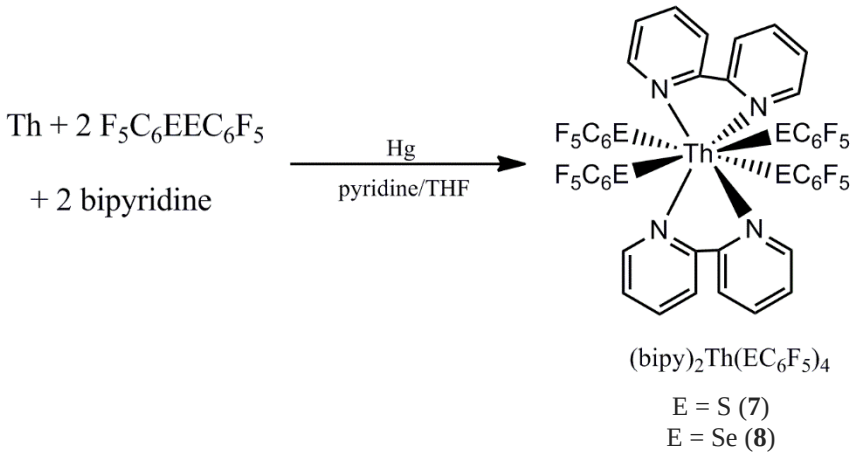

Scheme 7. Synthesis of bipyridine thorium monomers with fluorinated chalcogenido ligands.

All four bis-bipy products were isolated and characterized by conventional methods and low temperature single crystal x-ray diffraction. Because reliable elemental analyses are often difficult to obtain, due to the facile loss of lattice solvent at room

temperature and the possibility that other phases may also precipitate from the same flask, all compounds were also characterized by powder x-ray diffraction. Observed diffraction profiles were compared with profiles calculated from respective single crystal results to determine the level of purity of the bulk isolated material.

All four bipy compounds are thermochromic in the solid state, reversibly becoming darker as the temperature increases. Thermochromic properties are rare in actinide systems, with a mere two reports outlining thermochroic behavior in uranyl systems.[203,204] Because the analogous pyridine derivatives are colorless at room and elevated temperatures, the most likely source of the color change for the bipy compounds may be a low energy ligand-to-ligand charge transfer (LLCT) process in which an electron on the relatively electropositive EPh anion is transferred to a delocalized π* orbital on the bipy.[28–34] Well-defined absorption maxima that could be assigned to such an LLCT process were not observed, but the hypothesis can be tested by replacing bipy with terpy, where the more extended π* orbitals on the terpy ligand should lower the energy requirements of a LLCT process even more.[205] Addition of terpy to a solution of $Th(ER)_4$ led to the successful isolation and characterization of the thiolate product $(py)(terpy)Th(SPh)_4$, **5**, which was characterized by IR/UV/vis spectroscopic methods, PXRD, and low-temperature single crystal x-ray diffraction. Compound **5** is the first thorium compound containing terpy.

Although not quantitative because of variable crystal thicknesses, the yellow color of **5** is darker than the colorless $(py)_4Th(SPh)_4$ (104) and the light yellow $(bipy)_2Th(SPh)_4$, **5** implying that the electronic transition responsible for complex color is shifted increasingly into the visible spectrum as the extent of conjugation in the neutral

donor is extended. This behavior is consistent with the above LLCT assignment. Unfortunately, there was no well-defined adsorption maximum in the UV/vis spectrum of $(py)(terpy)Th(SPh)_4$ (Scheme 8).

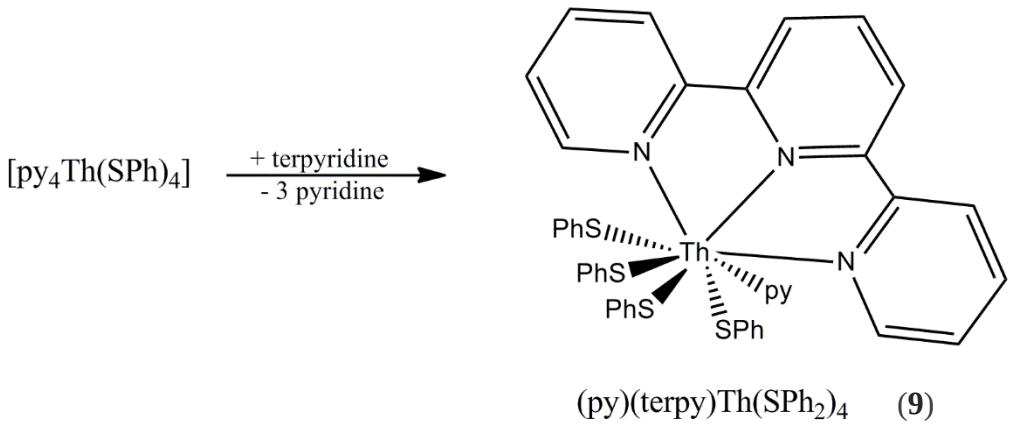

$(py)(terpy)Th(SPh_2)_4$ (**9**)

Scheme 8. Synthesis of the monomeric terpyridine thorium thiolate.

All five compounds are eight coordinate, with four chalcogenolate ligands and two neutral chelating ligands. These compounds crystallize in four structural types that differ greatly in overall conformation, but only slightly in the geometry of the ThE_4N_4 core coordination (see below). For **5 – 9**, this situation contrasts that for the 7-coordinate $(py)_3Th(ER)_4$ derivatives (ER = SePh, SC_6F_5).[111] Unexpectedly, for $(py)_3Th(SePh)_4$,[111] a seven coordinate structure is even maintained in pyridine solution, as determined by ^{77}Se NMR data and DFT calculations.[144]

In contrast to the relatively less crowded 7-coordinate Th compound $(py)_3Th(SC_6F_5)_4$,[206] eight -coordinate $(bipy)_2Th(SC_6F_5)_4$, **7**, contains no dative Th···F bonds, most likely due to space constraints when the two bidentate bipy ligands are present as in Fig. 12. This hypothesis is also supported by the absence of Th···F dative bonds in the 8-coordinate $(py)_4Th(SeC_6F_5)_4$. Many dative actinide···F interactions are found in the Cambridge Structure Database (CSD),[137] but only seven were found to involve an F atom from a ligand containing a C_6F_5 moiety.[28–34,207] The three py in $(py)_3Th(SC_6F_5)_4$[111] are all located on one side of the molecule, so that the molecular dipole is very large, in contrast to all of the 8-coordinate molecules presented here, which have pairs of ER located on opposite (**5**, **7**, **8**) or on nearly opposite (**6**, **9**) sides of the molecule.

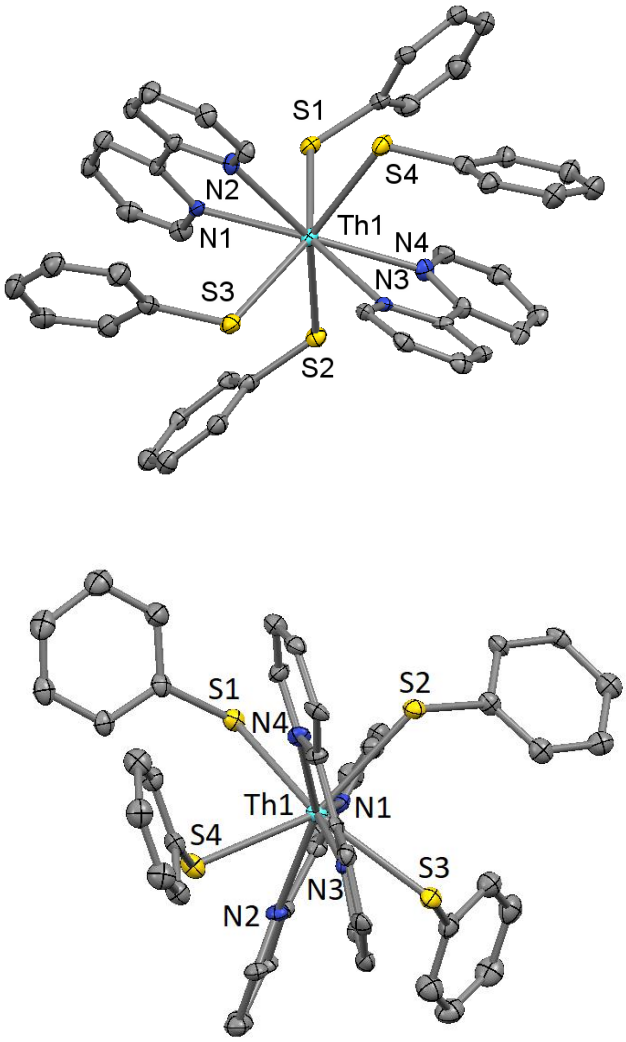

Fig. 10: Thermal ellipsoid diagram of $(bipy)_2Th(SPh)_4$, **5**, with the H atoms removed for clarity and ellipsoids at the 50% probability level. (TOP) View showing distorted square antiprismic coordination; (BOTTOM) view showing nearly regular bicapped trigonal prismic coordination with π···π interactions evident between the aromatic bipy and SPh groups comprising each trigonal face, namely, N1, N2, and S3 (below the viewing plane), or N3, N4, and S4 (above the viewing plane); capping ligands are the SPh with S1 and S2. Of the four unique molecules in **5**, two are nearly the same and the other two are nearly their inversion mates.

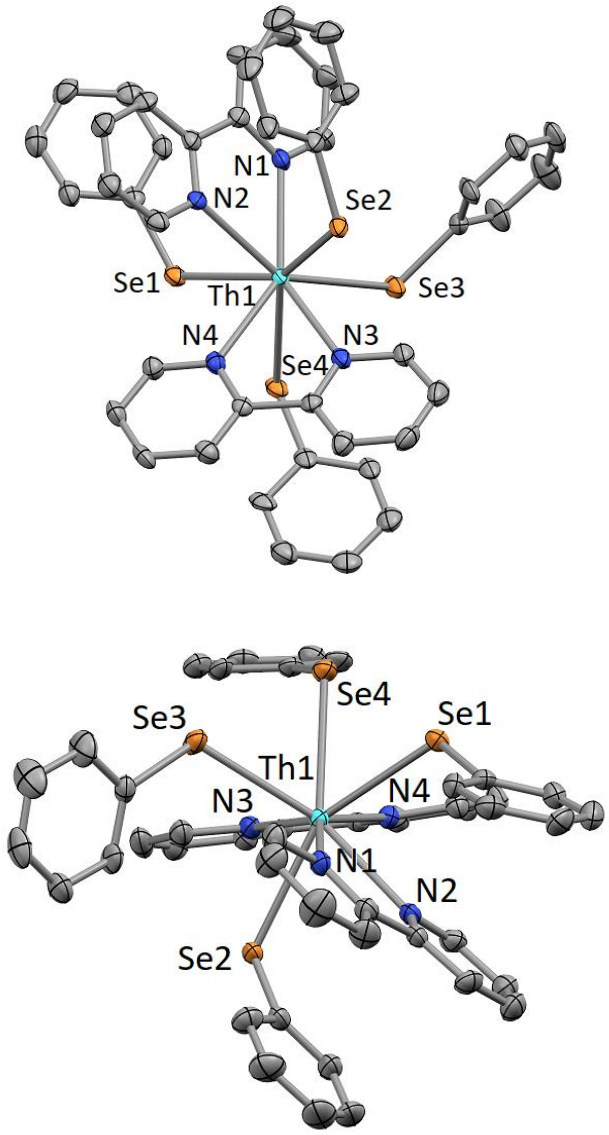

Fig. 11: Thermal ellipsoid diagram of $(bipy)_2Th(SePh)_4$, **6**, with the H atoms removed for clarity and ellipsoids at the 50% probability level. (TOP) View showing distorted square antiprismic coordination; (BOTTOM) view showing distorted bicapped trigonal prismic coordination with different connectivity than in **5**; The distortion and connectivity in **6** allow π···π interactions between the aromatic bipy and SePh groups comprising the trigonal faces, namely, N3, N4, and Se4 (below the viewing plane), and N1, N2, and Se2 (above the viewing plane); capping ligands are the SePh with Se3 and Se1, with the latter SePh rotated to provide additional π···π interaction to bipy containing N1 and N2.

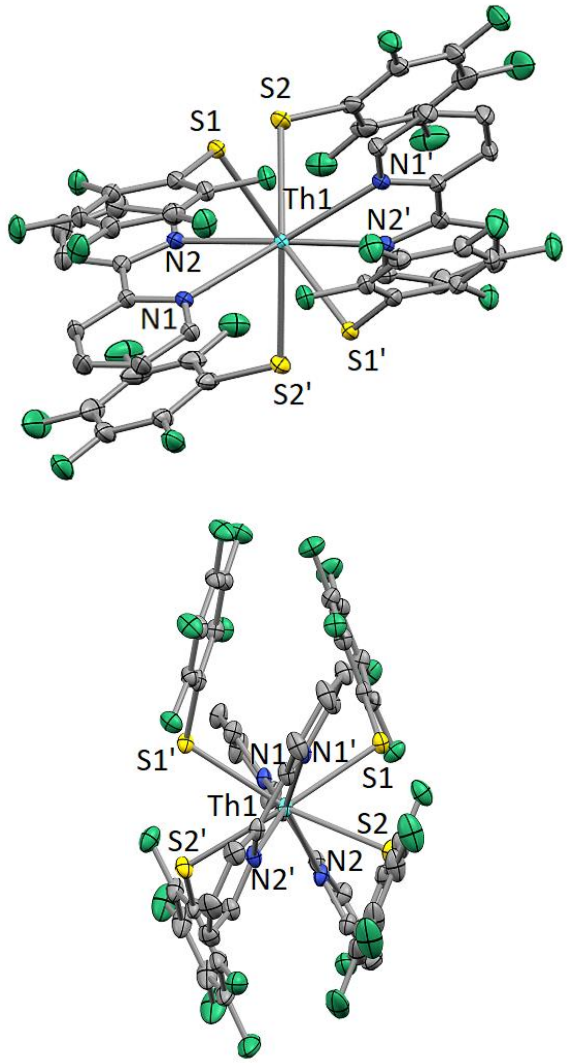

Fig. 12: Thermal ellipsoid diagram of $(py)_3Th(SC_6F_5)_4$, **7**, with the H atoms removed for clarity and ellipsoids at the 50% probability level. Symmetry transformation *-x, y, 1/2-z* used to generate equivalent atoms (primed labels). (TOP) View showing distorted square antiprismic coordination; (BOTTOM) view showing nearly regular bicapped trigonal prismic coordination with more symmetrical connectivity than in **1** due to the crystallographic C_2 site symmetry. The π···π interactions are between the aromatic bipy and SC_6F_5 groups comprising each trigonal face, namely, N1, N2, and S1 (below the viewing plane), or N1', N2', and S1' (above the viewing plane); capping ligands are the SC_6F_5 with S2 and S2', and their aromatic rings are considerably rotated with respect to analogous Ph rings in **5** to yield the maximum number of intramolecular π···π interactions for **7** and **8**.

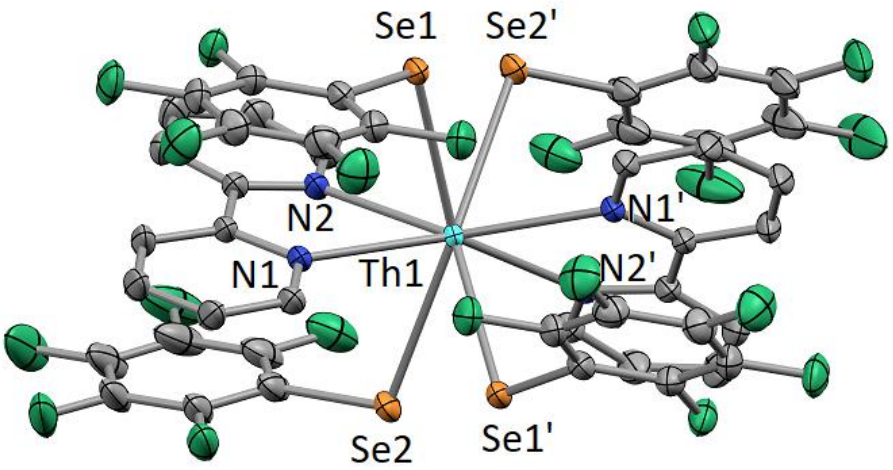

Fig. 13. Thermal ellipsoid diagram of $(py)_4Th(SeC_6F_5)_4$, **8**, with the H atoms removed for clarity and ellipsoids at the 50% probability level. Compound **8** is isomorphous to **7**, with very similar coordination angles, e.g., Se-Th-Se and Se-Th-N, and intramolecular π···π interaction geometries, despite the 0.15 A longer Th-Se bond *versus* Th-S bond, on average.

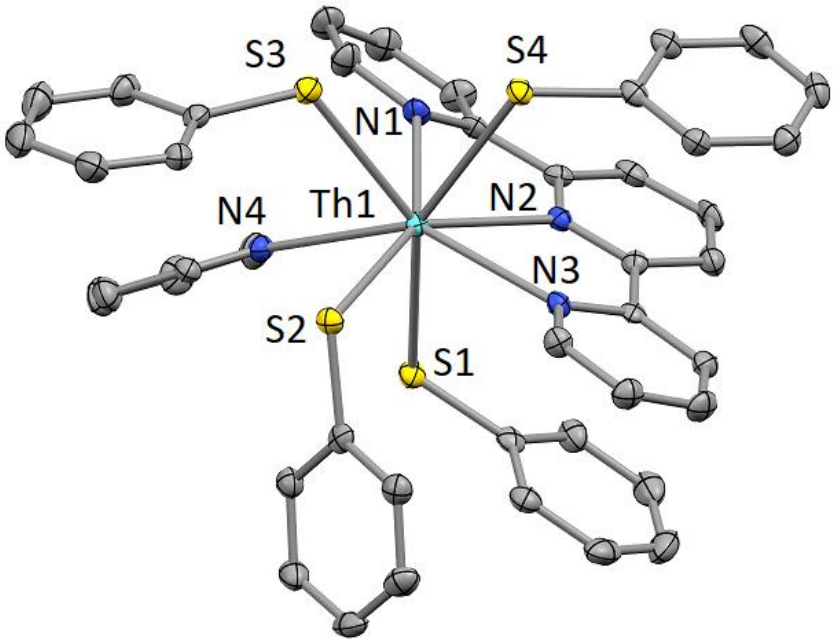

Fig. 14. Thermal ellipsoid diagram of (py)(terpy)Th(SPh_2)$_4$, **9**, with the H atoms removed for clarity and ellipsoids at the 50% probability level. With two narrow adjacent N-Th-N angles, a distorted square antiprism description for **9** appears to be better suited than a bicapped trigonal prism one. Only two intramolecular π…π interactions are found in **9**, involving both sides of the terpy ligand and thiolates with S1 and S4, unlike **5**-**8**, are located on only one side of the molecule. The rotationally flexible thiolate ligands with S2 and S3 and the py ligand are all available for intermolecular π…π interactions, but only the py ligand appears to have a π···π interaction, and only with a py of solvation (see text).

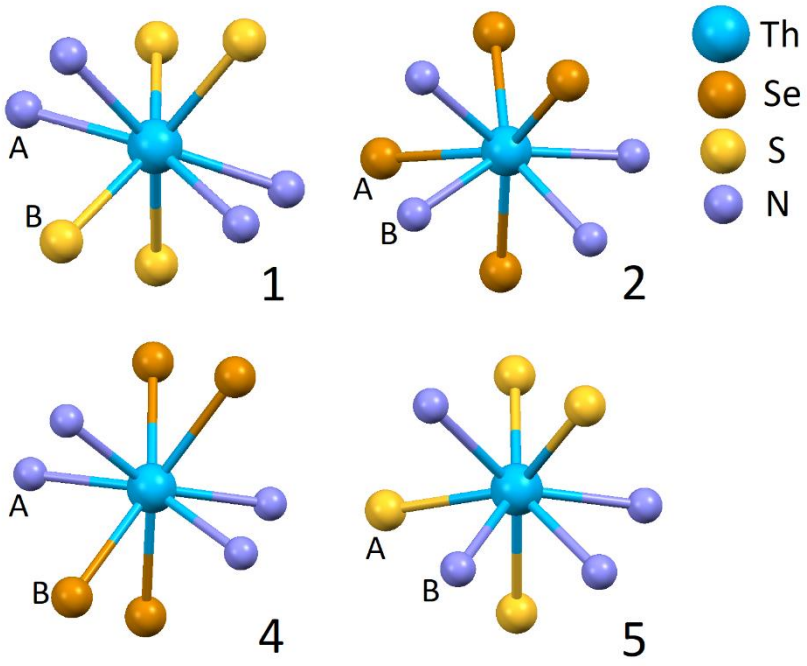

Fig. 15. Ball and stick diagrams of the atoms in the coordination sphere of the title compounds. Compound **7** (not shown) is the S-containing isomorphous analog of **8**. The coordination motifs are very similar in that six of the eight E or N relative positions are essentially the same and the other two, labeled A and B here, are switched in **2** and **5**, with respect to **5** and **8**. This switching has significant consequences for the intra- and inter-molecular interactions of the aromatic ring portions of the ligands (see text).

As shown in Fig. 15, the primary ThE_4N_4 coordination spheres in **5 - 9** can be viewed as having distorted square antiprism (SAP) symmetry.[208] However, based upon the ligand-Th-ligand bond angles (Tab. S4, S11, S18, S25, and S32 for **5** – **9**, respectively), a bicapped trigonal prism (BTP) coordination, with capping N atoms – one from each bipy, is a more accurate description. The coordination scheme for $(bipy)_2Th(SPh)_4$, $(bipy)_2Th(SC_6F_5)_4$, and $(bipy)_2Th(SeC_6F_5)_4$ is described by Kepert[206] as the *trans* configuration for two bidentate and four unidentate ligands, and contrasts the *cis* configuration of two bidentate ligands demonstrated by $(bipy)_2Th(SePh)_4$, and possibly $(py)(terpy)Th(SPh)_4$, if, for the sake of analysis, one considers N(2) and N(3) to belong to one bidentate ligand and N(1) and N(4) to belong to the other (see Fig. 14). For $(bipy)_2Th(SC_6F_5)_4$, as in Fig. 12 (top), and $(bipy)_2Th(SeC_6F_5)_4$, as in and Fig. 13, all ER are positioned to provide two instances of double π···π (e.g., ER…bipy…ER) stacking within a single molecule. However, for $(bipy)_2Th(SPh)_4$, and $(bipy)_2Th(SePh)_4$, with a comparatively smaller and more electropositive ER ligand, the double π···π stacking motif, which may exist in solution, certainly is not observed in the solid state. For a fuller comparison of π···π interaction geometries, Table 6 includes the Th angles to the centroids of the neutral ligands as well as the coordination bond angles.

Table 6 Selected Inter-atomic and Inter-ligand geometries for **5-9.**

Length, Angle, or Torsion[a]	$(bipy)_2Th(SPh)_4$ E = S, R = Ph	$(bipy)_2Th(SePh)_4 \cdot py$ E = Se, R = Ph	$(bipy)_2Th(SC_6F_5)_4 \cdot 2THF$[h] E = S, R = C_6F_5	$(bipy)_2Th(SeC_6F_5)_4 \cdot 2THF$[i] E = Se, R = C_6F_5	$(py)(terpy)Th(SPh)_4 \cdot 2py$ E = S, R = Ph
Th-N (Å)	2.606-2.691	2.620-2.653	2.628-2.631	2.613-2.618	2.598-2.734
Th-E (Å)	2.826- 2.867	2.954-3.015	2.843-2.873	2.970-3.016	2.828-2.848
E'-Th-E (°)	83.9-85.0, 89.2-120.4, 142.4-144.2	65.6-67.8, 98.0-105.5, 143.8-149.1	67.7-67.7, 114.9-128.8, 147.6-147.6	65.0-65.0, 117.7-130.8, 148.6-148.6	67.9-78.2, 91.4-105.6, 143.3-148.2
E-Th-N (°)[b]	10, 63.0 – 87.5	10, 64.7 – 84.9	12, 74.1 – 82.5	12, 74.1 – 82.8	10, 64.4 – 84.9
N'-Th-N (°)[c]	60.9 – 61.7, 106.2 – 108.8	61.4 – 61.8, 83.7	62.4 – 62.4, 115.5	62.7 – 62.7, 113.8	62.4 – 72.5, 62.8

Th-E-C1-C2 (°)[d]	63.0 – 70.0 63.6 – 70.2 77.9 – 86.2 76.5 – 82.2	67.4 81.7 28.9 78.7	84.6 82.5 84.6 82.5	83.2 83.8 83.2 83.8	77.9 76.2 84.1 88.7
twist (°)[e]	40.3, 38.8, 40.7, 41.3	48.8	60.3	57.0	53.0
Th…com (Å)	3.44 – 3.45	3.16, 3.18	3.42, 3.42	3.41, 3.41	3.40, 3.32
com-Th-com (°)	164.5, 164.2, 163.1 164.3	133.2	170.0	170.2	120.0
#, C-H…E (Å)[f]	9-10, 2.70-3.00	6, 2.74 – 2.91	4, 2.77 – 2.78	4, 2.87 – 2.92	8, 2.74 – 2.99
#, C-H…F, N(py) (Å)	n/a	n/a	12, 2.40 – 2.61	12, 2.32 – 2.60	n/a

#, C'…C intra (Å)[g]	4, 3.30 – 3.44	3, 3.09 – 3.28	2, 3.12 – 3.14	2, 3.16 – 3.17	4, 3.11 – 3.26
#, C'…C inter (Å)	8, 3.13 – 3.32	1, 3.37	3.34	3.40	n/a
#, π dihedral intra (°)	4, 1.2 – 3.2	3, 7.6 – 27.1	2, 15.0 – 15.1	2, 7.2 – 8.9	4, 8.2 – 19.5
#, π dihedral inter (°)	8, 11.6 – 26.6	1, 25.7	0.00	0.00	n/a

[a] The ESD values for Th-E related bonds, angles, and torsions are approximately 0.001 Å, 0.02 °, and 0.05 °, respectively.

[b] The number () and values of E-Th-N angles reported here are only for the acute angles.

[c] The first two N-Th-N values are for N atoms in the same bipy ligand; the third is the smallest angle using one N atom from either bipy.

[d] For Th-E-C-C', the atom labeled C' is the closer to Th of the 2- or 6-position atom on the ring; absolute values are listed, and for each E in order of label.

[e] The "twist" is the interplanar dihedral for the mean planes of the bipy ligands. Pseudo-atom center of mass "com" is the centroid of the bipy (for **5**, the centroid of the N3 and N2 rings and the centroid of the N1 and N4 rings were used).

[f] The number per molecule and range of H…E distances for intra-and inter-molecular H-bonding are for distances less than the

corresponding van der Waals radii sum.[21]

[g] The "C···C" distance is the shortest interatomic distance between pairs of 6-membered rings having a π···π interaction, and the "π,π dihedral" is the angle between those two rings.

[h] Compound made by Wen Wu.

[I] Compound made by Matthew Stuber.

The Th-Se, Th-S, and Th-N bond geometries in **5** - **9** are consistent with prior literature,[137] and are summarized in Table 6. The twist (dihedral) angle between the pair of mean bipy planes, the distance and angles from Th to the bipy center-of-mass, and the acute E-Th-N angles are also in Table 6. Because of the geometry of pairs of ligands in an 8-coordinate environment for **5** - **9**, the E'-Th-E bond angles in Table 6 may be grouped into 3 ranges, namely *cis* at 66 – 85 ° (e.g., acute angles), *meta* at 90 – 131 °, and nearly *trans* at 142 -149 °. None of the conformations of **5 – 9** include truly *trans* (e.g., E'-Th-E of 180 °), and, further, all of the molecules have a substantial molecular dipole.

By examination of Fig. 10 – 14, it is apparent that the torsion angles about the Th-E and E-C bonds are good measures of any conformational flexibility of ER ligands and the steric effects of nearest neighbor organic ligands. Interestingly, the Th-E-C-C' torsion angles have a narrow range, 82 – 85 ° for $(bipy)_2Th(SC_6F_5)_4$, and $(bipy)_2Th(SeC_6F_5)_4$, (Table 6), which may be due to a lower influence of packing interactions for their larger F-containing rings versus the smaller Ph rings of $(bipy)_2Th(SPh)_4$, and $(bipy)_2Th(SePh)_4$. The number and ranges for the weak intramolecular H bonding between the aromatic C-H donors and S or Se acceptors given in Table 6 indicate that more of these interactions are possible in the more "open" structures of **5** and **9** compared to the more compact structures of **7** and **8**. Compound **6**, with positions of one selenolate and one bipy switched with respect to those in **5** and **7**, has an intermediate number of H bonding interactions. With respect to close H···F contacts,[209] the values in Table 6 for **7** and **8** include one intra- and 2 inter-molecular H···F per EC_6F_5 for a total of 12 H···F per molecule. Because the E atoms are buried

near the core of the molecule, there are no intermolecular H-bonding interactions to S or Se in **5 – 9**. Also, it is clear that there is little or no charge residing on the bipy ligands, as evidenced by the central C-C bond lengths here that range from 1.46 to 1.50 Å, an observation which is consistent with the descriptions of neutral bipy ligands[113,150,154,166,174,178,180] of actinide compounds. The unit cell packing in each crystal structure of **5 – 9** is comprised of 2-dimensional sheets containing closely associated molecules but separated by more remote intermolecular H···H contacts of likely dispersive interactions. Non-typically and perhaps because of its larger terpy ligand, the intermolecular interactions in **5** more closely approximate H(Ar)···Ar type of crystal packing interaction.[210–212] Supplementary Fig.S22 – S26[213] show edge-on views of these 2-D sheets in the unit cell packing diagrams of **5 – 9**, respectively. The combination of the *trans* or near *trans* pair[214] of bipy ligands in **5 – 8** and the apparent requirement of bidirectional π···π interactions, likely creates the observed 2D sheet motif in all of these structures.

Solution structure. ^{77}Se NMR data for **6** and **8** provide information about the solution structure of these molecules, much as this technique has been informative for establishing the solution structure of related thorium selenolates and selenido cluster compounds. The SePh and SeC_6F_5 compounds **6** and **8** have ^{77}Se NMR resonances with chemical shifts that indicate their eight coordinate solid-state structures are maintained in solution. Shifts for the SePh compound cannot be compared directly with the related pyridine derivative because the latter crystallized with three coordinated pyridines and had a ^{77}Se resonance at 659 ppm[41] while **6** is eight coordinate with four neutral nitrogen donors. Given this experimental value and DFT calculations of the ^{77}Se NMR chemical

shifts for a hypothetical $(py)_4Th(SePh)_4$ (calculated 565 ppm)[144] and $(py)_3Th(SePh)_4$ (calculated 644 ppm[144] and experimental 659 ppm[41]), it is reasonable to conclude that the 586 ppm resonance found for $(bipy)_2Th(SePh)_4$ (**6**) is consistent with a solution structure in which all four nitrogen donors remain coordinated, and no additional pyridine is present in the primary coordination sphere.

The fluorinated selenolate compounds behave similarly. In this case, both $(py)_4Th(SeC_6F_5)_4$ (experimental 400 ppm)[41] and $(bipy)_2Th(SeC_6F_5)_4$ (**8**) (361 ppm) have ^{77}Se resonances in the range expected for eight coordinate structures, consistent with DFT calculations for $(py)_4Th(SeC_6F_5)_4$ (402 ppm),[144] and in contrast with calculations that predict a significantly upfield shifted resonance for the hypothetical seven coordinate $(py)_3Th(SeC_6F_5)_4$ (490 ppm).[41]

Unfortunately, thiolates do not have an equally informative sulfur isotope with which to probe solution conformation. Still, from ^1H NMR data it appears that complex **5** retains some form of asymmetry in solution, as judged by the inequivalence of the bipy and SPh resonances that are split into 8 and 6 distinct peaks respectively, with all resonances broadening and coalescing at elevated temperatures. A rigid eight coordinate Th coordination sphere was also noted in cubane clusters,[41,144] where exchange between bridging and terminal selenolate ligands was slow on the NMR timescale.

Conclusions

Bipyridine forms bis-chelate compounds with thorium chalcogenolates. Upon isolation, lattice solvent dissociates to leave thermally stable compounds. These compounds are all colored, most likely due to ligand to ligand (ER to bipy) charge

transfer, consistent with intermolecular π···π stacking. All bipyridine complexes adopt similar eight coordinate structures, and both fluorinated compounds here exhibit π-π stacking interactions and no dative Th-F bonds. The single terpy product (terpy)(py)Th(EPh)$_4$ similarly forms an eight-coordinate product with one py and one terpy coordinating to the Th(IV) center with the four N atoms positioned similar to those of the two bipy ligands in the other four compounds. From the ^{77}Se NMR chemical shifts it is clear that the eight coordinate structures of the Th(ER)$_4$ derivatives are maintained in solution.

Chapter 3

Actinide Mercury Heterometallic Clusters: Literature Comparison and Differentiation

Introduction

The growing demand for interesting physical and chemical properties can be satiated with heterometallic compounds. The synergistic effects of each metal and possible tunability in applications like nanomaterials provides a wide range of chemical compositions, and geometries. From a fundamental viewpoint the small difference in covalency between 4f and 5f metals may help improve the separation of fission products.[215–217] From a practical standpoint solid state heterometallics can be applied to hydrogen storage,[218–220] superconductivity[221–223], explosives detection,[224,225] catalysis,[226,227] corrosion resistance,[228,229] ferromagnetism,[230] electrocatalytic activity,[231] and CO_2 uptake[232] just to name a few. Furthermore, recent developments of nanocrystalline metals show some of the most wear resistant materials made to date are heterometallic.[233] Historically, heterometallics have played a large part in everyday life being an invaluable part of almost every industry including arms, transportation, medicine and even consumer goods like décor and utensils.

In comparison to their main group counterparts, An-M bonds are incredibly rare[234–236] despite being first discovered thirty years ago.[237] Much like the rest of the actinide literature, actinide heterometallics are plagued by limited synthetic routes. Salt metathesis and elimination reactions are favored with only a small group of examples reported.[238–243] Laying the fundamental groundwork by understanding the nature of f orbital bonds with respect to coordination number and oxidation states will allow for the evolution and wider application of the field.[244] Many examples exist in aqueous conditions such as $[NaU(Mo_6P_4O_{31}H_7)_2]\cdot 5Na\cdot (H2O)_n$ in which $\{Mo_6P_4\}$ clusters are linked into one-dimensional chains with alternating Na^+ and U^{4+} cations,[245]

$Na_2U_2M(C_2O_4)_6(H_2O)_4$ (M = Mn^{2+}, Fe^{2+}, Co^{2+}, and Zn^{2+}) series of isostructural materials that consist of UO_{10} and MO_6 polyhedra bridged by oxalate groups,[246] and $[Th_2Al_6(OH)_{14}(H_2O)_{12}(hedta)_2](NO_3)_6(H_2O)_{12}$ (hedta = hydroxyethylenediaminetriacetic acid) and $[Th_2Al_8(OH)_{12}(H_2O)_{10}(hdpta)_4](H_2O)_{21}$ (hdpta = hydroxyl-1,3-diaminopropane, N,N,N′,N′-tetraacetic acid). Each complex showing its unique structure, magnetic properties in the case of the UM series, and the thermal degradation in the case of the Th Al complexes shows the vast range of heterometallic possibilities. Unlike their traditional actinide complexes that require air and water free conditions, these compounds allow for more practical uses.

Mercury's unique features and applications make it an ideal ligand for actinide compounds. Being the only metallic compound to form a liquid under standard temperature and pressure, mercury has a unique ability to incorporate into a cluster forming both M and E or ligand bonds, stabilize a cluster as an anion, or stay on the peripheral as a terminal ligand. Compounds like $Hg(EPh)_2$ (E = Se, Te; Ph = phenyl) are efficient sources for the synthesis of more complex clusters.[247–250] When acting as a catalyst, this same moiety is present before Th displaces the Hg. However, when there is enough excess Hg it can be incorporated in the cluster.

The following chapter explores heterometallic mercury-actinide chemistry. Combinations of E′/EPh ligands (E′ = S, Se; E =Se) with both thorium and uranium have been synthesized $(py)_8Th_4[Hg(SePh)_2]_4(\mu_3\text{-}Se)_4(\mu_2\text{-}SePh)_4(\eta\text{-}SePh)_4$ (**10**), $(py)_8Th_4[Hg(SePh)_2]_4(\mu_3\text{-}S)_4(\mu_2\text{-}SePh)_4(\eta\text{-}SePh)_4$ (**11**), $(py)_8U_4[Hg(SePh)_2]_4(\mu_3\text{-}Se)_4(\mu_2\text{-}SePh)_4(\eta\text{-}SePh)_4$ (**12**), $(py)_8U_4[Hg(SePh)_2]_4(\mu_3\text{-}S)_4(\mu_2\text{-}SePh)_4(\eta\text{-}SePh)_4$ (**13**). Though these compounds have not been fully characterized due to problems with complete occupancy

of the Hg moiety, they serve as an interesting addition to the compounds already known in literature. Additionally, three cation/anion pairs have been synthesized $[ThF_2bipy_2py_3][Ag_4SePh_6]$ (**14**), and $[Th_8S_{13}I_4py_{18}][HgI_4]$ (**15**), $[U_8S_{13}I_3py_{17}][HgI_4][HgI_3py]$ (**16**). These compounds exhibit mercury's ability to effective hold charge as a counter ion instead of incorporating them into the internal structure or core.

Discussion

Mercury inserts into the PhE-EPh (E = S, Se) bond which catalyzes the reductive cleavage the E-E bond by Th metal through transmetalation. In the case of Th/Hg cubanes **10-13** Hg is not just a catalyst but also serves as a terminal ligand. This one pot synthesis is an attractive synthetic approach due to the minimal reagents and steps, the ease of isolation of a single product, and the utility of the heterometallic products for potential solid-state applications. One draw-back is that higher occupancy of the Hg moiety is correlated to the use excess Hg in the reaction mechanism, however these products can be isolated albeit sacrificing yield with as little as 0.300 mmol of Hg (Scheme 9). Attempts of cubanes with SPh as the terminal ligand were unsuccessful regardless of Hg ratio and resulted in (**1)** for Th and no significant product for U.

$$4An + 8(SePh)_2 \xrightarrow[py]{\substack{1.XHg \\ 2.1E}} (py)_8Th_4Hg_4E_4(\mu_2\text{-}SePh)_4(SePh)_4 + 4(SePh)_2$$

An = U, Th
X = 0.30, 1.0 or 2.0
E = S, Se

Scheme 9: Synthesis of actinide mercury cubanes **10-13**

Compounds **10−13** were characterized by spectroscopic methods and by low-temperature single-crystal X-ray diffraction, with POVRAY diagrams for **10−13** given in Figures 10−13, respectively. Unlike both the $Th_4(\mu_3\text{-}E)_4(\mu_2\text{-}EPh)_4(\eta\text{-}E'C_6F_5)_4$[41] cubanes that crystallize only in the tetragonal I4- cell, compounds **10−13** crystallize in multiple space groups like compounds **1−4**. Average An-N bond lengths of 2.60 are only slightly smaller than the 2.67 reported for compounds **1-9**. The Th-μ_3Se bonds, 2.94 Å, and the Th-μ_2SePh bonds, 3.12 Å, are similar to the previously reported cubanes, while the Th-μ_3S bonds, 2.80 Å, are an exact match. For the Hg-SePh bonds, regardless of An identity, the bond lengths are similar. The bridging moieties are a bit longer for the U cubanes most likely indicating differences in electronic density, since size difference should be negligible. Additionally, for each Hg moiety that has two bridging SePh groups, one is slightly longer than the other in both the Th and U derivatives. Overall the bond lengths of each cubane are more similar to the cubane containing the same An than that containing the same chalcogenido core. The most significant difference in that in the Th cubanes two $Hg(SePh)_2$ terminal ligands have one bridging Se bond while the other two have two bridging Se bonds, but in the U cubanes all $Hg(SePh)_2$ terminal ligands have two bridging Se bonds. All bond lengths can be seen in Table 7.

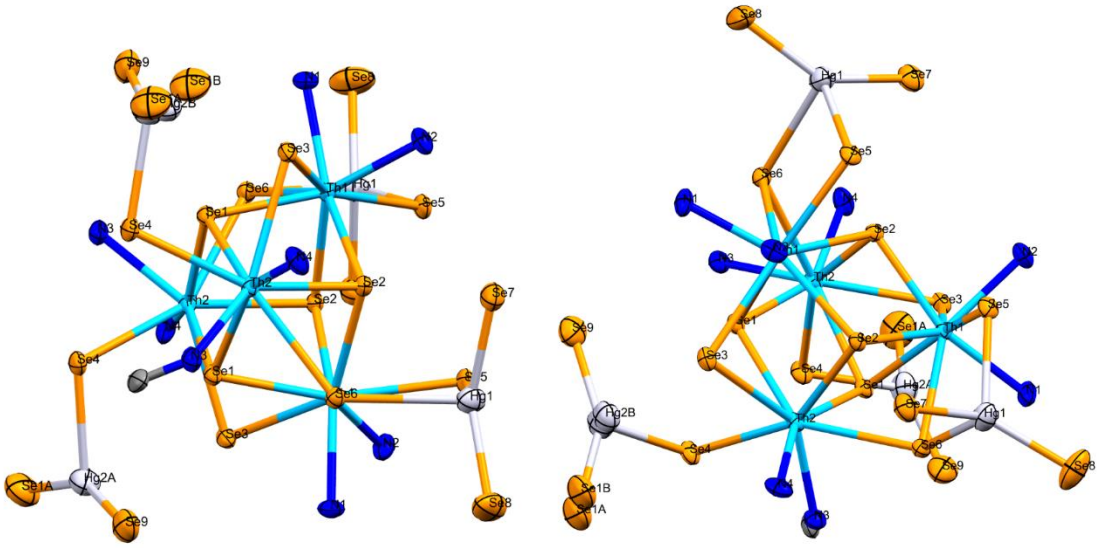

Figure 10. Thermal ellipsoid diagram of $(py)_8Th_4[Hg(SePh)_2]_4(\mu_3\text{-}Se)_4(\mu_2\text{-}SePh)_4(\eta\text{-}SePh)_4 \cdot 6Py$ (**10**) with the H and C atoms removed for clarity and ellipsoids at the 50% probability level. Significant bond-length averages are given in Table 7.

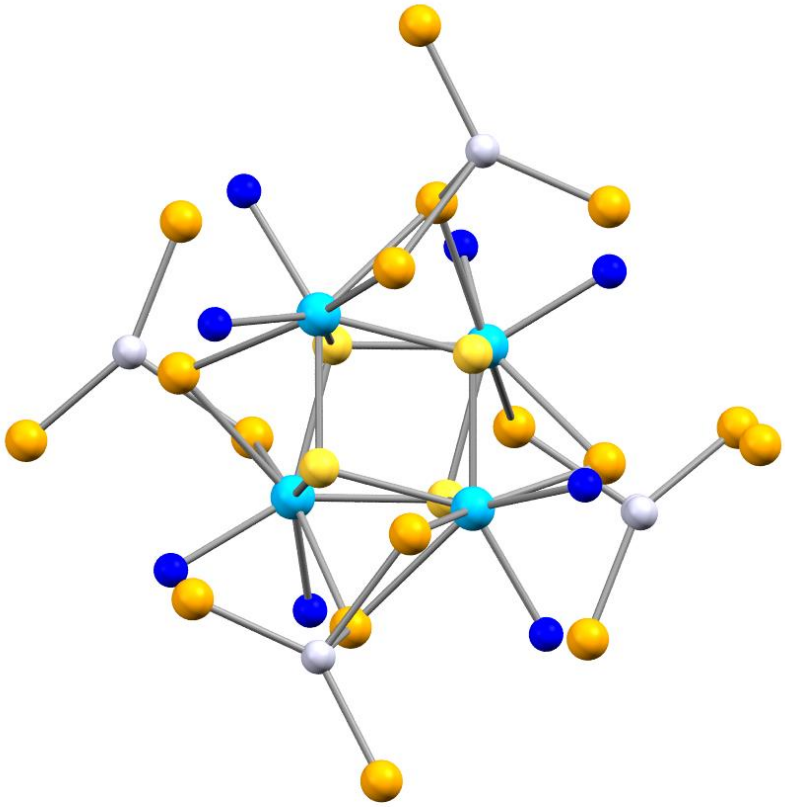

Figure 11. Thermal ellipsoid diagram of $(py)_8Th_4[Hg(SePh)_2]_4(\mu_3\text{-}S)_4(\mu_2\text{-}SePh)_4(\eta\text{-}SePh)_4 \cdot 6Py$ (**11**) with the H and C atoms removed for clarity and ellipsoids at the 50% probability level. Significant bond-length averages are given in Table 7.

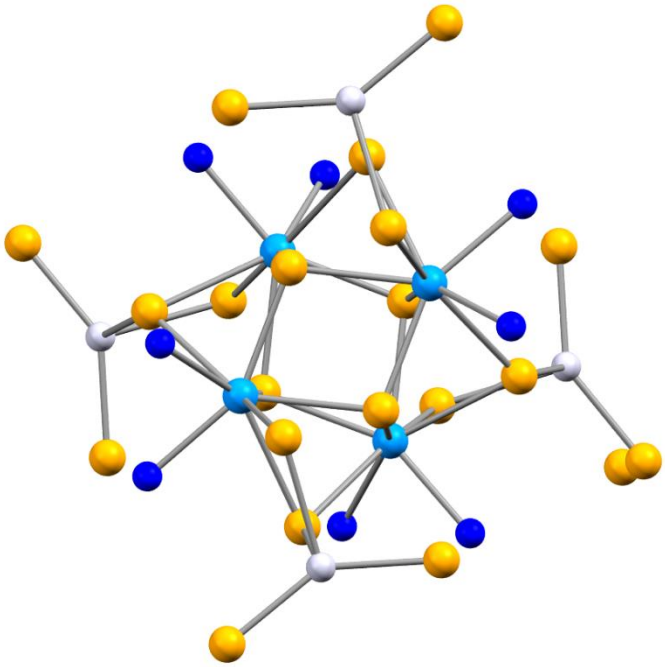

Figure 12. Thermal ellipsoid diagram of $(py)_8U_4[Hg(SePh)_2]_4(\mu_3\text{-}Se)_4(\mu_2\text{-}SePh)_4(\eta\text{-}SePh)_4 \cdot 6Py$ (**12**) with the H and C atoms removed for clarity and ellipsoids at the 50% probability level. Significant bond-length averages are given in Table 7.

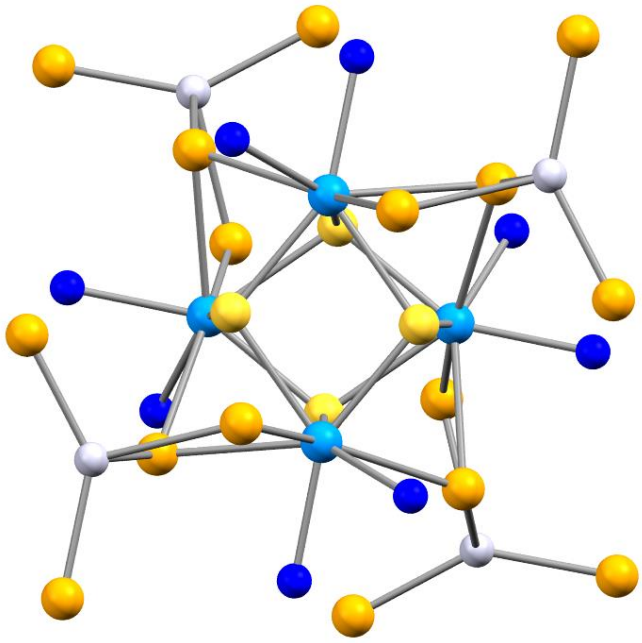

Figure 13. Thermal ellipsoid diagram of $(py)_8U_4[Hg(SePh)_2]_4(\mu_3\text{-}S)_4(\mu_2\text{-}SePh)_4(\eta\text{-}SePh)_4 \cdot 6Py$ (**13**) with the H and C atoms removed for clarity and ellipsoids at the 50% probability level. Significant bond-length averages are given in Table 7.

Table 7: Averages and ranges of selected bond distances (Å) of **10-13.**

	10	**11**	**12**	**13**
An-N	2.62 (2.60-2.64)	2.61 (2.59-2.64)	2.58 (2.55-2.61)	2.55 (2.51-2.60)
An-E	2.92 (2.89-2.98)	2.80 (2.77-2.86)	2.88 (2.83-2.93)	2.73 (2.69-2.80)
An-EPh bridging	3.12 (3.03-3.17)	3.10 (3.04-3.14)	3.06 (2.98-3.11)	3.04 (2.99-3.08)
Hg-EPh terminal	2.50 (2.47-2.51)	2.50 (2.49-2.51)	2.53 (2.50-2.58)	2.50 (2.48-2.52)
Hg-EPh bridging	2.87 (2.73-3.06)	2.85 (2.69-3.05)	2.99 (2.82-3.17)	2.97 (2.79-3.17)

In addition to the Hg cubanes a series of An cation anion compounds $[ThF_2bipy_2py_3][Ag_4SePh_6]$ (**14**), $[Th_8S_{13}I_4py_{18}][HgI_4]$ (**15**), and $[U_8S_{13}I_3py_{17}][HgI_4][HgI_3py]$ (**16**) have been synthesized. Compounds **14−16** were characterized by spectroscopic methods and by low-temperature single-crystal X-ray diffraction, with POVRAY diagrams for **14−16** given in Figures 20−22, respectively. The Th/Ag cation anion (Scheme 10) was attempted with other ER (E= S, Se; R=Ph, C_6F_5) ligands in place of $(SePh)_2$ and with AgCl instead of AgF, but neither yielded crystalline product. Regardless of bipy ratio, 0.50-2.00 mmol, or the identity of the fluorine source, AgF or AgF_2, the same product was formed.

$$1Th + 1.5(SePh)_2 + 0.5(SC_6F_5)_2 + 2Bipy \xrightarrow[Py]{cat\ Hg} 1.5AgF$$

Scheme 10: Synthesis of Th/Ag cation anion pair (**14).**

Compounds **14−16** were characterized by spectroscopic methods and by low-temperature single-crystal X-ray diffraction, with POVRAY diagrams Figures 14−16, respectively. The two An_8 compounds are essentially identical except for the counter ion. All bond lengths can be seen in Table 8. These compounds are most similar to Th_8O_{13}[251] complexes found in literature. The average Th-O distances were 2.48 Å,[50] and thus slightly shorter than the average Th-S bonds, 2.82 Å, in compounds **15-16** which are in range of other An-Se bonds.

$$1An + 1(SePh)_2 + 1(I)_2 + 1Hg \xrightarrow[Py]{cat\ Hg} 1.5S$$

An = Th, U

Scheme 10: Synthesis of An_8/Hg cation-anion pairs (**15-16**).

Figure 14. Thermal ellipsoid diagram $[ThF_2bipy_2py_3][Ag_4SePh_6]$ (**14**), with the H and C atoms removed for clarity and ellipsoids at the 50% probability level. Significant bond-length averages are given in Table 8.

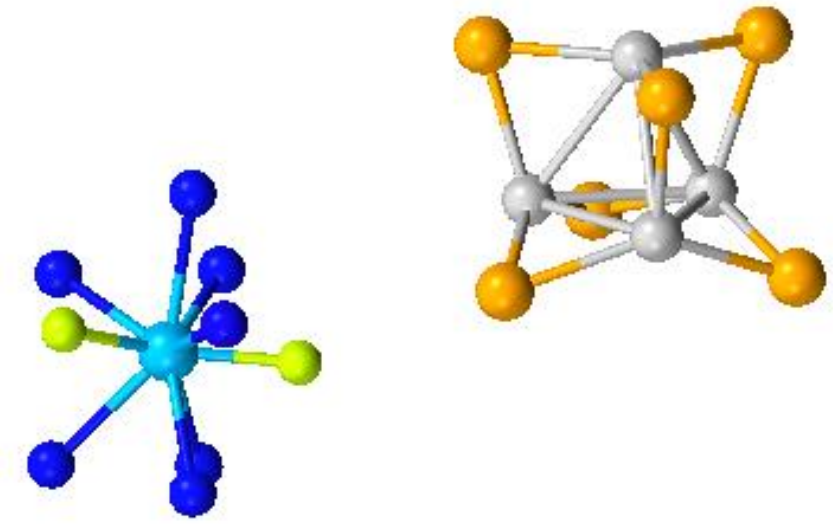

Figure 15. Thermal ellipsoid diagram of $[py_{18}Th_8I_4S_{13}]^{2+}[HgI_4]^{2-} \cdot 12Py$ (**15**) with the H atoms and HgI_4 anion removed for clarity and ellipsoids at the 50% probability level. Significant bond-length averages are given in Table 8.

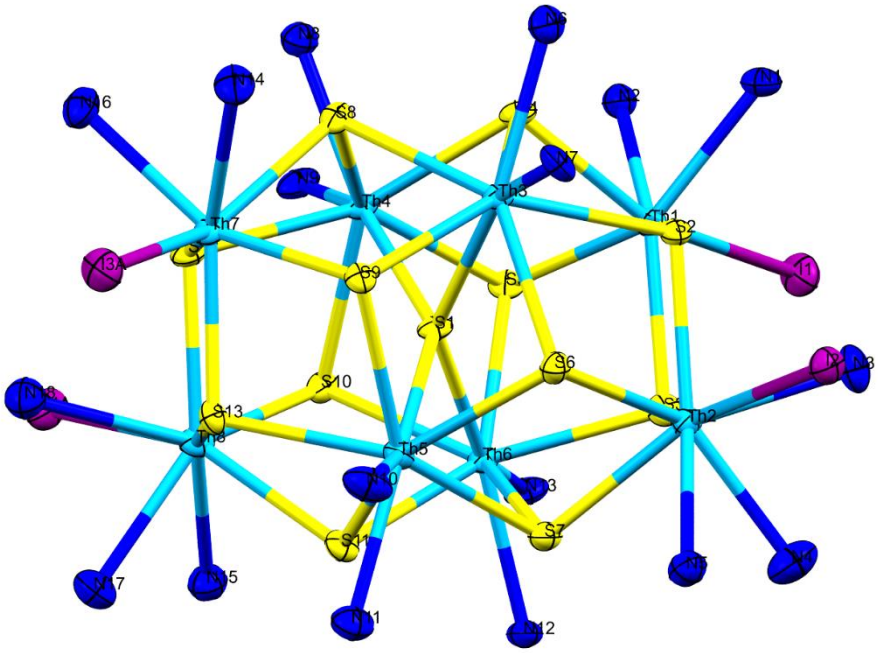

Figure 16. Thermal ellipsoid diagram $[U_8S_{13}I_3py_{17}][HgI_4][HgI_3py]$ (**16**) with the H atoms and HgI_4 anion removed for clarity and ellipsoids at the 50% probability level. Significant bond-length averages are given in Table 8.

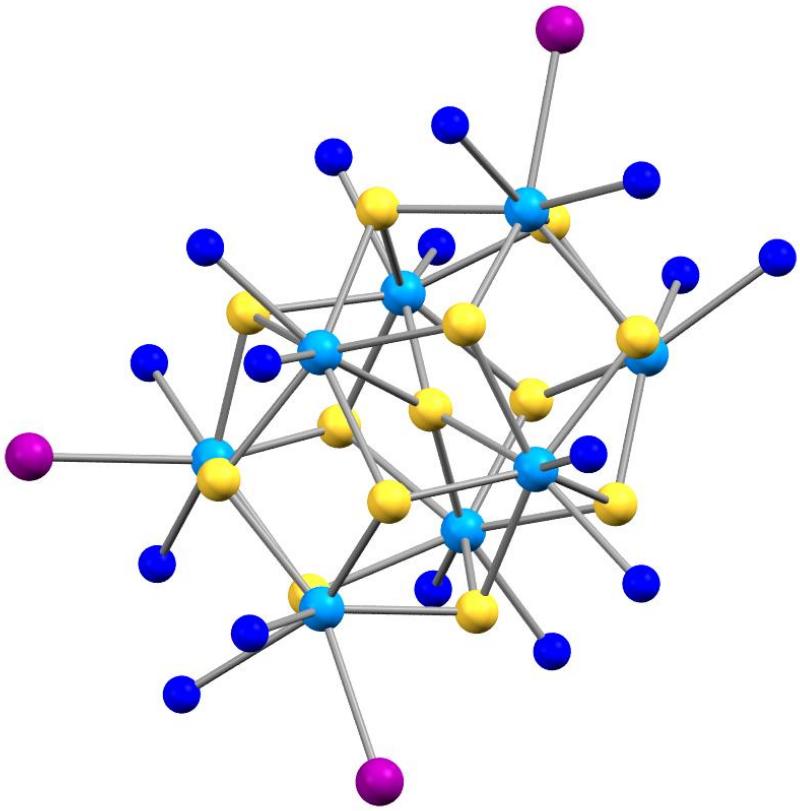

Table 8: Averages and ranges of selected bond distances (Å) of **14-16.**

	14	15	16
Th-N	2.69 (2.63-2.73)	2.73 (2.62-2.90)	2.64 (2.56-2.77)
Th-E		2.82 (2.70-2.96)	2.76 (2.62-3.00)
Th-I		3.23 (3.11-3.36)	3.11 (3.11-3.12)
Th-F	2.14 (2.13-2.15)		

(*) indicates data awaiting final confirmation from single crystal x-ray analysis.

Conclusion

In conclusion a series of heterometallic cubanes were synthesized $(py)_8Th_4[Hg(SePh)_2]_4(\mu_3\text{-}Se)_4(\mu_2\text{-}SePh)_4(\eta\text{-}SePh)_4$ (**10**), $(py)_8Th_4[Hg(SePh)_2]_4(\mu_3\text{-}S)_4(\mu_2\text{-}SePh)_4(\eta\text{-}SePh)_4$ (**11**), $(py)_8U_4[Hg(SePh)_2]_4(\mu_3\text{-}Se)_4(\mu_2\text{-}SePh)_4(\eta\text{-}SePh)_4$ (**12**), $(py)_8U_4[Hg(SePh)_2]_4(\mu_3\text{-}S)_4(\mu_2\text{-}SePh)_4(\eta\text{-}SePh)_4$ (**13**). These novel cubanes mimic those previously reported but incorporate Hg as a terminal moiety. Additionally, three cation/anion pairs were synthesized $[ThF_2bipy_2py_3][Ag_4SePh_6]$ (**14**), $[Th_8S_{13}I_4py_{18}][HgI_4]$ (**15**), and $[U_8S_{13}I_3py_{17}][HgI_4][HgI_3py]$ (**16**). Both An_8 compounds form isostructural cations but are coupled with different anions. The ability of Hg to be both a ligand and anion are demonstrated. Further analysis will prove if they can be used to synthesize heterometallic solid state materials.

References

(1) Liddle, S. T. The Renaissance of Non-Aqueous Uranium Chemistry. *Angew. Chemie Int. Ed.* **2015**, *54* (30), 8604–8641. https://doi.org/10.1002/anie.201412168.

(2) Clark, D. L.; Miller, M. M.; Watkin, J. G. Synthesis, Characterization, and X-Ray Structure of the Uranium Thiolate Complex U(S-2,6-Me2C6H3)[N(SiMe3)2]3. *Inorg. Chem.* **1993**, *32* (5), 772–774. https://doi.org/10.1021/ic00057a044.

(3) Domingos, Â.; de Matos, A. P.; Santos, I. Synthesis and Characterization of the Uranium Alkylthiolate Complex U(SPri)2(HBPz3)2. *Polyhedron* **1992**, *11* (13), 1601–1606. https://doi.org/10.1016/S0277-5387(00)83713-4.

(4) Jones, R. G.; Karmas, G.; Martin, G. A.; Gilman, H. Organic Compounds of Uranium. II. Uranium(IV) Amides, Alkoxides and Mercaptides. *J. Am. Chem. Soc.* **1956**, *78* (17), 4285–4286. https://doi.org/10.1021/ja01598a026.

(5) Lescop, C.; Arliguie, T.; Lance, M.; Nierlich, M.; Ephritikhine, M. Bispentamethylcyclopentadienyl Uranium(IV) Thiolate Compounds. Synthesis and Reactions with CO2 and CS2. *J. Organomet. Chem.* **1999**, *580* (1), 137–144. https://doi.org/10.1016/S0022-328X(98)01139-5.

(6) Leverd, P. C.; Arliguie, T.; Lance, M.; Nierlich, M.; Vigner, J.; Ephritikhine, M. Monocyclooctatetraene Uranium Thiolate Complexes. Crystal Structure of [{U(η-C 8 H 8)(μ-SPr i) 2 } 2]. *J. Chem. Soc., Dalt. Trans.* **1994**, No. 4, 501–504. https://doi.org/10.1039/DT9940000501.

(7) Leverd, P. C.; Lance, M.; Nierlich, M.; Vigner, J.; Ephritikhine, M. Synthesis and Crystal Structure of Homoleptic Uranium Hexathiolates: [NEt 2 H 2] 2 [U(SPh) 6] and [(Ph 3 P)Cu(μ-SPh) 3 -U(μ-SPh) 3 Cu(PPh 3)]. *J. Chem. Soc., Dalt. Trans.* **1994**, No. 24, 3563–3567. https://doi.org/10.1039/DT9940003563.

(8) Leverd, P. C.; Lance, M.; Vigner, J.; Nierlich, M.; Ephritikhine, M. Synthesis and Reactions of Uranium(IV) Tetrathiolate Complexes. *J. Chem. Soc. Dalt. Trans.* **1995**, No. 2, 237. https://doi.org/10.1039/dt9950000237.

(9) Smiles, D. E.; Wu, G.; Hrobárik, P.; Hayton, T. W. Use of 77 Se and 125 Te NMR Spectroscopy to Probe Covalency of the Actinide-Chalcogen Bonding in [Th(E n){N(SiMe 3) 2 } 3] − (E = Se, Te; n = 1, 2) and Their Oxo-Uranium(VI) Congeners. *J. Am. Chem. Soc.* **2016**, *138* (3), 814–825. https://doi.org/10.1021/jacs.5b07767.

(10) Mora, E.; Maria, L.; Biswas, B.; Camp, C.; Santos, I. C.; Pécaut, J.; Cruz, A.; Carretas, J. M.; Marçalo, J.; Mazzanti, M. Diamine Bis(Phenolate) as Supporting Ligands in Organoactinide(IV) Chemistry. Synthesis, Structural Characterization, and Reactivity of Stable Dialkyl Derivatives. *Organometallics* **2013**, *32* (5), 1409–1422. https://doi.org/10.1021/om3010806.

(11) Franke, S. M.; Heinemann, F. W.; Meyer, K. Reactivity of Uranium(<scp>iv</Scp>) Bridged Chalcogenido Complexes U^{IV}–E–U^{IV} (E = S, Se) with

Elemental Sulfur and Selenium: Synthesis of Polychalcogenido-Bridged Uranium Complexes. *Chem. Sci.* **2014**, *5* (3), 942–950. https://doi.org/10.1039/C3SC52799A.

(12) Leverd, P. C.; Ephritikhine, M.; Lance, M.; Vigner, J.; Nierlich, M. Triscyclopentadienyl Uranium Thiolates and Selenolates. *J. Organomet. Chem.* **1996**, *507* (1–2), 229–237. https://doi.org/10.1016/0022-328X(95)05773-I.

(13) Levered, P. C.; Lance, M.; Nierlich, M.; Vigner, J.; Ephritikhine, M. Synthesis and Crystal Structure of the Homoleptic Uranium (<scp>IV</Scp>) Thiolates [(Thf) $_3$ Na(μ-SR) $_3$ U(μ-SR) $_3$ NA(Thf) $_3$](Thf = Tetrahydrofuran; R = Bu ^{t} or Ph). *J. Chem. Soc., Dalt. Trans.* **1993**, No. 14, 2251–2254. https://doi.org/10.1039/DT9930002251.

(14) Lin, Z.; Brock, C. P.; Marks, T. J. Synthesis, Structural Characterization, and Properties of the Organothorium Alkylthiolate Complex [(CH3)5C5]2Th(SCH2CH2CH3)2. *Inorganica Chim. Acta* **1988**, *141* (1), 145–149. https://doi.org/10.1016/S0020-1693(00)86388-4.

(15) Rose, D.; Chang, Y.-D.; Chen, Q.; Zubieta, J. Reactions of Uranyl Thiolate Complexes with Molecular Oxygen: Syntheses and Crystal and Molecular Structures of the Uranyl Thiolate Peroxo Species (HNEt3)2[(UO2)2(O2)(SC4N2H3)4] and (HNEt3)[H(UO2)2(O2)(SC4N2H2Me)4].Cntdot.Me2CO.Cntdot.0.5Et3N and of the U. *Inorg. Chem.* **1994**, *33* (23), 5167–5168. https://doi.org/10.1021/ic00101a004.

(16) Rose, D. J.; Chen, Q.; Zubieta, J. Synthesis and Characterization of Uranyl Thiolate Complexes. Crystal and Molecular Structures of [Me4N][UO2(NO3)2(C5H4NS)] and [C16H25N2S2Si2][UO2(NO3)2(C8H12NSSi)]. *Inorganica Chim. Acta* **1998**, *268* (1), 163–167. https://doi.org/10.1016/S0020-1693(97)05732-0.

(17) Tatsumi, K.; Matsubara, I.; Inoue, Y.; Nakamura, A.; Cramer, R. E.; Tagoshi, G. J.; Golen, J. A.; Gilje, J. W. A Homoleptic Uranium Thiolate: Synthesis, Structure, and Fluxional Behavior of [Li(Dme)]4[U(SCH2CH2S)4] and Reaction with Carbon Disulfide. *Inorg. Chem.* **1990**, *29* (24), 4928–4938. https://doi.org/10.1021/ic00349a021.

(18) Ventelon, L.; Lescop, C.; Arliguie, T.; Ephritikhine, M.; Leverd, P. C.; Lance, M.; Nierlich, M. Synthesis and X-Ray Crystal Structure of [Na(18-Crown-6)][U(Cp*)2(SBut)(S)], the First f-Element Compound Containing a Metal–sulfur Double Bond. *Chem. Commun.* **1999**, No. 7, 659–660. https://doi.org/10.1039/a900466a.

(19) Falcone, M.; Chatelain, L.; Mazzanti, M. Nucleophilic Reactivity of a Nitride-Bridged Diuranium(IV) Complex: CO 2 and CS 2 Functionalization. *Angew. Chemie Int. Ed.* **2016**, *55* (12), 4074–4078. https://doi.org/10.1002/anie.201600158.

(20) Cantat, T.; Scott, B. L.; Morris, D. E.; Kiplinger, J. L. What a Difference a 5f Element Makes: Trivalent and Tetravalent Uranium Halide Complexes Supported by One and Two Bis[2-(Diisopropylphosphino)-4-Methylphenyl]Amido (PNP) Ligands. *Inorg. Chem.* **2009**, *48* (5), 2114–2127. https://doi.org/10.1021/ic802061x.

(21) Perry, D. L.; Zalkin, A.; Ruben, H.; Templeton, D. H. Synthesis, Characterization, and Structure of a Uranyl Complex with a Disulfide Ligand, Bis(Di-n-Propylammonium) Disulfidobis(Di-n-Propylthiocarbamato)Dioxouranate(VI). *Inorg. Chem.* **1982**, *21* (1), 237–240. https://doi.org/10.1021/ic00131a044.

(22) Castro-Rodriguez, I.; Meyer, K. Carbon Dioxide Reduction and Carbon Monoxide Activation Employing a Reactive Uranium(III) Complex. *J. Am. Chem. Soc.* **2005**, *127* (32), 11242–11243. https://doi.org/10.1021/ja053497r.

(23) Qiu, J.; Burns, P. C. Clusters of Actinides with Oxide, Peroxide, or Hydroxide Bridges. *Chem. Rev.* **2013**, *113* (2), 1097–1120. https://doi.org/10.1021/cr300159x.

(24) Behrle, A. C.; Barnes, C. L.; Kaltsoyannis, N.; Walensky, J. R. Systematic Investigation of Thorium(IV)– and Uranium(IV)–Ligand Bonding in Dithiophosphonate, Thioselenophosphinate, and Diselenophosphonate Complexes. *Inorg. Chem.* **2013**, *52* (18), 10623–10631. https://doi.org/10.1021/ic401642a.

(25) Smiles, D. E.; Wu, G.; Kaltsoyannis, N.; Hayton, T. W. Thorium–ligand Multiple Bonds via Reductive Deprotection of a Trityl Group. *Chem. Sci.* **2015**, *6* (7), 3891–3899. https://doi.org/10.1039/C5SC01248A.

(26) Gaunt, A. J.; Reilly, S. D.; Enriquez, A. E.; Scott, B. L.; Ibers, J. A.; Sekar, P.; Ingram, K. I. M.; Kaltsoyannis, N.; Neu, M. P. Experimental and Theoretical Comparison of Actinide and Lanthanide Bonding in M[N(EPR 2) 2] 3 Complexes (M = U, Pu, La, Ce; E = S, Se, Te; R = Ph, i Pr, H). *Inorg. Chem.* **2008**, *47* (1), 29–41. https://doi.org/10.1021/ic701618a.

(27) Gaunt, A. J.; Scott, B. L.; Neu, M. P. U(IV) Chalcogenolates Synthesized via Oxidation of Uranium Metal by Dichalcogenides. *Inorg. Chem.* **2006**, *45* (18), 7401–7407. https://doi.org/10.1021/ic060560k.

(28) Fernández-Moreira, V.; Sastre-Martín, H. Photophysical and Bioactivity Behavior of Fac-Rhenium(I) Derivatives Containing Ditopic Sulfurpyridine Ligands. *Inorganica Chim. Acta* **2017**, *460*, 127–133. https://doi.org/10.1016/J.ICA.2016.07.038.

(29) Monti, F.; Baschieri, A.; Gualandi, I.; Serrano-Pérez, J. J.; Junquera-Hernández, J. M.; Tonelli, D.; Mazzanti, A.; Muzzioli, S.; Stagni, S.; Roldan-Carmona, C.; et al. Iridium(III) Complexes with Phenyl-Tetrazoles as Cyclometalating Ligands. *Inorg. Chem.* **2014**, *53* (14), 7709–7721. https://doi.org/10.1021/ic500999k.

(30) Verma, S.; Kar, P.; Das, A.; Ghosh, H. N. Photophysical Properties of Ligand Localized Excited State in Ruthenium(Ii) Polypyridyl Complexes: A Combined Effect of Electron Donor–acceptor Ligand. *Dalt. Trans.* **2011**, *40* (38), 9765. https://doi.org/10.1039/c1dt10266d.

(31) Christopoulos, K.; Karidi, K.; Tsipis, A.; Garoufis, A. Synthesis, Characterization, DNA-Binding Properties and Electronic Structure (DFT) of Ruthenium Oligopyridine Complexes. *Inorg. Chem. Commun.* **2008**, *11* (11), 1341–1346. https://doi.org/10.1016/j.inoche.2008.08.015.

(32) Patel, S.; Li, Y.; Odom, A. L. Synthesis, Structure, and LLCT Transitions in Terminal Hydrazido(2−) Bipyridine Complexes of Titanium. *Inorg. Chem.* **2007**, *46* (16), 6373–6381. https://doi.org/10.1021/ic700426s.

(33) Tzeng, B.-C.; Fu, W.-F.; Che, C.-M.; Chao, H.-Y.; Cheung, K.-K.; Peng, S.-M. Structures and Photoluminescence of Dinuclear Platinum(II) and Palladium(II) Complexes with Bridging Thiolates and 2,2′-Bipyridine or 2,2′:6′,2″-Terpyridine Ligands. *J. Chem. Soc. Dalt. Trans.* **1999**, No. 6, 1017–1024. https://doi.org/10.1039/a809287g.

(34) Noy, A. Z.; Galin, A. M.; Razskazovskii, Y. V.; Mel'nikov, M. Y. Photophysical and Photochemical Properties of Dithiolate-Diimine Zinc Complexes: Complexes with 3,4-Toluenedithiolate Ligand: (Tdt)Zn(Bpy), (Tdt)Zn(Phen), (Tdt)Zn(Biqu). *Proc. Indian Acad. Sci. - Chem. Sci.* **1995**, *107* (6), 789–794. https://doi.org/10.1007/BF02869970.

(35) Arliguie, T.; Lescop, C.; Ventelon, L.; Leverd, P. C.; Thuéry, P.; Nierlich, M.; Ephritikhine, M. C−H and C−S Bond Cleavage in Uranium(III) Thiolato Complexes. *Organometallics* **2001**, *20* (17), 3698–3703. https://doi.org/10.1021/om0102551.

(36) Melman, J. H.; Rohde, C.; Emge, T. J.; Brennan, J. G. Trivalent Lanthanide Compounds with Fluorinated Thiolate Ligands: Ln−F Dative Interactions Vary with Ln and Solvent. *Inorg. Chem.* **2002**, *41* (1), 28–33. https://doi.org/10.1021/ic0104813.

(37) Lee, J.; Freedman, D.; Melman, J. H.; Brewer, M.; Sun, L.; Emge, T. J.; Long, F. H.; Brennan, J. G. TRIVALENT LANTHANIDE CHALCOGENOLATES - LN(SEPH)(3), LN(2)(EPH)(6), LN(4)(SPH)(12), AND [LN(EPH)3](N), (E=S, SE) - HOW METAL, CHALCOGEN, AND SOLVENT INFLUENCE STRUCTURE. *Inorg. Chem.* **1998**, *37*, 2512–2519.

(38) Berardini, M.; Lee, J.; Freedman, D.; Lee, J.; Emge, T. J.; Brennan, J. G. Early- and Late-Lanthanide Pyridinethiolates: Synthesis, Redox Stability, and Structure. *Inorg. Chem.* **1997**, *36* (25), 5772–5776. https://doi.org/10.1021/ic9706865.

(39) Mashima, K.; Nakayama, Y.; Shibahara, T.; Fukumoto, H.; Nakamura, A. Synthesis of Arenethiolate Complexes of Divalent and Trivalent Lanthanides from Metallic Lanthanides and Diaryl Disulfides: Crystal Structures of [{Yb(Hmpa) 3 } 2 (μ-SPh) 3][SPh] and Ln(SPh) 3 (Hmpa) 3 (Ln = Sm, Yb; Hmpa = Hexamethylphosphoric Triamide). *Inorg. Chem.* **1996**, *35* (1), 93–99. https://doi.org/10.1021/ic950050i.

(40) Lee, J.; Brewer, M.; Berardini, M.; Brennan, J. G. Trivalent Lanthanide Chalcogenolates: Synthesis, Structure, and Thermolysis Chemistry. *Inorg. Chem.*

1995, *34* (12), 3215–3219. https://doi.org/10.1021/ic00116a013.

(41) Stuber, M. A.; Kornienko, A. Y.; Emge, T. J.; Brennan, J. G. Tetrametallic Thorium Compounds with Th 4 E 4 (E = S, Se) Cubane Cores. *Inorg. Chem.* **2017**, *56* (17), 10247–10256. https://doi.org/10.1021/acs.inorgchem.7b00950.

(42) Arliguie, T.; Thuéry, P.; Floch, P. Le; Mézailles, N.; Ephritikhine, M. A Homoleptic SPS-Based Complex and a Double-Cubane-Type Sulfur Cluster of an Actinide Element. *Polyhedron* **2009**, *28* (8), 1578–1582. https://doi.org/10.1016/j.poly.2009.03.027.

(43) Arliguie, T.; Blug, M.; Le Floch, P.; Mézailles, N.; Thuéry, P.; Ephritikhine, M. Organouranium Complexes with Phosphinine-Based SPS Pincer Ligands. Variations with the Substituent at the Phosphorus Atom. *Organometallics* **2008**, *27* (16), 4158–4165. https://doi.org/10.1021/om8003493.

(44) Fong, S.-W. A.; Yap, W. T.; Vittal, J. J.; Henderson, W.; Hor, T. S. A. Mass Spectrometry-Directed Synthesis of 'Early–late' Sulfide-Bridged Heterobimetallic Complexes from the Metalloligand [Pt2(PPh3)4(μ-S)2] and Oxo Compounds of Vanadium(v), Molybdenum(vi) and Uranium(Vi). *J. Chem. Soc. Dalt. Trans.* **2002**, *0* (8), 1826–1831. https://doi.org/10.1039/b107939p.

(45) Gibson, J. K.; Haire, R. G. Synthesis and Investigation of Plutonium Oxide Cluster Ions: PuxOy+ (X≤18). *J. Alloys Compd.* **2001**, *322* (1–2), 143–152. https://doi.org/10.1016/S0925-8388(01)01178-1.

(46) Krivovichev, S. V.; Burns, P. C.; Tananaev, I. G.; Myasoedov, B. F. Nanostructured Actinide Compounds. *J. Alloys Compd.* **2007**, *444–445*, 457–463. https://doi.org/10.1016/j.jallcom.2006.10.077.

(47) Patel, D.; Tuna, F.; McInnes, E. J. L.; Lewis, W.; Blake, A. J.; Liddle, S. T. An Actinide Zintl Cluster: A Tris(Triamidouranium)μ 3 -η 2 :η 2 :η 2 -Heptaphosphanortricyclane and Its Diverse Synthetic Utility. *Angew. Chemie Int. Ed.* **2013**, *52* (50), 13334–13337. https://doi.org/10.1002/anie.201306492.

(48) Cronin, L.; Müller, A. From Serendipity to Design of Polyoxometalates at the Nanoscale, Aesthetic Beauty and Applications. *Chem. Soc. Rev.* **2012**, *41* (22), 7333. https://doi.org/10.1039/c2cs90087d.

(49) Liao, Z.; Ling, J.; Reinke, L. R.; Szymanowski, J. E. S.; Sigmon, G. E.; Burns, P. C. Cage Clusters Built from Uranyl Ions Bridged through Peroxo and 1-Hydroxyethane-1,1-Diphosphonic Acid Ligands. *Dalt. Trans.* **2013**, *42* (19), 6793. https://doi.org/10.1039/c3dt33025g.

(50) Qian, X.-Y.; Zhou, T.-H.; Mao, J.-G. New Thorium(<scp>iv</Scp>)–arsonates with a $[Th_8O_{13}]^{6+}$ Octanuclear Core. *Dalt. Trans.* **2015**, *44* (30), 13573–13580. https://doi.org/10.1039/C5DT01370D.

(51) Knope, K. E.; Soderholm, L. Plutonium(IV) Cluster with a Hexanuclear [Pu 6 (OH) 4 O 4] 12+ Core. *Inorg. Chem.* **2013**, *52* (12), 6770–6772. https://doi.org/10.1021/ic4007185.

(52) Dembowski, M.; Colla, C. A.; Yu, P.; Qiu, J.; Szymanowski, J. E. S.; Casey, W. H.; Burns, P. C. The Propensity of Uranium-Peroxide Systems to Preserve Nanosized Assemblies. *Inorg. Chem.* **2017**, *56* (16), 9602–9608. https://doi.org/10.1021/acs.inorgchem.7b01095.

(53) Berthet, J.-C.; Thuéry, P.; Ephritikhine, M. Advances in F-Element Cyanide Chemistry. *Dalt. Trans.* **2015**, *44* (17), 7727–7742. https://doi.org/10.1039/C5DT00692A.

(54) Berthet, J.-C.; Thuéry, P.; Ephritikhine, M. Polyimido Clusters of Neodymium and Uranium, Including a Cluster with an M 6 (μ 3 -N) 8 Core. *Eur. J. Inorg. Chem.* **2008**, *2008* (35), 5455–5459. https://doi.org/10.1002/ejic.200800947.

(55) Berthet, J.-C.; Thuéry, P.; Ephritikhine, M. Polyimido Uranium(IV) Clusters: Imidometalates with an M 7 (μ 3 -N) 6 (μ 2 -N) 6 Core Analogous to the Anderson-Type Polyoxometalate Motif. *Angew. Chemie Int. Ed.* **2008**, *47* (30), 5586–5589. https://doi.org/10.1002/anie.200801420.

(56) Thuéry, P. Increasing Complexity in the Uranyl Ion–Kemp's Triacid System: From One- and Two-Dimensional Polymers to Uranyl–Copper(II) Dodeca- and Hexadecanuclear Species. *Cryst. Growth Des.* **2014**, *14* (5), 2665–2676. https://doi.org/10.1021/cg500353k.

(57) Travia, N. E.; Scott, B. L.; Kiplinger, J. L. A Rare Tetranuclear Thorium(IV) μ 4 -Oxo Cluster and Dinuclear Thorium(IV) Complex Assembled by Carbon-Oxygen Bond Activation of 1,2-Dimethoxyethane (DME). *Chem. - A Eur. J.* **2014**, *20* (51), 16846–16852. https://doi.org/10.1002/chem.201404551.

(58) Liang, L.; Zhang, R.; Zhao, J.; Liu, C.; Weng, N. S. Two Actinide-Organic Frameworks Constructed by a Tripodal Flexible Ligand: Occurrence of Infinite {(UO 2)O 2 (OH) 3 } 4n and Hexanuclear {Th 6 O 4 (OH) 4 } Motifs. *J. Solid State Chem.* **2016**, *243*, 50–56. https://doi.org/10.1016/j.jssc.2016.07.026.

(59) Chatelain, L.; White, S.; Scopelliti, R.; Mazzanti, M. Isolation of a Star-Shaped Uranium(V/VI) Cluster from the Anaerobic Photochemical Reduction of Uranyl(VI). *Angew. Chemie Int. Ed.* **2016**, *55* (46), 14325–14329. https://doi.org/10.1002/anie.201608754.

(60) Zheng, Z. *Recent Development in Clusters of Rare Earths and Actinides: Chemistry and Materials*; Zheng, Z., Ed.; Structure and Bonding; Springer Berlin Heidelberg: Berlin, Heidelberg, 2017; Vol. 173. https://doi.org/10.1007/978-3-662-53303-1.

(61) Thuéry, P.; Nierlich, M.; Souley, B.; Asfari, Z.; Vicens, J. Complexation of a Hexameric Uranium(VI) Cluster by p-Benzylcalix[7]Arene. *J. Chem. Soc. Dalt. Trans.* **1999**, No. 15, 2589–2594. https://doi.org/10.1039/a903289d.

(62) Hayden, L. A.; Burns, P. C. A Novel Uranyl Sulfate Cluster in the Structure of Na6(UO2)(SO4)4(H2O)2. *J. Solid State Chem.* **2002**, *163* (1), 313–318. https://doi.org/10.1006/jssc.2001.9417.

(63) Zhang, L.; Zhang, C.; Hou, G.; Zi, G.; Walter, M. D. Small-Molecule Activation Mediated by a Uranium Bipyridyl Metallocene. *Organometallics* **2017**, *36* (6), 1179–1187. https://doi.org/10.1021/acs.organomet.7b00064.

(64) Falcone, M.; Chatelain, L.; Scopelliti, R.; Živković, I.; Mazzanti, M. Nitrogen Reduction and Functionalization by a Multimetallic Uranium Nitride Complex. *Nature* **2017**, *547* (7663), 332–335. https://doi.org/10.1038/nature23279.

(65) Andrez, J.; Pécaut, J.; Scopelliti, R.; Kefalidis, C. E.; Maron, L.; Rosenzweig, M. W.; Meyer, K.; Mazzanti, M. Synthesis and Reactivity of a Terminal Uranium(<scp>iv</Scp>) Sulfide Supported by Siloxide Ligands. *Chem. Sci.* **2016**, *7* (9), 5846–5856. https://doi.org/10.1039/C6SC00675B.

(66) Johnson, S. A.; Higgins, R. F.; Abu-Omar, M. M.; Shores, M. P.; Bart, S. C. Mechanistic Insights into Concerted C–C Reductive Elimination from Homoleptic Uranium Alkyls. *Organometallics* **2017**, *36* (18), 3491–3497. https://doi.org/10.1021/acs.organomet.7b00438.

(67) Sinclair, F.; Hlina, J. A.; Wells, J. A. L.; Shaver, M. P.; Arnold, P. L. Ring Opening Polymerisation of Lactide with Uranium(<scp>iv</Scp>) and Cerium(<scp>iv</Scp>) Phosphinoaryloxide Complexes. *Dalt. Trans.* **2017**, *46* (33), 10786–10790. https://doi.org/10.1039/C7DT02167D.

(68) Hellebrandt, S.; Lee, S. S.; Knope, K. E.; Lussier, A. J.; Stubbs, J. E.; Eng, P. J.; Soderholm, L.; Fenter, P.; Schmidt, M. A Comparison of Adsorption, Reduction, and Polymerization of the Plutonyl(VI) and Uranyl(VI) Ions from Solution onto the Muscovite Basal Plane. *Langmuir* **2016**, *32* (41), 10473–10482. https://doi.org/10.1021/acs.langmuir.6b02513.

(69) Graves, C. R.; Vaughn, A. E.; Schelter, E. J.; Scott, B. L.; Thompson, J. D.; Morris, D. E.; Kiplinger, J. L. Probing the Chemistry, Electronic Structure and Redox Energetics in Organometallic Pentavalent Uranium Complexes. *Inorg. Chem.* **2008**, *47* (24), 11879–11891. https://doi.org/10.1021/ic8017375.

(70) Erickson, K. A.; Kiplinger, J. L. Catalytic Dehydrogenation of Dimethylamine Borane by Highly Active Thorium and Uranium Metallocene Complexes. *ACS Catal.* **2017**, *7* (7), 4276–4280. https://doi.org/10.1021/acscatal.7b00967.

(71) Camp, C.; Cooper, O.; Andrez, J.; Pécaut, J.; Mazzanti, M. CS 2 Activation at Uranium(Iii) Siloxide Ate Complexes: The Effect of a Lewis Acidic Site. *Dalt. Trans.* **2015**, *44* (6), 2650–2656. https://doi.org/10.1039/C4DT02585G.

(72) Dutkiewicz, M. S.; Farnaby, J. H.; Apostolidis, C.; Colineau, E.; Walter, O.; Magnani, N.; Gardiner, M. G.; Love, J. B.; Kaltsoyannis, N.; Caciuffo, R.; et al. Organometallic Neptunium(III) Complexes. *Nat. Chem.* **2016**, *8* (8), 797–802. https://doi.org/10.1038/nchem.2520.

(73) Wang, Q.; Zhou, Z.-Y.; Lai, Y.-J.; You, Y.; Liu, J.-G.; Wu, X.-L.; Terefe, E.; Chen, C.; Song, L.; Rauf, M.; et al. Phenylenediamine-Based FeN x /C Catalyst with High Activity for Oxygen Reduction in Acid Medium and Its Active-Site Probing. *J. Am. Chem. Soc.* **2014**, *136* (31), 10882–10885.

https://doi.org/10.1021/ja505777v.

(74) Banik, N. L.; Vallet, V.; Réal, F.; Belmecheri, R. M.; Schimmelpfennig, B.; Rothe, J.; Marsac, R.; Lindqvist-Reis, P.; Walther, C.; Denecke, M. A.; et al. First Structural Characterization of Pa(<scp>iv</Scp>) in Aqueous Solution and Quantum Chemical Investigations of the Tetravalent Actinides up to Bk(<scp>iv</Scp>): The Evidence of a Curium Break. *Dalt. Trans.* **2016**, *45* (2), 453–457. https://doi.org/10.1039/C5DT03560K.

(75) Bera, J. K.; Samuelson, A. G.; Chandrasekhar, J. Ab Initio Study of Structures, Energetics, and Bonding in Formally High-Oxidation-State Copper Organometallics. *Organometallics* **1998**, *17* (19), 4136–4145. https://doi.org/10.1021/om980373x.

(76) Suski, W. Physics of the F-Electron Intermetallics. *Phys. Solid State* **1999**, *41* (5), 733–737. https://doi.org/10.1134/1.1131084.

(77) Antunes, M. A.; Coutinho, J. T.; Santos, I. C.; Marçalo, J.; Almeida, M.; Baldoví, J. J.; Pereira, L. C. J.; Gaita-Ariño, A.; Coronado, E. A Mononuclear Uranium(IV) Single-Molecule Magnet with an Azobenzene Radical Ligand. *Chem. - A Eur. J.* **2015**, *21* (49), 17817–17826. https://doi.org/10.1002/chem.201503133.

(78) Pagano, J. K.; Erickson, K. A.; Scott, B. L.; Morris, D. E.; Waterman, R.; Kiplinger, J. L. Synthesis and Characterization of a New and Electronically Unusual Uranium Metallacyclocumulene, (C 5 Me 5) 2 U(η 4 -1,2,3,4-PhC 4 Ph). *J. Organomet. Chem.* **2017**, *829*, 79–84. https://doi.org/10.1016/j.jorganchem.2016.10.034.

(79) Schelter, E. J.; Morris, D. E.; Scott, B. L.; Thompson, J. D.; Kiplinger, J. L. Toward Actinide Molecular Magnetic Materials: Coordination Polymers of U(IV) and the Organic Acceptors TCNQ and TCNE †. *Inorg. Chem.* **2007**, *46* (14), 5528–5536. https://doi.org/10.1021/ic0700295.

(80) Hlina, J. A.; Pankhurst, J. R.; Kaltsoyannis, N.; Arnold, P. L. Metal–Metal Bonding in Uranium–Group 10 Complexes. *J. Am. Chem. Soc.* **2016**, *138* (10), 3333–3345. https://doi.org/10.1021/jacs.5b10698.

(81) Zamani, H. A.; Feizyzadeh, B.; Faridbod, F.; Ganjali, M. R. Thulium(III) Sensor Based on a Derivative of Thiourea Doped in Polymeric Membrane. *Sens. Lett.* **2011**, *9* (5), 1767–1773. https://doi.org/10.1166/sl.2011.1708.

(82) Magill, J.; Schenkel, R. New Challenges in Nuclear Science: Recent Activities at ITU. *ATW-INTERNATIONALE ZEITSCHRIFT FUR KERNENERGIE* **2001**, *46* (12), 775–782.

(83) Tressaud, A.; Bartlett, N. Preparation, Magnetic Properties, and Pressure-Induced Transitions of Some MIIMIVF6 (MII=Ni, Pd, Cu; MIV=Pd, Pt, Sn) Complex Fluorides. *J. Solid State Chem.* **2001**, *162* (2), 333–340. https://doi.org/10.1006/jssc.2001.9331.

(84) Fillaux, C.; Den Auwer, C.; Guillaumont, D.; Shuh, D. K.; Tyliszczak, T.

Investigation of Actinide Compounds by Coupling X-Ray Absorption Spectroscopy and Quantum Chemistry. *J. Alloys Compd.* **2007**, *444–445*, 443–446. https://doi.org/10.1016/j.jallcom.2007.04.021.

(85) Arai, Y. Fundamental Research on Actinide Materials for Sustainable Fuel Cycles in JAEA. *Procedia Chem.* **2012**, *7*, 425–430. https://doi.org/10.1016/j.proche.2012.10.066.

(86) Ivanova, B.; Spiteller, M. Behaviour of Complexes of F–elements in the Environment – An Experimental and Theoretical Analysis. *J. Mol. Struct.* **2017**, *1127*, 199–211. https://doi.org/10.1016/j.molstruc.2016.07.101.

(87) Nocton, G.; Horeglad, P.; Pécaut, J.; Mazzanti, M. Polynuclear Cation−Cation Complexes of Pentavalent Uranyl: Relating Stability and Magnetic Properties to Structure. *J. Am. Chem. Soc.* **2008**, *130* (49), 16633–16645. https://doi.org/10.1021/ja804766r.

(88) Mounce, A. M.; Yasuoka, H.; Koutroulakis, G.; Lee, J. A.; Cho, H.; Gendron, F.; Zurek, E.; Scott, B. L.; Trujillo, J. A.; Slemmons, A. K.; et al. Nuclear Magnetic Resonance Measurements and Electronic Structure of Pu(IV) in [(Me) 4 N] 2 PuCl 6. *Inorg. Chem.* **2016**, *55* (17), 8371–8380. https://doi.org/10.1021/acs.inorgchem.6b00735.

(89) Conradson, S. D.; Andersson, D. A.; Bagus, P. S.; Boland, K. S.; Bradley, J. A.; Byler, D. D.; Clark, D. L.; Conradson, D. R.; Espinosa-Faller, F. J.; Lezama Pacheco, J. S.; et al. Anomalous Dispersion and Band Gap Reduction in UO 2+ x and Its Possible Coupling to the Coherent Polaronic Quantum State. *Nucl. Instruments Methods Phys. Res. Sect. B Beam Interact. with Mater. Atoms* **2016**, *374*, 45–50. https://doi.org/10.1016/j.nimb.2015.10.073.

(90) Ephritikhine, M. Molecular Actinide Compounds with Soft Chalcogen Ligands. *Coord. Chem. Rev.* **2016**, *319*, 35–62. https://doi.org/10.1016/j.ccr.2016.04.020.

(91) Zhang, Y.-J.; Collison, D.; Livens, F. .; Powell, A. .; Wocadlo, S.; Eccles, H. Synthesis, Spectroscopic, and X-Ray Crystallographic Characterisation of Thorium(IV) and Uranium(IV) Malonato and Substituted Malonato Compounds. *Polyhedron* **2000**, *19* (14), 1757–1767. https://doi.org/10.1016/S0277-5387(00)00465-4.

(92) Emery, J.; Dacheux, N.; Clavier, N. Investigation in Thorium Phosphate by NMR II-Phosphorus Dipolar Networks. *Solid State Nucl. Magn. Reson.* **2006**, *29* (4), 294–304. https://doi.org/10.1016/j.ssnmr.2005.10.006.

(93) Gardner, B. M.; Lewis, W.; Blake, A. J.; Liddle, S. T. Thorium Triamidoamine Complexes: Synthesis of an Unusual Dinuclear Tuck-In–Tuck-over Thorium Metallacycle Featuring the Longest Known Thorium−σ-Alkyl Bond. *Organometallics* **2015**, *34* (11), 2386–2394. https://doi.org/10.1021/om501177s.

(94) Behrle, A. C.; Kerridge, A.; Walensky, J. R. Dithio- and Diselenophosphinate Thorium(IV) and Uranium(IV) Complexes: Molecular and Electronic Structures, Spectroscopy, and Transmetalation Reactivity. *Inorg. Chem.* **2015**, *54* (24),

11625–11636. https://doi.org/10.1021/acs.inorgchem.5b01342.

(95) Ward, A. L.; Buckley, H. L.; Lukens, W. W.; Arnold, J. Synthesis and Characterization of Thorium(IV) and Uranium(IV) Corrole Complexes. *J. Am. Chem. Soc.* **2013**, *135* (37), 13965–13971. https://doi.org/10.1021/ja407203s.

(96) SZABO, Z.; TORAISHI, T.; VALLET, V.; GRENTHE, I. Solution Coordination Chemistry of Actinides: Thermodynamics, Structure and Reaction Mechanisms. *Coord. Chem. Rev.* **2006**, *250* (7–8), 784–815. https://doi.org/10.1016/j.ccr.2005.10.005.

(97) Aparna, K.; Krishnamurthy, S. S.; Nethaji, M. Synthetic, Spectroscopic and Structural Studies on Uranium and Thorium Complexes of Diphosphazane Dioxides. *J. Chem. Soc. Dalt. Trans.* **1995**, No. 18, 2991. https://doi.org/10.1039/dt9950002991.

(98) Smiles, D. E.; Wu, G.; Hrobárik, P.; Hayton, T. W. Synthesis, Thermochemistry, Bonding, and 13 C NMR Chemical Shift Analysis of a Phosphorano-Stabilized Carbene of Thorium. *Organometallics* **2017**, *36* (23), 4519–4524. https://doi.org/10.1021/acs.organomet.7b00202.

(99) Crawford, M.-J.; Karaghiosoff, K.; Mayer, P. The Homoleptic U(NCSe)84- Anion in (Pr4N)4U(NCSe)8·2CFCl3 and Th(NCSe)4(OP(NMe2)3)4·0.5CH3CN·0.5H2O: First Structurally Characterised Actinide Isoselenocyanates. *Zeitschrift für Anorg. und Allg. Chemie* **2010**, *636* (11), 1903–1906. https://doi.org/10.1002/zaac.201000114.

(100) Cruz, C. A.; Emslie, D. J. H.; Robertson, C. M.; Harrington, L. E.; Jenkins, H. A.; Britten, J. F. Cationic Thorium Alkyl Complexes of Rigid NON- and NNN-Donor Ligands: π-Arene Coordination as a Persistent Structural Motif. *Organometallics* **2009**, *28* (6), 1891–1899. https://doi.org/10.1021/om800624t.

(101) Rabinovich, E.; Aharonovich, S.; Botoshansky, M.; Eisen, M. S. Thorium 2-Pyridylamidinates: Synthesis, Structure and Catalytic Activity towards the Cyclo-Oligomerization of ε-Caprolactone. *Dalt. Trans.* **2010**, *39* (29), 6667. https://doi.org/10.1039/c000661k.

(102) Jeanson, A.; Berthon, C.; Coantic, S.; Den Auwer, C.; Floquet, N.; Funke, H.; Guillaneux, D.; Hennig, C.; Martinez, J.; Moisy, P.; et al. The Role of Aspartyl-Rich Pentapeptides in Comparative Complexation of Actinide(Iv) and Iron(Iii). Part 1. *New J. Chem.* **2009**, *33* (5), 976. https://doi.org/10.1039/b813523a.

(103) Settineri, N. S.; Garner, M. E.; Arnold, J. A Thorium Chalcogenolate Series Generated by Atom Insertion into Thorium–Carbon Bonds. *J. Am. Chem. Soc.* **2017**, *139* (17), 6261–6269. https://doi.org/10.1021/jacs.7b02356.

(104) Dulong, F.; Thuéry, P.; Ephritikhine, M.; Cantat, T. Synthesis of N -Aryloxy-β-Diketiminate Ligands and Coordination to Zirconium, Ytterbium, Thorium, and Uranium. *Organometallics* **2013**, *32* (5), 1328–1340. https://doi.org/10.1021/om3010355.

(105) Dunbar, A. C.; Gozum, J. E.; Girolami, G. S. Synthesis and Characterization of Phosphine Adducts of Thorium Borohydride, Th(BH4)4. *J. Organomet. Chem.* **2010**, *695* (25–26), 2804–2808. https://doi.org/10.1016/j.jorganchem.2010.09.033.

(106) Pedrick, E. A.; Hrobárik, P.; Seaman, L. A.; Wu, G.; Hayton, T. W. Synthesis, Structure and Bonding of Hexaphenyl Thorium(<scp>iv</Scp>): Observation of a Non-Octahedral Structure. *Chem. Commun.* **2016**, *52* (4), 689–692. https://doi.org/10.1039/C5CC08265J.

(107) Garner, M. E.; Hohloch, S.; Maron, L.; Arnold, J. A New Supporting Ligand in Actinide Chemistry Leads to Reactive Bis(NHC)Borate-Supported Thorium Complexes. *Organometallics* **2016**, *35* (17), 2915–2922. https://doi.org/10.1021/acs.organomet.6b00467.

(108) Ortu, F.; Formanuik, A.; Innes, J. R.; Mills, D. P. New Vistas in the Molecular Chemistry of Thorium: Low Oxidation State Complexes. *Dalt. Trans.* **2016**, *45* (18), 7537–7549. https://doi.org/10.1039/C6DT01111J.

(109) Formanuik, A.; Ortu, F.; Beekmeyer, R.; Kerridge, A.; Adams, R. W.; Mills, D. P. White Phosphorus Activation by a Th(<scp>iii</Scp>) Complex. *Dalt. Trans.* **2016**, *45* (6), 2390–2393. https://doi.org/10.1039/C5DT04528B.

(110) Button, Z. E.; Higgins, J. A.; Suvova, M.; Cloke, F. G. N.; Roe, S. M. Mixed Sandwich Thorium Complexes Incorporating Bis(Tri-Isopropylsilyl)Cyclooctatetraenyl and Pentamethylcyclopentadienyl Ligands: Synthesis, Structure and Reactivity. *Dalt. Trans.* **2015**, *44* (6), 2588–2596. https://doi.org/10.1039/C4DT02362E.

(111) Rehe, D.; Kornienko, A. Y.; Emge, T. J.; Brennan, J. G. Thorium Compounds with Bonds to Sulfur or Selenium: Synthesis, Structure, and Thermolysis. *Inorg. Chem.* **2016**, *55* (14), 6961–6967. https://doi.org/10.1021/acs.inorgchem.6b00645.

(112) Domingos, Â.; Marçalo, J.; de Matos, A. P. Bis[Hydrotris(Pyrazolyl)Borate] Thorium(IV) Complexes: Synthesis and Characterization of Alkyl, Thiolate, Alkoxide and Aryloxide Derivatives and the x-Ray Crystal Structure of Th(HBPz3)2(OPh)2. *Polyhedron* **1992**, *11* (8), 909–915. https://doi.org/10.1016/S0277-5387(00)83340-9.

(113) Ren, W.; Zi, G.; Walter, M. D. Synthesis, Structure, and Reactivity of a Thorium Metallocene Containing a 2,2′-Bipyridyl Ligand. *Organometallics* **2012**, *31* (2), 672–679. https://doi.org/10.1021/om201015f.

(114) Weiss, C. J.; Wobser, S. D.; Marks, T. J. Organoactinide-Mediated Hydrothiolation of Terminal Alkynes with Aliphatic, Aromatic, and Benzylic Thiols. *J. Am. Chem. Soc.* **2009**, *131* (6), 2062–2063. https://doi.org/10.1021/ja808764q.

(115) Kelly, R. P.; Falcone, M.; Lamsfus, C. A.; Scopelliti, R.; Maron, L.; Meyer, K.; Mazzanti, M. Metathesis of a U V Imido Complex: A Route to a Terminal U V Sulfide. *Chem. Sci.* **2017**, *8* (8), 5319–5328. https://doi.org/10.1039/C7SC01111C.

(116) Kornienko, A. Y.; Emge, T. J.; Brennan, J. G. Chalcogen-Rich Lanthanide Clusters: Cluster Reactivity and the Influence of Ancillary Ligands on Structure. *J. Am. Chem. Soc.* **2001**, *123* (48), 11933–11939. https://doi.org/10.1021/ja011487u.

(117) Berg, J. M.; Clark, D. L.; Huffman, J. C.; Morris, D. E.; Sattelberger, A. P.; Streib, W. E.; Van der Sluys, W. G.; Watkin, J. G. Early Actinide Alkoxide Chemistry. Synthesis, Characterization, and Molecular Structures of Thorium(IV) and Uranium(IV) Aryloxide Complexes. *J. Am. Chem. Soc.* **1992**, *114* (27), 10811–10821. https://doi.org/10.1021/ja00053a017.

(118) Zhou, E.; Ren, W.; Hou, G.; Zi, G.; Fang, D.-C.; Walter, M. D. Small Molecule Activation Mediated by a Thorium Terminal Imido Metallocene. *Organometallics* **2015**, *34* (14), 3637–3647. https://doi.org/10.1021/acs.organomet.5b00454.

(119) Prakash, J.; Mesbah, A.; Beard, J.; Lebègue, S.; Malliakas, C. D.; Ibers, J. A. Synthesis, Crystal Structure, Optical, and Electronic Study of the New Ternary Thorium Selenide Ba3ThSe3(Se2)2. *J. Solid State Chem.* **2015**, *231*, 163–168. https://doi.org/10.1016/j.jssc.2015.08.012.

(120) Mesbah, A.; Ringe, E.; Lebègue, S.; Van Duyne, R. P.; Ibers, J. A. Ba 2 An(S 2) 2 S 2 (An = U, Th): Syntheses, Structures, Optical, and Electronic Properties. *Inorg. Chem.* **2012**, *51* (24), 13390–13395. https://doi.org/10.1021/ic302223m.

(121) Schomaker, V.; Stevenson, D. P. Some Revisions of the Covalent Radii and the Additivity Rule for the Lengths of Partially Ionic Single Covalent Bonds *. *J. Am. Chem. Soc.* **1941**, *63* (1), 37–40. https://doi.org/10.1021/ja01846a007.

(122) Shannon, R. D. Revised Effective Ionic Radii and Systematic Studies of Interatomic Distances in Halides and Chalcogenides. *Acta Crystallogr. Sect. A* **1976**, *32* (5), 751–767. https://doi.org/10.1107/S0567739476001551.

(123) Krogh-Jespersen, K.; Romanelli, M. D.; Melman, J. H.; Emge, T. J.; Brennan, J. G. Covalent Bonding and the Trans Influence in Lanthanide Compounds. *Inorg. Chem.* **2010**, *49* (2), 552–560. https://doi.org/10.1021/ic901571m.

(124) Luthra, N. P.; Dunlap, R. B.; Odom, J. D. Selenium-77 NMR Studies of Organic Selenenyl Sulfides. *J. Magn. Reson.* **1982**, *46* (1), 152–157. https://doi.org/10.1016/0022-2364(82)90175-5.

(125) Duddeck, H. Selenium-77 Nuclear Magnetic Resonance Spectroscopy. *Prog. Nucl. Magn. Reson. Spectrosc.* **1995**, *27* (1–3), 1–323. https://doi.org/10.1016/0079-6565(94)00005-F.

(126) Bottomley, F.; Day, R. W. Preparation and Properties of (.Eta.-C5H5)2TiCl(SeH), (.Eta.-C5H5)2Ti(SeH)2, [(.Eta.-C5H5)Ti]4(.Mu.2-Se)3(.Mu.3-Se)3, and Related Cyclopentadienyl Selenides of Titanium. *Organometallics* **1991**, *10* (8), 2560–2563. https://doi.org/10.1021/om00054a012.

(127) Furin, G. G.; Rezvukhin, A. I.; Fedotov, M. A.; Yakobson, G. G. 15N, 17O, 31P and 77Se Nuclear Magnetic Resonance Spectra of Polyfluoroaromatic Compounds. *J. Fluor. Chem.* **1983**, *22* (3), 231–252.

https://doi.org/10.1016/S0022-1139(00)84954-4.

(128) Huebner, L.; Kornienko, A.; Emge, T. J.; Brennan, J. G. Lanthanide Clusters with Internal Ln: Fragmentation and the Formation of Dimers with Bridging Se 2- and Se 2 2- Ligands. *Inorg. Chem.* **2005**, *44* (14), 5118–5122. https://doi.org/10.1021/ic050150g.

(129) Büyükyazi, M.; Fischer, T.; Yu, P.; Coll, M.; Mathur, S. A Cobalt(II)Heteroarylalkenolate Precursor for Homogeneous Co3O4coatings by Atomic Layer Deposition. *Dalt. Trans.* **2017**, *46* (38), 12996–13001. https://doi.org/10.1039/c7dt02757e.

(130) Jamil, A.; Schläfer, J.; Gönüllü, Y.; Lepcha, A.; Mathur, S. Precursor-Derived Rare Earth Metal Pyrochlores: Nd 2 Sn 2 O 7 Nanofibers and Thin Films As Efficient Photoabsorbers. *Cryst. Growth Des.* **2016**, *16* (9), 5260–5267. https://doi.org/10.1021/acs.cgd.6b00815.

(131) Fuhrmann, D.; Dietrich, S.; Krautscheid, H. Copper Zinc Thiolate Complexes as Potential Molecular Precursors for Copper Zinc Tin Sulfide (CZTS). *Chem. - A Eur. J.* **2017**, *23* (14), 3338–3346. https://doi.org/10.1002/chem.201604717.

(132) Gaber, A.-A. M.; Wentrup, C. Pyrolysis of Hydrazine Derivatives and Related Compounds with N N Single Bonds. *J. Anal. Appl. Pyrolysis* **2017**, *125*, 258–278. https://doi.org/10.1016/j.jaap.2017.03.016.

(133) Holligan, K.; Rogler, P.; Rehe, D.; Pamula, M.; Kornienko, A. Y.; Emge, T. J.; Krogh-Jespersen, K.; Brennan, J. G. Copper, Indium, Tin, and Lead Complexes with Fluorinated Selenolate Ligands: Precursors to MSe X. *Inorg. Chem.* **2015**, *54* (18), 8896–8904. https://doi.org/10.1021/acs.inorgchem.5b00452.

(134) Zachariasen, W. H. Crystal Chemical Studies of the 5 f -Series of Elements. X. Sulfides and Oxysulfides. *Acta Crystallogr.* **1949**, *2* (5), 291–296. https://doi.org/10.1107/S0365110X49000758.

(135) D'Eye, R. W. M. 343. The Crystal Structures of ThSe2 and Th7Se12. *J. Chem. Soc.* **1953**, *0* (0), 1670. https://doi.org/10.1039/jr9530001670.

(136) Ribaudo, G.; Bellanda, M.; Menegazzo, I.; Wolters, L. P.; Bortoli, M.; Ferrer-Sueta, G.; Zagotto, G.; Orian, L. Mechanistic Insight into the Oxidation of Organic Phenylselenides by H 2 O 2. *Chem. - A Eur. J.* **2017**, *23* (10), 2405–2422. https://doi.org/10.1002/chem.201604915.

(137) Groom, C. R.; Bruno, I. J.; Lightfoot, M. P.; Ward, S. C. The Cambridge Structural Database. *Acta Crystallogr. Sect. B Struct. Sci. Cryst. Eng. Mater.* **2016**. https://doi.org/10.1107/S2052520616003954.

(138) Ripan, R.; Popper, E. Konduktometrische Bestimmung Des Thalliumi-Ions Mit Alkalipseudohalogeniden. *Zeitschrift f*[illegible]*r Anal. Chemie* **1943**, *125* (7–8), 269–276. https://doi.org/10.1007/BF01459160.

(139) Joensen, P.; Crozier, E. D.; Alberding, N.; Frindt, R. F. A Study of Single-Layer

and Restacked MoS 2 by X-Ray Diffraction and X-Ray Absorption Spectroscopy. *J. Phys. C Solid State Phys.* **1987**, *20* (26), 4043–4053. https://doi.org/10.1088/0022-3719/20/26/009.

(140) Murphy, D. W.; Hull, G. W. Monodispersed Tantalum Disulfide and Adsorption Complexes with Cations. *J. Chem. Phys.* **1975**, *62* (3), 973–978. https://doi.org/10.1063/1.430513.

(141) Liu, C.; Singh, O.; Joensen, P.; Curzon, A. E.; Frindt, R. F. X-Ray and Electron Microscopy Studies of Single-Layer TaS2 and NbS2. *Thin Solid Films* **1984**, *113* (2), 165–172. https://doi.org/10.1016/0040-6090(84)90025-7.

(142) Bruker. GADDS. Bruker: Madison, WI 2015.

(143) JADE 7. MDI: Livermore, CA 2004.

(144) Ringgold, M.; Rehe, D.; Hrobárik, P.; Kornienko, A. Y.; Emge, T. J.; Brennan, J. G. Thorium Cubanes–Synthesis, Solid-State and Solution Structures, Thermolysis, and Chalcogen Exchange Reactions. *Inorg. Chem.* **2018**, *57* (12), 7129–7141. https://doi.org/10.1021/acs.inorgchem.8b00836.

(145) Bruker SMART, SHELXT, SAINT. Bruker: Madison, WI.

(146) Ingram, K. I. M.; Tassell, M. J.; Gaunt, A. J.; Kaltsoyannis, N. Covalency in the f Element−Chalcogen Bond. Computational Studies of M[N(EPR 2) 2] 3 (M = La, Ce, Pr, Pm, Eu, U, Np, Pu, Am, Cm; E = O, S, Se, Te; R = H, i Pr, Ph). *Inorg. Chem.* **2008**, *47* (17), 7824–7833. https://doi.org/10.1021/ic800835k.

(147) Jensen, M. P.; Bond, A. H. Comparison of Covalency in the Complexes of Trivalent Actinide and Lanthanide Cations. *J. Am. Chem. Soc.* **2002**, *124* (33), 9870–9877. https://doi.org/10.1021/ja0178620.

(148) Garner, M. E.; Arnold, J. Reductive Elimination of Diphosphine from a Thorium–NHC–Bis(Phosphido) Complex. *Organometallics* **2017**, *36* (23), 4511–4514. https://doi.org/10.1021/acs.organomet.7b00301.

(149) Carter, K. P.; Kalaj, M.; Surbella, R. G.; Ducati, L. C.; Autschbach, J.; Cahill, C. L. Engaging the Terminal: Promoting Halogen Bonding Interactions with Uranyl Oxo Atoms. *Chem. - A Eur. J.* **2017**, *23* (61), 15355–15369. https://doi.org/10.1002/chem.201702744.

(150) Andreev, G. B.; Fedosseev, A. M.; Budantseva, N. A.; Antipin, M. Y. Structural and Spectral Investigation of a Neptunium(V) Complex with 2,2'-Bipyridine. *Mendeleev Commun.* **2001**, *11* (2), 58–59. https://doi.org/10.1070/MC2001V011N02ABEH001438.

(151) Thangavelu, S. G.; Pope, S. J. A.; Cahill, C. L. Synthetic, Structural, and Luminescence Study of Uranyl Coordination Polymers Containing Chelating Terpyridine and Trispyridyltriazine Ligands. *CrystEngComm* **2015**, *17* (32), 6236–6247. https://doi.org/10.1039/C5CE00984G.

(152) Andreev, G. B.; Budantseva, N. A.; Tananaev, I. G.; Myasoedov, B. F. Interaction

of Transuranium Elements with Biologically Relevant Ligands. Synthesis, Crystal Structure, IR and Electronic Spectra of Neptunium Glycolate [NpO2(C2O3H3)(Bipy)] · 2.5H2O. *Inorg. Chem. Commun.* **2009**, *12* (2), 109–111. https://doi.org/10.1016/J.INOCHE.2008.11.016.

(153) Antunes, M. A.; Pereira, L. C. J.; Santos, I. C.; Mazzanti, M.; Marçalo, J.; Almeida, M. $[U(Tp^{Me2})_2(Bipy)]^+$: A Cationic Uranium(III) Complex with Single-Molecule-Magnet Behavior. *Inorg. Chem.* **2011**, *50* (20), 9915–9917. https://doi.org/10.1021/ic200705p.

(154) Thuéry, P. 2,2′-Bipyridine and 1,10-Phenanthroline as Coligands or Structure-Directing Agents in Uranyl-Organic Assemblies with Polycarboxylic Acids. *Eur. J. Inorg. Chem.* **2013**, *2013* (26), 4563–4573. https://doi.org/10.1002/ejic.201300502.

(155) Thuéry, P.; Harrowfield, J. Ag^{I} and Pb^{II} as Additional Assembling Cations in Uranyl Coordination Polymers and Frameworks. *Cryst. Growth Des.* **2017**, *17* (4), 2116–2130. https://doi.org/10.1021/acs.cgd.7b00081.

(156) Brown, M. L.; Ovens, J. S.; Leznoff, D. B. Dicyanoaurate-Based Heterobimetallic Uranyl Coordination Polymers. *Dalt. Trans.* **2017**, *46* (22), 7169–7180. https://doi.org/10.1039/C7DT00942A.

(157) Thuéry, P.; Harrowfield, J. Complexation of Uranyl Ion with Sulfonates: One- to Three-Dimensional Assemblies with 1,5- and 2,7-Naphthalenedisulfonates. *Eur. J. Inorg. Chem.* **2017**, *2017* (5), 979–987. https://doi.org/10.1002/ejic.201601374.

(158) Kraft, S. J.; Fanwick, P. E.; Bart, S. C. Synthesis and Characterization of a Uranium(III) Complex Containing a Redox-Active 2,2′-Bipyridine Ligand. *Inorg. Chem.* **2010**, *49* (3), 1103–1110. https://doi.org/10.1021/ic902008w.

(159) Mohammad, A.; Cladis, D. P.; Forrest, W. P.; Fanwick, P. E.; Bart, S. C. Reductive Heterocoupling Mediated by $Cp^*_2U(2,2'\text{-Bpy})$. *Chem. Commun.* **2012**, *48* (11), 1671–1673. https://doi.org/10.1039/C2CC16200H.

(160) Kraft, S. J.; Walensky, J.; Fanwick, P. E.; Hall, M. B.; Bart, S. C. Crystallographic Evidence of a Base-Free Uranium(IV) Terminal Oxo Species. *Inorg. Chem.* **2010**, *49* (17), 7620–7622. https://doi.org/10.1021/ic101136j.

(161) Fortier, S.; Veleta, J.; Pialat, A.; Le Roy, J.; Ghiassi, K. B.; Olmstead, M. M.; Metta-Magaña, A.; Murugesu, M.; Villagrán, D. $[U(Bipy)_4]$: A Mistaken Case of U^0? *Chem. - A Eur. J.* **2016**, *22* (6), 1931–1936. https://doi.org/10.1002/chem.201504982.

(162) Diaconescu, P. L.; Cummins, C. C. Radical Anionic versus Neutral 2,2′-Bipyridyl Coordination in Uranium Complexes Supported by Amide and Ketimide Ligands. *Dalt. Trans.* **2015**, *44* (6), 2676–2683. https://doi.org/10.1039/C4DT02422B.

(163) Spencer, L. P.; Yang, P.; Scott, B. L.; Batista, E. R.; Boncella, J. M. Uranium(VI) Bis(Imido) Chalcogenate Complexes: Synthesis and Density Functional Theory Analysis. *Inorg. Chem.* **2009**, *48* (6), 2693–2700.

https://doi.org/10.1021/ic802212m.

(164) Arnaudet, L.; Bougon, R.; Buu, B.; Lance, M.; Nierlich, M.; Vigner, J. Interaction between Uranium(V) and -(VI) Fluorides and Nitrogen Bases. Characterization and Crystal Structures of the Dimorphic Adduct UF5.Cntdot.Bipy (Bipy = 2,2'-Bipyridyl). *Inorg. Chem.* **1994**, *33* (20), 4510–4516. https://doi.org/10.1021/ic00098a017.

(165) Ren, W.; Song, H.; Zi, G.; Walter, M. D. A Bipyridyl Thorium Metallocene: Synthesis, Structure and Reactivity. *Dalt. Trans.* **2012**, *41* (19), 5965. https://doi.org/10.1039/c2dt00051b.

(166) Berthet, J.-C.; Thuéry, P.; Ephritikhine, M. Thorocene Adducts of the Neutral 2,2′-Bipyridine and Its Radical Anion. Synthesis and Crystal Structures of [Th(H8-C8H8)2(K2-Bipy)] and [Th(μ-H8:H5-C8H8)2(K2-Bipy)K(Py)2]∞. *Comptes Rendus Chim.* **2014**, *17* (6), 526–533. https://doi.org/10.1016/J.CRCI.2013.09.006.

(167) Garner, M. E.; Lohrey, T. D.; Hohloch, S.; Arnold, J. Synthesis, Characterization, and Epoxide Ring-Opening Reactivity of Thorium-NHC-Bpy Complexes. *J. Organomet. Chem.* **2018**, *857*, 10–15. https://doi.org/10.1016/J.JORGANCHEM.2017.09.006.

(168) Wiley, R. O.; Von Dreele, R. B.; Brown, T. M. Synthesis, Characterization, and Molecular Structure of Tetraethylammonium Pentakis(Isothiocyanato)Bis(2,2'-Bipyridine)Uranate(IV). *Inorg. Chem.* **1980**, *19* (11), 3351–3356. https://doi.org/10.1021/ic50213a028.

(169) Takase, M. K.; Fang, M.; Ziller, J. W.; Furche, F.; Evans, W. J. Reduction Chemistry of the Mixed Ligand Metallocene [(C5Me5)(C8H8)U]2(μ-C8H8) with Bipyridines. *Inorganica Chim. Acta* **2010**, *364* (1), 167–171. https://doi.org/10.1016/J.ICA.2010.07.074.

(170) Spencer, L. P.; Yang, P.; Scott, B. L.; Batista, E. R.; Boncella, J. M. Uranium(VI) Bis(Imido) Disulfonamide and Dihalide Complexes: Synthesis Density Functional Theory Analysis. *Comptes Rendus Chim.* **2010**, *13* (6–7), 758–766. https://doi.org/10.1016/J.CRCI.2010.01.016.

(171) Spencer, L. P.; Yang, P.; Scott, B. L.; Batista, E. R.; Boncella, J. M. Oxidative Addition to U(V)−U(V) Dimers: Facile Routes to Uranium(VI) Bis(Imido) Complexes. *Inorg. Chem.* **2009**, *48* (24), 11615–11623. https://doi.org/10.1021/ic901581r.

(172) Jilek, R. E.; Spencer, L. P.; Kuiper, D. L.; Scott, B. L.; Williams, U. J.; Kikkawa, J. M.; Schelter, E. J.; Boncella, J. M. A General and Modular Synthesis of Monoimidouranium(IV) Dihalides. *Inorg. Chem.* **2011**, *50* (10), 4235–4237. https://doi.org/10.1021/ic200377b.

(173) Mehdoui, T.; Berthet, J.-C.; Thuéry, P.; Salmon, L.; Rivière, E.; Ephritikhine, M. Lanthanide(III)/Actinide(III) Differentiation in the Cerium and Uranium Complexes [M(C5Me5)2(L)]0,+ (L=2,2′-Bipyridine, 2,2′:6′,2″-Terpyridine): Structural, Magnetic, and Reactivity Studies. *Chem. - A Eur. J.* **2005**, *11* (23),

6994–7006. https://doi.org/10.1002/chem.200500479.

(174) Brown, J. L.; Mokhtarzadeh, C. C.; Lever, J. M.; Wu, G.; Hayton, T. W. Facile Reduction of a Uranyl(VI) β-Ketoiminate Complex to U(IV) Upon Oxo Silylation. *Inorg. Chem.* **2011**, *50* (11), 5105–5112. https://doi.org/10.1021/ic200387n.

(175) Brown, J. L.; Batista, E. R.; Boncella, J. M.; Gaunt, A. J.; Reilly, S. D.; Scott, B. L.; Tomson, N. C. A Linear *Trans* -Bis(Imido) Neptunium(V) Actinyl Analog: $Np^{V}(NDipp)_2(^{t}Bu_2Bipy)_2Cl$ (Dipp = 2,6-$^{i}Pr_2C_6H_3$). *J. Am. Chem. Soc.* **2015**, *137* (30), 9583–9586. https://doi.org/10.1021/jacs.5b06667.

(176) Jilek, R. E.; Spencer, L. P.; Lewis, R. A.; Scott, B. L.; Hayton, T. W.; Boncella, J. M. A Direct Route to Bis(Imido)Uranium(V) Halides via Metathesis of Uranium Tetrachloride. *J. Am. Chem. Soc.* **2012**, *134* (24), 9876–9878. https://doi.org/10.1021/ja2108432.

(177) Jilek, R. E.; Tomson, N. C.; Shook, R. L.; Scott, B. L.; Boncella, J. M. Preparation and Reactivity of the Versatile Uranium(IV) Imido Complexes $U(NAr)Cl_2(R_2Bpy)_2$ (R = Me, ^{t}Bu) and $U(NAr)Cl_2(Tppo)_3$. *Inorg. Chem.* **2014**, *53* (18), 9818–9826. https://doi.org/10.1021/ic5014208.

(178) Rivière, C.; Nierlich, M.; Ephritikhine, M.; Madic, C. Complexation Studies of Iodides of Trivalent Uranium and Lanthanides (Ce and Nd) with 2,2‘-Bipyridine in Anhydrous Pyridine Solutions. *Inorg. Chem.* **2001**, *40* (17), 4428–4435. https://doi.org/10.1021/ic001411j.

(179) Haiges, R.; Vasiliu, M.; Dixon, D. A.; Christe, K. O. The Uranium(VI) Oxoazides $[UO_2(N_3)_2 \cdot CH_3CN]$, $[(Bipy)_2(UO_2)_2(N_3)_4]$, $[(Bipy)UO_2(N_3)_3]^-$, [. *Chem. - A Eur. J.* **2017**, *23* (3), 652–664. https://doi.org/10.1002/chem.201604154.

(180) Newell, B. S.; Schwaab, T. C.; Shores, M. P. Synthesis and Characterization of a Novel Tetranuclear 5f Compound: A New Synthon for Exploring U(IV) Chemistry. *Inorg. Chem.* **2011**, *50* (23), 12108–12115. https://doi.org/10.1021/ic201670z.

(181) Spencer, L. P.; Schelter, E. J.; Yang, P.; Gdula, R. L.; Scott, B. L.; Thompson, J. D.; Kiplinger, J. L.; Batista, E. R.; Boncella, J. M. Cation-Cation Interactions, Magnetic Communication, and Reactivity of the Pentavalent Uranium Ion $[U(N\,t\,Bu)_2]^+$. *Angew. Chemie Int. Ed.* **2009**, *48* (21), 3795–3798. https://doi.org/10.1002/anie.200806190.

(182) Jilek, R. E.; Tomson, N. C.; Scott, B. L.; Boncella, J. M. [2 + 2] Cycloaddition Reactions at Terminal Imido Uranium(IV) Complexes to Yield Isolable Cycloadducts. *Inorganica Chim. Acta* **2014**, *422*, 78–85. https://doi.org/10.1016/J.ICA.2014.07.032.

(183) Alcock, N. W.; Flanders, D. J.; Brown, D. Actinide Structural Studies. Part 7. The Crystal and Molecular Structures of (2,2′-Bipyridyl)Dinitratodioxo-Uranium(VI) and -Neptunium(VI), and Diacetato-(2,2′-Bipyridyl)Dioxo-Uranium(VI) and -Neptunium(VI). *J. Chem. Soc., Dalt. Trans.* **1985**, *0* (5), 1001–1007. https://doi.org/10.1039/DT9850001001.

(184) Deacon, G. B.; Mackinnon, P. I.; Taylor, J. C. Preparations, Structures and Thermal Decomposition of Some Bis(Pentafluorobenzoato)Dioxouranium(VI) Complexes. *Polyhedron* **1985**, *4* (1), 103–113. https://doi.org/10.1016/S0277-5387(00)84229-1.

(185) Carter, K. P.; Thomas, K. E.; Pope, S. J. A.; Holmberg, R. J.; Butcher, R. J.; Murugesu, M.; Cahill, C. L. Supramolecular Assembly of Molecular Rare-Earth–3,5-Dichlorobenzoic Acid–2,2′:6′,2″-Terpyridine Materials: Structural Systematics, Luminescence Properties, and Magnetic Behavior. *Inorg. Chem.* **2016**, *55* (14), 6902–6915. https://doi.org/10.1021/acs.inorgchem.6b00408.

(186) Thangavelu, S. G.; Cahill, C. L. Uranyl-Promoted Peroxide Generation: Synthesis and Characterization of Three Uranyl Peroxo [(UO $_2$) $_2$ (O $_2$)] Complexes. *Inorg. Chem.* **2015**, *54* (9), 4208–4221. https://doi.org/10.1021/ic502767k.

(187) Thuéry, P.; Harrowfield, J. Anchoring Flexible Uranyl Dicarboxylate Chains through Stacking Interactions of Ancillary Ligands on Chiral U(vi) Centres. *CrystEngComm* **2016**, *18* (21), 3905–3918. https://doi.org/10.1039/C6CE00603E.

(188) Yang, W.; Dang, S.; Wang, H.; Tian, T.; Pan, Q.-J.; Sun, Z.-M. Synthesis, Structures, and Properties of Uranyl Hybrids Constructed by a Variety of Mono- and Polycarboxylic Acids. *Inorg. Chem.* **2013**, *52* (21), 12394–12402. https://doi.org/10.1021/ic4012444.

(189) Thuéry, P.; Harrowfield, J. Coordination Polymers and Cage-Containing Frameworks in Uranyl Ion Complexes with *Rac* - and (1 *R* ,2 *R*)- *Trans* -1,2-Cyclohexanedicarboxylates: Consequences of Chirality. *Inorg. Chem.* **2017**, *56* (3), 1455–1469. https://doi.org/10.1021/acs.inorgchem.6b02537.

(190) Panchanan, S.; Hämäläinen, R.; Roy, P. S. Synthesis, Chiroptical and Electrochemical Studies of Dioxouranium(VI) Complexes of Aldimine Derivatives of L -/ D -Histidine and Crystal Structure of (2,2′-Bipyridyl)Dioxo(N-o-Vanillylidene- L -Histidinato)Uranium(VI)–water–methanol(1/1/1). *J. Chem. Soc., Dalt. Trans.* **1994**, *0* (16), 2381–2390. https://doi.org/10.1039/DT9940002381.

(191) Schettini, M. F.; Wu, G.; Hayton, T. W. Coordination of N-Donor Ligands to a Uranyl(V) β-Diketiminate Complex. *Inorg. Chem.* **2009**, *48* (24), 11799–11808. https://doi.org/10.1021/ic9018508.

(192) Lu, E.; Cooper, O. J.; Tuna, F.; Wooles, A. J.; Kaltsoyannis, N.; Liddle, S. T. Uranium-Carbene-Imido Metalla-Allenes: Ancillary-Ligand-Controlled *Cis* -/ *Trans* -Isomerisation and Assessment of *Trans* Influence in the R $_2$ C=U ^{IV} =NR′ Unit (R=Ph $_2$ PNSiMe $_3$; R′=CPh <sub>3<. *Chem. - A Eur. J.* **2016**, *22* (33), 11559–11563. https://doi.org/10.1002/chem.201602690.

(193) Yang, P.; Zhou, E.; Fang, B.; Hou, G.; Zi, G.; Walter, M. D. Preparation of (η ^{5} -C $_5$ Me $_5$) $_2$ Th(Bipy) and Its Reactivity toward Small Molecules. *Organometallics* **2016**, *35* (12), 2129–2139. https://doi.org/10.1021/acs.organomet.6b00357.

(194) Mehdoui, J. C.; Berthet, P. T.; Ephritikhine, M. No Title. *CCDC* **2014**, 958632.

(195) Rabinovich, D.; Chamberlin, R. M.; Scott, B. L.; Nielsen, J. B.; Abney, K. D. Synthesis of [Li(THF) 4] 2 [Th(η 5 -C 2 B 9 H 11) 2 X 2] (X = Cl, Br, I): The First Dicarbollide Complexes of Thorium. *Inorg. Chem.* **1997**, *36* (19), 4216–4217. https://doi.org/10.1021/ic970198x.

(196) Fairley, M.; Unruh, D. K.; Donovan, A.; Abeysinghe, S.; Forbes, T. Z. Synthesis and Characterization of Homo- and Heteronuclear Molecular Al3+ and Th4+ Species Chelated by the Ethylenediaminetetraacetate (Edta) Ligand. *Dalt. Trans.* **2013**, *42* (37), 13706. https://doi.org/10.1039/c3dt51517f.

(197) Zalkin, A.; Brennan, J. G.; Andersen, R. A. Dibenzyl[1,2-Bis(Dimethylphosphino)Ethane]Bis(Cyclopentadienyl)Thorium(IV). *Acta Crystallogr. Sect. C Cryst. Struct. Commun.* **1987**, *43* (3), 421–423. https://doi.org/10.1107/S0108270187095532.

(198) Edwards, P. G.; Harman, M.; Hursthouse, M. B.; Parry, J. S. The Synthesis and Crystal Structure of the Thorium Tetraphosphido Complex, Th[P(CH $_2$ CH $_2$ PMe $_2$) $_2$] $_4$, an Actinide Complex with Only Metal–phosphorus Ligand Bonds. *J. Chem. Soc., Chem. Commun.* **1992**, *0* (19), 1469–1470. https://doi.org/10.1039/C39920001469.

(199) Edwards, P. G.; Hursthouse, M. B.; Malik, K. M. A.; Parry, J. S. Direct Conversion of Carbon Monoxide to a Coordinated Secondary Alcohol Derivative by a Thorium Phosphido Complex. *J. Chem. Soc. Chem. Commun.* **1994**, *0* (10), 1249. https://doi.org/10.1039/c39940001249.

(200) Hashem, E.; Lorusso, G.; Evangelisti, M.; McCabe, T.; Schulzke, C.; Platts, J. A.; Baker, R. J. Fingerprinting the Oxidation State of U(Iv) by Emission Spectroscopy. *Dalt. Trans.* **2013**, *42* (41), 14677. https://doi.org/10.1039/c3dt52151f.

(201) Kiernicki, J. J.; Zeller, M.; Bart, S. C. Facile Reductive Silylation of UO_2^{2+} to Uranium(IV) Chloride. *Angew. Chemie Int. Ed.* **2017**, *56* (4), 1097–1100. https://doi.org/10.1002/anie.201609838.

(202) Berthet, J.-C.; Nierlich, M.; Ephritikhine, M. A Novel Coordination Geometry for the Uranyl Ion. Rhombohedral Uranium Environment in [UO2(OTf)2(Bpy)2] and [UO2(Phen)3][OTf]2. *Chem. Commun.* **2003**, *0* (14), 1660. https://doi.org/10.1039/b303255h.

(203) Surbella, R. G.; Ducati, L. C.; Autschbach, J.; Deifel, N. P.; Cahill, C. L. Thermochromic Uranyl Isothiocyanates: Influencing Charge Transfer Bands with Supramolecular Structure. *Inorg. Chem.* **2018**, *57* (5), 2455–2471. https://doi.org/10.1021/acs.inorgchem.7b02702.

(204) Hu, K.-Q.; Wu, Q.-Y.; Mei, L.; Zhang, X.-L.; Ma, L.; Song, G.; Chen, D.-Y.; Wang, Y.-T.; Chai, Z.-F.; Shi, W.-Q. Novel Viologen Derivative Based Uranyl Coordination Polymers Featuring Photochromic Behaviors. *Chem. - A Eur. J.* **2017**, *23* (71), 18074–18083. https://doi.org/10.1002/chem.201704478.

(205) Vogler, A.; Kunkely, H. Excited State Properties of Organometallics Based on

Interligand Interactions between Aromatic Ligands. *Coord. Chem. Rev.* **2005**, *249* (13–14), 1511–1516. https://doi.org/10.1016/j.ccr.2005.03.008.

(206) Kepert, D. L. *Inorganic Stereochemistry*, 1st ed.; Inorganic Chemistry Concepts; Springer-Verlag Berlin Heidelberg: Berlin, Heidelberg, 1982; Vol. 6. https://doi.org/10.1007/978-3-642-68046-5.

(207) Macrae, C. F.; Bruno, I. J.; Chisholm, J. A.; Edgington, P. R.; McCabe, P.; Pidcock, E.; Rodriguez-Monge, L.; Taylor, R.; van de Streek, J.; Wood, P. A. Mercury CSD 2.0 – New Features for the Visualization and Investigation of Crystal Structures. *J. Appl. Crystallogr.* **2008**, *41* (2), 466–470. https://doi.org/10.1107/S0021889807067908.

(208) Burdett, J. K.; Hoffmann, R.; Fay, R. C. Eight-Coordination. *Inorg. Chem.* **1978**, *17* (9), 2553–2568. https://doi.org/10.1021/ic50187a041.

(209) Bondi, A. Van Der Waals Volumes and Radii. *J. Phys. Chem.* **1964**, *68* (3), 441–451. https://doi.org/10.1021/j100785a001.

(210) Hunter, C. A.; Sanders, J. K. M. The Nature of π-π Interactions. *J. Am. Chem. Soc.* **1990**. https://doi.org/10.1021/ja00170a016.

(211) Adams, H.; Cockroft, S. L.; Guardigli, C.; Hunter, C. A.; Lawson, K. R.; Perkins, J.; Spey, S. E.; Urch, C. J.; Ford, R. Experimental Measurement of Noncovalent Interactions Between Halogens and Aromatic Rings. *ChemBioChem* **2004**, *5* (5), 657–665. https://doi.org/10.1002/cbic.200400018.

(212) *No Title*; John Wiley & Sons, Ltd, 2012.

(213) Ringgold, M.; Wu, W.; Stuber, M.; Kornienko, A. Y.; Emge, T. J.; Brennan, J. G. Monomeric Thorium Chalcogenolates with Bipyridine and Terpyridine Ligands. *Dalt. Trans.* **2018**, *47* (41), 14652–14661. https://doi.org/10.1039/C8DT02543F.

(214) and, H. C. A.; Cunningham, S. A.; and, P. M.; Macaudiere, P. Lanthanide Tris(Tert-Butylthiolates) and the Crystal Structure of [Yb(SBut)2(M2-SBut)(Bipy)]2. **1998**. https://doi.org/10.1021/IC9800684.

(215) Kozimor, S. A.; Yang, P.; Batista, E. R.; Boland, K. S.; Burns, C. J.; Clark, D. L.; Conradson, S. D.; Martin, R. L.; Wilkerson, M. P.; Wolfsberg, L. E. Trends in Covalency for D- and f-Element Metallocene Dichlorides Identified Using Chlorine K-Edge X-Ray Absorption Spectroscopy and Time-Dependent Density Functional Theory. *J. Am. Chem. Soc.* **2009**, *131* (34), 12125–12136. https://doi.org/10.1021/ja9015759.

(216) INTERNATIONAL ATOMIC ENERGY AGENCY. *Spent Fuel Reprocessing Options*; INTERNATIONAL ATOMIC ENERGY AGENCY: Vienna, 2008.

(217) Arnold, P. L.; Turner, Z. R.; Kaltsoyannis, N.; Pelekanaki, P.; Bellabarba, R. M.; Tooze, R. P. Covalency in CeIV and UIV Halide and N-Heterocyclic Carbene Bonds. *Chem. - A Eur. J.* **2010**, *16* (31), 9623–9629. https://doi.org/10.1002/chem.201001471.

(218) Kirchheim, R.; Mütschele, T.; Kieninger, W.; Gleiter, H.; Birringer, R.; Koblé, T. D. Hydrogen in Amorphous and Nanocrystalline Metals. *Mater. Sci. Eng.* **1988**, *99* (1–2), 457–462. https://doi.org/10.1016/0025-5416(88)90377-1.

(219) Kamakoti, P. A Comparison of Hydrogen Diffusivities in Pd and CuPd Alloys Using Density Functional Theory. *J. Memb. Sci.* **2003**, *225* (1–2), 145–154. https://doi.org/10.1016/j.memsci.2003.07.008.

(220) Shao, H.; Xu, H.; Wang, Y.; Li, X. Preparation and Hydrogen Storage Properties of Mg 2 Ni Intermetallic Nanoparticles. *Nanotechnology* **2004**, *15* (3), 269–274. https://doi.org/10.1088/0957-4484/15/3/006.

(221) Cava, R. J.; Takagi, H.; Zandbergen, H. W.; Krajewski, J. J.; Peck, W. F.; Siegrist, T.; Batlogg, B.; van Dover, R. B.; Felder, R. J.; Mizuhashi, K.; et al. Superconductivity in the Quaternary Intermetallic Compounds LnNi2B2C. *Nature* **1994**, *367* (6460), 252–253. https://doi.org/10.1038/367252a0.

(222) Cava, R. J.; Takagi, H.; Batlogg, B.; Zandbergen, H. W.; Krajewski, J. J.; Peck, W. F.; van Dover, R. B.; Felder, R. J.; Siegrist, T.; Mizuhashi, K.; et al. Superconductivity at 23 K in Yttrium Palladium Boride Carbide. *Nature* **1994**, *367* (6459), 146–148. https://doi.org/10.1038/367146a0.

(223) He, T.; Huang, Q.; Ramirez, A. P.; Wang, Y.; Regan, K. A.; Rogado, N.; Hayward, M. A.; Haas, M. K.; Slusky, J. S.; Inumara, K.; et al. Superconductivity in the Non-Oxide Perovskite MgCNi3. *Nature* **2001**, *411* (6833), 54–56. https://doi.org/10.1038/35075014.

(224) Wang, K.; Tian, X.; Jin, Y.; Sun, J.; Zhang, Q. Heterometallic Hybrid Open Frameworks: Synthesis and Application for Selective Detection of Nitro Explosives. *Cryst. Growth Des.* **2017**, *17* (4), 1836–1842. https://doi.org/10.1021/acs.cgd.6b01808.

(225) Wang, K.; Liu, T.; Liu, Y.; Tian, X.; Sun, J.; Zhang, Q. Fluorescent Heterometallic MOFs: Tunable Framework Charges and Application for Explosives Detection. *CrystEngComm* **2016**, *18* (42), 8301–8308. https://doi.org/10.1039/C6CE01818A.

(226) Solis Maldonado, C.; Rivera de la Rosa, J.; Lucio-Ortiz, C. J.; Sandoval-Rangel, L.; Martínez-Vargas, D. X.; Luna Sánchez, R. A. Applications of Heterometallic Complexes in Catalysis. *Direct Synth. Met. Complexes* **2018**, 369–377. https://doi.org/10.1016/B978-0-12-811061-4.00010-4.

(227) Shao, L.; Zhang, W.; Armbrüster, M.; Teschner, D.; Girgsdies, F.; Zhang, B.; Timpe, O.; Friedrich, M.; Schlögl, R.; Su, D. S. Nanosizing Intermetallic Compounds Onto Carbon Nanotubes: Active and Selective Hydrogenation Catalysts. *Angew. Chemie Int. Ed.* **2011**, *50* (43), 10231–10235. https://doi.org/10.1002/anie.201008013.

(228) Deacon, G. B.; Forsyth, C. M.; Behrsing, T.; Konstas, K.; Forsyth, M. Heterometallic CeIII???FeIII???Salicylate Networks: Models for Corrosion Mitigation of Steel Surfaces by the ???Green??? Inhibitor, Ce(Salicylate)3. *Chem. Commun.* **2002**, No. 23, 2820–2821. https://doi.org/10.1039/b207722a.

(229) Chausov, F. F.; Somov, N. V.; Zakirova, R. M.; Alalykin, A. A.; Reshetnikov, S. M.; Petrov, V. G.; Aleksandrov, V. A.; Shumilova, M. A. Linear Organic–inorganic Heterometallic Copolymers [(Fe, Zn)(H2O)3{NH(CH2PO3H)3}] n and [(Fe, Cd)(H2O)3{NH(CH2PO3H)3}] N : The Missing Link in the Mechanism of Inhibiting Local Steel Corrosion with Phosphonates. *Bull. Russ. Acad. Sci. Phys.* **2017**, *81* (3), 365–367. https://doi.org/10.3103/S106287381703008X.

(230) Sun, S. Monodisperse FePt Nanoparticles and Ferromagnetic FePt Nanocrystal Superlattices. *Science (80-.).* **2000**, *287* (5460), 1989–1992. https://doi.org/10.1126/science.287.5460.1989.

(231) Casado-Rivera, E.; Volpe, D. J.; Alden, L.; Lind, C.; Downie, C.; Vázquez-Alvarez, T.; Angelo, A. C. D.; DiSalvo, F. J.; Abruña, H. D. Electrocatalytic Activity of Ordered Intermetallic Phases for Fuel Cell Applications. *J. Am. Chem. Soc.* **2004**, *126* (12), 4043–4049. https://doi.org/10.1021/ja038497a.

(232) Bratsos, I.; Tampaxis, C.; Spanopoulos, I.; Demitri, N.; Charalambopoulou, G.; Vourloumis, D.; Steriotis, T. A.; Trikalitis, P. N. Heterometallic In(III)–Pd(II) Porous Metal–Organic Framework with Square-Octahedron Topology Displaying High CO_2 Uptake and Selectivity toward CH_4 and N_2. *Inorg. Chem.* **2018**, *57* (12), 7244–7251. https://doi.org/10.1021/acs.inorgchem.8b00910.

(233) Curry, J. F.; Babuska, T. F.; Furnish, T. A.; Lu, P.; Adams, D. P.; Kustas, A. B.; Nation, B. L.; Dugger, M. T.; Chandross, M.; Clark, B. G.; et al. Achieving Ultralow Wear with Stable Nanocrystalline Metals. *Adv. Mater.* **2018**, *30* (32), 1802026. https://doi.org/10.1002/adma.201802026.

(234) Green, S. P.; Jones, C.; Stasch, A. Stable Magnesium(I) Compounds with Mg-Mg Bonds. *Science (80-.).* **2007**, *318* (5857), 1754–1757. https://doi.org/10.1126/science.1150856.

(235) *Multiple Bonds Between Metal Atoms*, 3rd ed.; Cotton, F. A., Murillo, C. A., Walton, R. A., Eds.; Springer-Verlag: New York, 2005. https://doi.org/10.1007/b136230.

(236) Schnöckel, H. Formation, Structure and Bonding of Metalloid Al and Ga Clusters. A Challenge for Chemical Efforts in Nanosciences. *Dalt. Trans.* **2008**, *0* (33), 4344. https://doi.org/10.1039/b718784j.

(237) Sternal, R. S.; Brock, C. P.; Marks, T. J. Metal-Metal Bonds Involving Actinides. Synthesis and Characterization of a Complex Having an Unsupported Actinide to Transition Metal Bond. *J. Am. Chem. Soc.* **1985**, *107* (26), 8270–8272. https://doi.org/10.1021/ja00312a081.

(238) Bucaille, A.; Le Borgne, T.; Ephritikhine, M.; Daran, J.-C. Synthesis and X-Ray Crystal Structure of a Urana[1]Ferrocenophane, the First Tris(1,1‘-Ferrocenylene) Metal Compound. *Organometallics* **2000**, *19* (23), 4912–4914. https://doi.org/10.1021/om000483f.

(239) Monreal, M. J.; Khan, S. I.; Kiplinger, J. L.; Diaconescu, P. L. Molecular Quadrangle Formation from a Diuranium μ-H6,H6-Toluene Complex. *Chem.*

Commun. **2011**, *47* (32), 9119. https://doi.org/10.1039/c1cc12367j.

(240) Gardner, B. M.; McMaster, J.; Lewis, W.; Liddle, S. T. Synthesis and Structure of [{N(CH2CH2NSiMe3)3}URe(H5-C5H5)2]: A Heterobimetallic Complex with an Unsupported Uranium–rhenium Bond. *Chem. Commun.* **2009**, *0* (20), 2851. https://doi.org/10.1039/b906554g.

(241) Gardner, B. M.; Patel, D.; Cornish, A. D.; McMaster, J.; Lewis, W.; Blake, A. J.; Liddle, S. T. The Nature of Unsupported Uranium-Ruthenium Bonds: A Combined Experimental and Theoretical Study. *Chem. - A Eur. J.* **2011**, *17* (40), 11266–11273. https://doi.org/10.1002/chem.201101394.

(242) Patel, D.; Moro, F.; McMaster, J.; Lewis, W.; Blake, A. J.; Liddle, S. T. A Formal High Oxidation State Inverse-Sandwich Diuranium Complex: A New Route to f-Block-Metal Bonds. *Angew. Chemie* **2011**, *123* (44), 10572–10576. https://doi.org/10.1002/ange.201104110.

(243) Napoline, J. W.; Kraft, S. J.; Matson, E. M.; Fanwick, P. E.; Bart, S. C.; Thomas, C. M. Tris(Phosphinoamide)-Supported Uranium–Cobalt Heterobimetallic Complexes Featuring Co → U Dative Interactions. *Inorg. Chem.* **2013**, *52* (20), 12170–12177. https://doi.org/10.1021/ic402343q.

(244) *The Chemistry of the Actinide and Transactinide Elements*; Morss, L. R., Edelstein, N. M., Fuger, J., Eds.; Springer Netherlands: Dordrecht, 2006. https://doi.org/10.1007/1-4020-3598-5.

(245) Deb, T.; Zakharov, L.; Falaise, C.; Nyman, M. Structure and Solution Speciation of U^{IV} Linked Phosphomolybdate (Mo^{V}) Clusters. *Inorg. Chem.* **2016**, *55* (2), 755–761. https://doi.org/10.1021/acs.inorgchem.5b02229.

(246) Yeon, J.; Smith, M. D.; Sefat, A. S.; zur Loye, H.-C. Crystal Growth, Structural Characterization, and Magnetic Properties of New Uranium(IV) Containing Mixed Metal Oxalates: $Na_2U_2M(C_2O_4)_6(H_2O)_4$ ($M = Mn^{2+}$, . *Inorg. Chem.* **2013**, *52* (4), 2199–2207. https://doi.org/10.1021/ic3026733.

(247) Stieler, R.; Bublitz, F.; Schulz Lang, E.; Manzoni de Oliveira, G. On the Synthesis and Structure of HgSe Clusters: Synthetic–structural Considerations and Optical Features of New Cluster Compounds. *Polyhedron* **2012**, *35* (1), 137–141. https://doi.org/10.1016/J.POLY.2012.01.006.

(248) Fenske, D.; Bettenhausen, M.; Okamoto, Y.; Yano, T. Mercury Bis(Phenyltellurolate) as a Precursor for the Synthesis of Binary and Ternary Nanoclusters. *Angew. Chem., Int. Ed* **2001**, *123* (4), 99. https://doi.org/10.1021/ic070006q.

(249) Arnold, A. P.; Canty, A. J.; Skelton, B. W.; White, A. H. Mercury(II) Selenolates. Crystal Structures of Polymeric Hg(SeMe)2 and the Tetrameric Pyridinates [{HgCl(Py)(SeEt)}4] and [{HgCl(Py)0.5(SeBut)}4]. *J. Chem. Soc. Dalt. Trans.* **1982**, *0* (3), 607. https://doi.org/10.1039/dt9820000607.

(250) Back, D. F.; de Oliveira, G. N. M.; Burrow, R. A.; Castellano, E. E.; Abram, U.;

Lang, E. S. Mercury Bis(Phenyltellurolate) as a Precursor for the Synthesis of Binary and Ternary Nanoclusters. *Inorg. Chem.* **2007**, *46* (7), 2356–2358. https://doi.org/10.1021/ic070006q.

(251) Qian, X.-Y.; Zhou, T.-H.; Mao, J.-G. New Thorium(IV)–arsonates with a [Th8O13]6+ Octanuclear Core. **2015**, *44*, 13573. https://doi.org/10.1039/c5dt01370d.

Experimentals

Caution. Thorium-232 is a strong α-emitter and potentially is a health hazard. Appropriate radioactive and personal safety trainings should be mandatory before reproducing this work.

General Methods. All syntheses were performed under ultrapure nitrogen (Welco Praxair), using conventional drybox or Schlenk techniques. Pyridine and hexane (Aldrich) were purified with a dualcolumn Solv-Tek solvent purification system and collected immediately prior to use. PhSeSePh (Aldrich) was purchased and recrystallized from hexanes. PhSSPh (Acros), thorium chips (International Bioanalytical Industries Inc.), and mercury (Strem Chemicals) were purchased and used as received. $(C_6F_5)_2Se_2$ was prepared according to literature procedure.[138] Melting points were recorded in sealed capillaries and are uncorrected. IR spectra were recorded on a Thermo Nicolet Avatar 360 FTIR spectrometer from 4000 to 450 cm^{-1} as mineral oil mulls on CsI plates. UV−Vis absorption spectra were recorded on a Varian DMS 100S spectrometer with the samples dissolved in pyridine, placed in either a 1.0 mm × 1.0 cm Spectrosil quartz cell or a 1.0 cm^2 special optical glass cuvette, and scanned from 400 to 1000 nm - all four compounds were found to be optically transparent. NMR data were collected on a Varian VNMRS 500 spectrometer at 25 °C with the compounds dissolved in pyridine-d_5. ^1H and ^{77}Se NMR spectra were obtained at 499 and 95 MHz, respectively. ^{77}Se NMR spectra were acquired with a longer relaxation delay (7.0 s) in hydrogen-decoupled mode using $(C_6F_5)_2Se_2$ as an external standard. Gas chromatography-mass spectrometry (GC-MS)

data were collected on a Varian Saturn 2100T instrument fitted with a capillary column (30 mm length, 0.25 mm ID, 0.25 mm film thickness). Elemental analyses were performed by Quantitative Technologies, Inc. Because some of these compounds rapidly lose both lattice pyridine within minutes of isolation, elemental analyses are time-dependent. Combustion analyses were obtained on freshly isolated materials from compounds that were desolvated fully under vacuum. Powder X-ray diffraction (PXRD) data were obtained on a Bruker Vantec500 area detector using Cu Kα radiation, as described below, to confirm that single-crystal X-ray data were consistent with bulk materials.

Synthesis of $(py)_8Th_4(\mu_3\text{-}S)_4(\mu_2\text{-}SPh)_4(\eta\text{-}SPh)_4\cdot 4py$ (1). Th (0.232 g, 1.00 mmol), Hg (0.015 g, 0.075 mmol), and PhSSPh (0.437 g, 2.00 mmol) were combined in pyridine (ca. 15 mL), and the mixture was stirred for 12 h at 25 °C. Elemental sulfur (0.032, 1.00 mmol) and additional pyridine (20 mL) were added to the mixture that was then stirred for additional 12 h (Scheme 1), filtered to remove a trace amount of air-sensitive white powder, concentrated to 20 mL, and layered with hexanes (12 mL) to yield colorless crystals (0.25 g, 32%) that melt at 264 °C and decompose at 313 °C. IR: 1601 (s), 1598 (s), 1576 (m), 1377 (s), 1221 (s), 1034 (m), 1153 (w), 1036 (m), 804 (w), 602 (s), 420 (s) cm^{-1}. Anal. Calcd for $C_{108}H_{100}N_{12}Th_4S_{12}$: C, 45.1; H, 3.50; N, 5.84. ($C_{88}H_{80}N_8Th_4S_{12}$: C, 41.2; H, 3.15; N, 4.37). Found: C, 41.9; H, 3.35; N, 4.70%. This compound was not sufficiently soluble to obtain NMR data.

Reproduced as entry MR-7-580 (**1**) was dissolved in py, $4(SePh)_2$ was added and heated to about 60 °C, did not affect structure; Reproduced as entry MR-8-728 Th+ $2.5(SPh)_2$+

1 hg →S, Hg did not incorporate and structure was not changed; Reproduced as entry MR-9-841 4,4'bipyridine as added after S addition, did not impact structure.

Synthesis of $(py)_8Th_4(\mu_3\text{-}Se)_4(\mu_2\text{-}SePh)_4(\eta\text{-}SePh)_4\cdot 6.25py$ (2). Th (0.232 g, 1.00 mmol), Hg (0.018 g, 0.090 mmol), and PhSeSePh (0.624 g, 2.00 mmol) were added to pyridine (ca. 15 mL) and stirred at 25 °C for 12 h. Elemental selenium (0.079, 1.00 mmol) and additional pyridine (20 mL) were added, and the mixture was stirred for 12 h (Scheme 1) to form a yellow solution with a black powder precipitate. The solution was filtered and concentrated to ca. 20 mL, layered with ca. 12 mL of hexanes, and left for a week to yield pale yellow crystals (0.37 g, 43%) that melt at 246 °C and decompose at 257 °C. IR: 2923 (w), 1629 (m), 1260 (s), 1151 (s), 1089 (m), 666 (s), 624 (s), 466 (s) cm^{-1}. Anal. Calcd for $C_{119.25}H_{111.25}N_{14.25}Th_4Se_{12}$: C, 39.6; H, 3.10; N, 5.52. ($C_{89}H_{81}N_8Th_4Se_{12}$: C, 34.1; H, 2.60; N, 3.57). Found: C, 38.4; H, 3.05; N, 5.01%. 1H NMR: 8.74 (bs, 2H, py), 8.17 (d, 2H, J = 5.5 Hz, SePh), 7.58 (tt, 1 H, 7.5 Hz, 2 Hz, py), 7.37 (m, 2H, SePh), 7.29 (t, 1H, J = 7.5 Hz, SePh), 7.22 (m, 2H, py), 7.08 (s, 2H, SePh), 6.60 (t, 1H, J = 7 Hz, SePh), 6.41 (t, 2H, J = 7 Hz, SePh) ^{77}Se NMR: 928(s, μ_3-Se), 573(s, η-SePh), 460 (s, μ_2-SePh).

Reproduced with entry MR-5-462 TMEDA added after Se addition, does not impact structure; entry MR-5-455 entry MR-9-840 addition of 4,4'-bipyridine after Se addition, does not impact structure; entry MR-7-612 dissolved cubane with addition 2 mmol Se, does not impact structure; entry MR-8-679 Zn + 5(SePh)→2Th→2Se, Zn does not incorporate

Synthesis of $(py)_8Th_4(\mu_3\text{-}S)_4(\mu_2\text{-}SePh)_4(\eta\text{-}SePh)_4\cdot 4py$ (3). Th (0.232 g, 1.00 mmol), Hg (0.020 g, 0.10 mmol), and PhSeSePh (0.624 g, 2.00 mmol) were added to pyridine (15

mL) and stirred for 12 h. Elemental sulfur (0.032, 1.00 mmol) and pyridine (20 mL) were added, and the mixture was stirred for 12 h (Scheme 1) to give a yellow solution with a greyish-green precipitate. The solution was filtered, concentrated to ca. 20 mL, layered with hexanes (12 mL), and left for a week at 25 °C to yield pale yellow crystals (0.31 g, 19%) that melt at 254 °C and decompose at 370 °C. IR: 2957 (w), 1599 (s), 1571 (s), 1218 (s), 1153 (m), 1094 (s), 800 (m), 662 (s), 625 (s), 465 (s) cm^{-1}. Anal. Calcd for $C_{108}H_{100}N_{12}Th_4Se_8S_4$: C, 39.9; H, 3.10; N, 5.16. ($C_{88}H_{80}N_8Th_4Se_8S_4$: C, 36.0; H, 2.75; N, 3.82). Found: C, 35.7; H, 2.88; N, 4.02%. This compound was not sufficiently soluble to obtain NMR data.

Synthesis of $(py)_8Th_4(\mu_3\text{-}Se)_4(\mu_2\text{-}SPh)_4(\eta\text{-}SPh)_4\cdot 2py$ (4). Method A. (Scheme 2) Th (0.232 g, 1.00 mmol), Hg (0.005 g, 0.025 mmol), PhSSPh (0.218 g, 1.00 mmol), and PhSeSePh (0.312 g, 1.00 mmol) were added to pyridine (15 mL), and the mixture was stirred for 12 h at 25 °C. Elemental selenium (0.079, 1.00 mmol) and toluene (14 mL) were added, and the mixture was stirred for 6 h to form a yellow solution with a black powder. The solution was filtered, concentrated to 20 mL, layered with 12 mL of hexanes, and left at 25 °C to yield colorless crystals (0.13 g, 18%). The product identity was confirmed by single-crystal analysis.

Method B. (Scheme 3) Th (0.232 g, 1.00 mmol), Hg (0.015 g, 0.075 mmol), and PhSeSePh (0.624 g, 2.00 mmol) were added to pyridine (15 mL), and the mixture was stirred for 12 h. Elemental Se (0.079 g, 1.00 mmol) was added, and the mixture was stirred for 8 h. PhSSPh (0.218 g, 1.00 mmol) was added, and after it was stirred for 20 min the solution was filtered, concentrated to 20 mL, and layered with hexanes (12 mL) to yield colorless crystals (0.38 g, 54%) that melt at 182 °C and decompose at 356 °C. IR:

2359 (w), 1598 (s), 1574 (m), 1220 (s), 1154 (m), 1034 (m), 1001 (m), 733 (m), 689 (s) cm^{-1}. Anal. Calcd for $C_{98}H_{90}N_{12}Th_4Se_4S_8$: C, 40.5; H, 3.12; N, 4.82. ($C_{88}H_{80}N_8Th_4Se_4S_8$: C, 38.4; H, 2.93; N, 4.08). Found: C, 38.7; H, 3.13; N, 4.45%. 1H NMR: 8.69 (d, 2H, J = 5.0 Hz, py), 8.07 (bs, 2H, SPh), 7.55 (tt, 1 H, 8.0 Hz, 1.5 Hz, py), 7.47 (bs, 2H, SPh), 7.22 (bs, 1H, SPh), 7.16 (m, 2H, py), 7.03 (bs, 2H, SPh), 6.45 (s, 1H, SPh), 6.32 (s, 2H, SPh). This compound was not soluble enough to obtain reliable ^{77}Se NMR data.

Synthesis of $(bipy)_2Th(SPh)_4$ (5). Th (0.232 g, 1.00 mmol), Hg (0.018 g, 0.090 mmol), and PhSSPh (0.437 g, 2.00 mmol) were combined in 20 mL of pyridine (20 mL) and stirred at 25ºC for three days to form a white precipitate in a light green solution. The mixture was heated for one hour at 60ºC to dissolve the precipitate and then a pyridine solution of 2,2'-bipyridine (0.312 g, 2.00 mmol in 10 mL of pyridine) was added, resulting in an immediate change in solution color to deep orange. After 30 min the hot solution was filtered, cooled to 25ºC and layered with 20 mL of hexanes to form pale yellow crystals (0.41 g, 33%) that reversibly turn orange at 186ºC, melt at 212°C and turn deep red, becoming black and condensing a colorless liquid at the top of the capillary at 319°C. Anal. Calcd for $C_{44}H_{36}N_4S_4Th$: C, 53.9; H, 3.70; N, 5.71. Found: C, 52.8; H, 3.89; N, 5.75. IR: 2926 (w), 1596 (s), 1573 (s), 1457 (w), 1376 (s), 1261 (m), 1240 (s), 1080 (s), 1012 (s), 764 (s), 731 (s), 699 (s), 690 (s) cm^{-1} ^{1}H NMR: 10.55 (d, 2H, J = 6 Hz, bipy), 10.38 (dd, 2H, J = 1, 5.5 Hz, bipy), 8.74 -8.68 (overlapping m, 5H, bipy and py), 7.95 (d, 5H, J = 8.5 Hz, bipy), 7.79-7.67 (overlapping m, 6H, bipy and SPh), 7.55 (m, 1H, py), 7.35-7.29 (m, 4H, bipy), 7.24-7.18 (overlapping m, 4H, bipy, SPh, py), 7.03 (t, 2H, J = 8.5 Hz, SPh), 6.90-6.68 (m, 3H, SPh). Crystallographic details for **1** (see Table S1 for combined details for **1-5**): M = 981.05, Monoclinic, Cc, *a* = 25.426(1)Å, *b*

= 25.274(1)Å, *c* = 24.336(1) Å, β= 90.948(2)°, V = 15636.8(13)Å^3, Z = 16, D(calc) = 1.667 g cm^{-3}, T = 100(2)K, μ = 4.066 mm^{-1}, R(int) = 0.0879, N(unique) = 28537, R(F, I > 2σ) = 0.0522, wR(F^2, I > 2σ) = 0.1175, CCDC no. 1841858.

Synthesis of (bipy)$_2$Th(SePh)$_4$· py (6). Th (0.232 g, 1.00 mmol), Hg (0.018 g, 0.090 mmol), and PhSeSePh (0.624 g, 2.00 mmol) were combined in pyridine (30 mL) and stirred at 25ºC for 5 hours to form a yellow solution. 2,2'-bipyridine (0.312 g, 2.00 mmol) was added and the color changed immediately to deep red. The solution was stirred for an hour at 25ºC, filtered and concentrated to 20 mL, layered with hexanes (20 mL), and left for one day to yield orange crystals (0.87 g, 70%) that melt at 186°C and decompose at 304°C. Anal. Calcd for $C_{49}H_{41}N_5Se_4Th$: C, 47.2; H, 3.31; N, 5.61 (lattice-desolvated $C_{44}H_{36}N_4Se_4Th$: C, 45.2; H, 3.10; N, 4.80). Found: C, 45.1; H, 3.43; N, 4.82. IR: 2922 (w), 1658 (s), 1562 (s), 1455 (w), 1377 (m), 1154 (m), 1067 (m), 1013 (s), 755 (s), 723 (s), 691(m) cm^{-1}. ^{1}H NMR: 10.25 (d, 2H, J = 4 Hz, bipy), 8.71 (d, 2H, J = 4 Hz, py, solvent), 7.89 (d, 2H, J = 8 Hz, bipy), 7.78 (overlapping td, J = 1.5, 7.5 Hz, 2H, bipy), 7.74 (overlapping td, J = 2, 7.5 Hz, 2H, py), 7.55 (tt, J = 2, 7.5 Hz, 1H, py, solvent), 7.46 (d, J = 8.5 Hz, 1H, py), 7.34 (overlapping d, 2H, J = 7.5 Hz, SePh), 7.30 (overlapping t, 2H, J = 6.5 Hz, bipy), 7.2 (overlapping dd, 2H, J = 4.5, 7.5 Hz, py), 7.19 (overlapping m, 2H, py, solvent), 6.80 (t, H, J = 7 Hz, SePh), 6.70 (t, 2H, J = 7.5 Hz, SePh). ^{77}Se NMR: 568 (s). Crystallographic details for **2**: M = 1247.75, Monoclinic, P2$_1$/c, *a* = 20.895(2)Å, *b* = 9.473(1)Å, *c* = 22.825(3)Å, β=100.916(1)°, V=4434.5(9)Å^3, Z=4, D(calc)=1.869 g cm^{-3}, T=100(2)K, μ=6.686 mm^{-1}, R(int)= 0.0586, N(unique)=10170, R(F, I > 2σ)=0.0404, wR(F^2, I > 2σ)=0.0879, CCDC no. 1841859.

Synthesis of $(bipy)_2Th(SC_6F_5)_4 \cdot 2THF$ (7) made by Wen Wu. Th (0.116 g, 0.50 mmol), $(SC_6F_5)_2$ (0.398 g, 1.00 mmol) and 2,2'-bipyridine (0.156 g, 1.00 mmol) were combined with Hg (0.010 g, 0.05 mmol) in THF (10 mL) and stirred for 24 h at 25°C. The solution was filtered to remove trace grey precipitate, concentrated to 3 mL, and cooled to -30°C to yield colorless crystals (0.31 g, 42%) that melt at 179°C and decompose at 318°C. Anal. Calcd for $C_{52}H_{32}F_{20}O_2N_4S_4Th$: C, 42.1; H, 2.17; N, 3.77 (lattice desolvated $C_{44}H_{16}F_{20}N_4S_4Th$: C, 39.4, H,1.20, N, 4.18). Found: C, 43.2; H, 2.68; N, 4.28. IR: 2924 (m), 2584 (w), 1599 (m), 1500 (w), 1458 (s), 1376 (s), 1162 (w), 1076 (m), 1012 (m), 969 (s), 862 (s), 766 (m), 734 (m), 646 (m), 628 (w) cm^{-1}. ^1H NMR (pyridine-d_5): 8.76 (d, 2H, J=5.0Hz, bipy), 8.71 (dt, 2H, J = 8.0, 1.2 Hz, bipy), 7.77 (td, 2H, J = 8.0, 1.5 Hz, bipy), 7.25 (ddd, 2H, J = 7.5, 4.8, 1.3 Hz, bipy), 3.67 (m, 3H, THF), 1.61 (m, 3H, THF). ^{19}F NMR (pyridine-d_5): -132 (m, 2F), -161 (s, 1F), -165 (m, 2F). Crystallographic details for **3**: M = 1485.09, Monoclinic, C2/c, a = 26.247(1)Å, b = 12.598(1)Å, c = 17.213(1)Å, β=114.189(1)°, V = 5191.9(4)$Å^3$, Z=4, D(calc) = 1.900 g cm^{-3}, T = 100(2) K, μ=3.153 mm^{-1}, R(int)= 0.0412, N(unique) = 7926, R(F, I > 2σ) = 0.0290, wR(F^2, I > 2σ) = 0.0643, CCDC no. 1841860.

Synthesis of $(bipy)_2Th(SeC_6F_5)_4 \cdot 2THF$ made by Matthew Stuber (8). Th (0.116 g, 0.50 mmol) and $(SeC_6F_5)_2$ (0.492 g, 1.00 mmol) were combined with Hg (0.020 g, 0.10 mmol) in pyridine (11 mL). The solution was stirred for 24 h. The solvent was removed under vacuum, 2,2'-bipyridine (0.156 g, 1.00 mmol) and THF (14 mL) were added and the mixture was stirred for 24 h. The resulting red solution was filtered to remove trace greenish precipitate and layered with hexane (10 mL) to form pale yellow (0.77 g, 46%) crystals that turn brown-deep orange at 101°C, melt at 105°C and decompose at 173°C.

Anal. Calcd for $C_{52}H_{32}F_{20}O_2N_4Se_4Th$: C, 37.3; H, 1.93; N, 3.35 (lattice desolvated $C_{44}H_{16}F_{20}N_4Se_4Th$: C, 34.6; H, 1.05; N, 3.67). Found: C, 36.7; H, 1.63; N, 3.36. UV-vis: This compound does not show an optical absorption maximum from 400 to 1000 nm. IR: 2957 (s), 2923 (s), 2853 (s), 2361 (w), 1598 (w), 1462 (m), 1376 (m), 1261 (m), 1153 (w), 1081 (m), 1013 (m), 967 (w), 800 (m), 722 (w) cm^{-1}. ^1H NMR (pyridine-d_5): 10.2 (d, 2H, J = 5.0Hz, bipy), 8.47 (dt, 2H, J = 8.5, 1.0 Hz, bipy), 8.21 (td, 2H, J = 7.7, 1.6 Hz, bipy), 7.73 (ddd, 2H, J = 7.5, 5.5, 1.1 Hz, bipy), 3.64 (m, 3H, THF), 1.61 (m, 3H, THF). ^{19}F NMR (pyridine-d_5): -124 (m, 2F), -161 (s, 1F), -163 (m, 2F). ^{77}Se NMR (pyridine-d_5): 361 (s). Crystallographic details for **4**: M = 1672.69 , Monoclinic, C2/c, a = 26.340(1) Å, b = 12.750(1) Å, c = 17.396(1) Å, β= 114.296(1)°, V = 5324.7(4) $Å^3$, Z = 4, D(calc) = 2.087 g cm^{-3}, T = 100(2) K, μ= 5.652 mm^{-1}, R(int) = 0.0357, N(unique) = 8110, R(F, I > 2σ) = 0.0271, wR(F^2, I > 2σ) = 0.0605, CCDC no. 1841861.

Synthesis of (py)(terpy)Th(SPh)$_4$ · 2py (9). Th (0.232 g, 1.00 mmol), and PhSSPh (0.437 g, 2.00 mmol) were combined with catalytic amount of Hg (0.018 g, 0.090 mmol) in pyridine (40 mL) and stirred for three days at 25°C to give a pale-yellow solution. 2,2:6,'2"-terpyridine (0.289 g, 1.24 mmol) was added and the color immediately turned to red orange. The solution was filtered to remove trace black powder and concentrated to 20 mL, then layered with 13 mL of hexanes and left for one day to yield orange crystals (1.41 g, 87%) that melt at 171°C and decompose at 390°C. Anal. Calcd for $C_{54}H_{46}N_6S_4$ Th: C, 56.9; H, 4.07; N, 7.38 (lattice-desolvated $C_{39}H_{31}N_3S_4Th$:C, 51.9; H, 3.46; N, 4.66). Found: C, 52.9; H, 3.83; N, 5.95. UV-vis: This compound does not show an optical absorption maximum from 400 to 1000 nm. IR: 2957 (w), 1463 (m), 1377 (s),

1260 (s), 1081 (m), 1021 (m), 799 (m), 722 (m) cm^{-1}. ^1H NMR (pyridine-d_5): 10.36 (d, 2H, J=4.5 Hz, terpy), 8.70 (m, 2H, py, solvent), 8.26 (d, 2H, J= 8.0 Hz, terpy), 8.14 (m, 3H, terpy), 7.88 (t, 2H, J = 15, 8 Hz, terpy), 7.56 (m, 1H, py, solvent), 7.36 (t, 2H, J= 6.5, 12 Hz, terpy), 7.26 (d, 2H, J= 7.5 Hz, SPh), 7.20 (m, 2H, py, solvent), 6.81 (t, 2H, J= 7.5, 15 Hz, SPh), 6.75 (m, 1H, SPh). Crystallographic details for **5**: M = 1139.25, Monoclinic, $P2_1/n$, a = 15.188(1) Å, b = 21.632(1) Å, c = 15.651(1) Å, β= 111.146(1)°, V = 4795.8(5)$Å^3$, Z = 4, D(calc)= 1.578 g cm^{-3}, T = 100(2)K, μ= 3.328 mm^{-1}, R(int) = 0.0398, N(unique) = 13310, R(F, I > 2σ) = 0.0371, wR(F^2, I > 2σ) = 0.0733, CCDC no. 1841862.

Synthesis of $(py)_8Th_4[Hg(SePh)_2]_4(\mu_3\text{-}Se)_4(\mu_2\text{-}SePh)_4(\eta\text{-}SePh)_4\cdot 6Py$ (10). To an oven dried flask with magnetic stir bar Th (0.232g, 1.00mmol), $(SePh)_2$ (0.624 g, 2.0 mmol), and Hg (0.060 g, 0.30 mmol) were added and dissolved in pyridine ca. 10 mL. In a separate flask was added Hg (0.200 g, 1.00 mmol) and $(SePh)_2$ (0.624 g, 2.0 mmol) dissolved in pyridine ca. 10 mL. After four days the first reaction (green with grey precipitate) was filtered into the second. After four days elemental Se (0.079 g, 1.00 mmol) was added. After two days an orange solution was filtered, concentrated slightly and layered with hexane ca. 15 mL. Large plates formed. MP, IR: 2923 (w), 1467 (m), 1376 (bs), 1261 (s), 1099 (bs), 1020 (s), 729 (s), 689 (s) cm^{-1}. PXRD

Reproduced as entry MR-8-692 Hg + $3(SePh)_2 \rightarrow Th \rightarrow$ 1Se+0.25SeO2, 90% at all 4 spots; Reproduced as entry MR-8-788 100% occ.; Reproduced as entry MR-3-185 Th and Hg were separate solutions and combined same product formed.

Synthesis of $(py)_8Th_4[Hg(SePh)_2]_4(\mu_3\text{-}S)_4(\mu_2\text{-}SePh)_4(\eta\text{-}SePh)_4$ (11). Th (0.232 g, 1.00 mmol), Hg (0.060 g, 0.030 mmol), and PhSeSePh (0.624 g, 2.00 mmol) were added to a

1:1 pyridine: toluene mixture (ca. 20 mL) and stirred at 25 °C for 72 h. Elemental sulfur (0.032, 1.00 mmol) was added, and the mixture was stirred for 12 h to form a yellow solution with grey/green powder precipitate. The solution was filtered and concentrated slightly and layered with ca. 15 mL of hexanes, and left for a week to yield small white crystals that melt at 190-192 °C and decompose at 290 °C.

Synthesis of $(py)_8U_4[Hg(SePh)_2]_4(\mu_3\text{-}Se)_4(\mu_2\text{-}SePh)_4(\eta\text{-}SePh)_4$ (12). To an oven dried flask with magnetic stir bar U (0.238 g, 1.00mmol), $(SePh)_2$ (0.624 g, 2.0 mmol), I_2 (0.010 g, catalytic), and Hg (0.200 g, 1.00 mmol) dissolved in pyridine ca. 20 mL. The next day $(SePh)_2$ (0.624 g, 2.0 mmol) was added. Two days later the solution was heated to about 60 °C. After two days elemental Se (0.079 g, 1.00 mmol) was added and stirred overnight. After three days the solution was filtered, and the black solution was layered with hexanes ca 20 mL and stored in -16 °C. The crystals formed only had 84% occupancy of the Hg. MP 134-136. IR: 2923 (w), 1456 (bs), 1377 (s), 1219 (s), 1063 (bs), 1019 (s), 801 (m), 725 (s) cm^{-1}. UV-vis and PXRD done.

Reproduced with entry MR-9-819 (90% occ.)

Synthesis of $(py)_8U_4[Hg(SePh)_2]_4(\mu_3\text{-}S)_4(\mu_2\text{-}SePh)_4(\eta\text{-}SePh)_4$ (13). U (0.238 g, 1.00 mmol), Hg (0.200 g, 1.00 mmol), $(SePh)_2$ (0.624 g, 2.00 mmol), and I_2 (0.010 g, catalytic) were added to pyridine (15 mL) and stirred. After four days elemental S (0.032, 1.00 mmol) was added, and the mixture was stirred for 2 hrs. After 9 days the dark solution was filtered and layered with hexanes. Black crystals formed.

Synthesis of $[py_3bipy_2ThF_2][Ag_4SePh_6]$ 2py (14)

To an oven dried flask with magnetic stir bar Th (0.232 g, 1.00 mmol), $(SePh)_2$ (0.468 g, 1.50 mmol), $(SC_6F_5)_2$ (0.199 g, 0.50 mmol), 2,2'-bipyridine (0.312 g, 2.00 mmol) and Hg (0.030 g, catalytic) were added and dissolved in pyridine ca. 20 mL. The next day AgF (0.190 g, 1.50 mmol) was added. After two days a deep red-orange solution was filtered and layered yielding small orange crystals. MP, Anal. Calcd for $C_{81}H_{71}N_9Ag_4S_6F_2Th$: C, 41.5; H, 3.05; N, 5.37 Found: C, 37.3; H, 3.04; N, 4.06. IR: 2923 (m), 1571 (s), 1463 (s), 1377 (s), 1066 (s), 1021 (m), 733 (s)cm^{-1}. PXRD, EA

Reproduced as entry MR-7-645 same product when second step is 1.00 mmol AgF_2; Attempted with entry MR-7-646 SPh replaced SePh, solid did not diffract; Attempted with SeC_6F_5 instead of SePh, resulted in dark red oil; Attempted with entry MR-7-641used AgCl instead of AgF resulted in red oil; Reproduced as entry MR-8-706, 1bipy used; Reproduced as entry MR-9-801, 0.51bipy used.

Synthesis of $[py_{18}Th_8\ I_4S_{13}][HgI_4]$ 11.5py (15)

To an oven dried flask with magnetic stir bar Th (0.232 g, 1.00 mmol), $(SePh)_2$ (0.312 g, 1.00 mmol), I_2 (0.252 g, 1.00 mmol), and Hg (0.200 g, 1.00 mmol) were dissolved in pyridine ca. 20 mL. The next day elemental S (0.048 g, 1.50 mmol) was added. After five days, the resulting yellow solution was filtered and layered yielding yellow crystals.

Synthesis of $[py_{17}U_8\ I_3S_{13}][HgI_4][HgI_3py]$ 7py (16)

To an oven dried flask with magnetic stir bar U (0.232 g, 1.00 mmol), $(SePh)_2$ (0.312 g, 1.00 mmol), I_2 (0.252 g, 1.00 mmol), and Hg (0.200 g, 1.00 mmol) were dissolved in pyridine ca. 20 mL. After two days elemental S (0.048 g, 1.50 mmol) was added. After one days the solution was settled and four days later the resulting black solution was

filtered and layered yielding black rods. IR: 2923 (w), 1597 (s), 1463 (b), 1377 (s), 1217 (s), 1150 (bs), 1063 (s), 1036 (s), 1002 (s), 749 (s), 694 (s), 621 (s) cm^{-1}.

Synthesis of $py_6Nd_2(SeC_6F_5)_6$ entry MR-1-6

To an oven dried flask with magnetic stir bar Nd (0.1442g, 1.00mmol), (SeC6F5)2 (0.7380 g, 1.5 mmol), pyridine (0.3560 g, 4.5 mmol), and Hg (0.025 g, catalytic) were added and dissolved in toluene ca. 20 mL. The reaction was stirred for four days. A clear green solution was filtered from black precipitate and concentrated to about 5 mL. Small square white crystals formed.

Synthesis of $py_4Nd(SeC_6F_5)_3$ entry MR-1-21

To an oven dried flask with magnetic stir bar Nd (0.144 g, 1.00mmol), $(SeC_6F_5)_2$ (0.738 g, 1.5 mmol), pyridine-d5 (0.378 g, 4.5 mmol), and Hg (0.025 g, catalytic) were added and dissolved in toluene ca. 15 mL. The reaction was stirred for two days. A clear green solution was filtered from black precipitate and concentrated to about 5 mL. Large green needles formed. MP:162-164

Synthesis of $HPy^+[py_2Er(SeC_6F_5)_4]\cdot py$ entry MR-1-36

To an oven dried flask with magnetic stir bar Er (0.167g, 1.00mmol), $(SeC_6F_5)_2$ (0.738 g, 1.5 mmol), pyridine (0.356 g, 4.5 mmol), and Hg (0.025 g, catalytic) were added and dissolved in toluene ca. 20 mL. The reaction was stirred for two days. A dark yellow solution was filtered from black precipitate and concentrated to about 5 mL. Small square light orange crystals formed.

Synthesis of $py_6Tm_2(SeC_6F_5)_6\cdot 6Tol$ entry MR-1-45

To an oven dried flask with magnetic stir bar Tm (0.169g, 1.0 mmol), $(SeC_6F_5)_2$ (0.738 g, 1.5 mmol), pyridine (0.356 g, 4.5 mmol), and Hg (0.025 g, catalytic) were added and dissolved in a 1:1 mixture of toluene and pyridine ca. 20 mL. The reaction was stirred for one week. A clear yellow solution was filtered from precipitate and concentrated to about 5 mL. crystals formed. IR. MP:147-149 and EA.

Synthesis of $py_3Tm(SeC_6F_5)_3 \cdot 3Tol$ entry MR-1-57

To an oven dried flask with magnetic stir bar Tm (0.169g, 1.0 mmol), $(SeC_6F_5)_2$ (0.738 g, 1.5 mmol), pyridine-$_{d5}$ (0.379 g, 4.5 mmol), and Hg (0.025 g, 0.15 mmol) were added and toluene ca. 20 mL. The reaction was stirred for one day. A light green solution was filtered and concentrated to about 5 mL. White crystals formed. MP:163-165

Synthesis of $py_4Th(SPh)_4$

Entry MR-9-797: To an oven dried flask with magnetic stir bar Th (0.232g, 1.0 mmol), $(SPh)_2$ (0.436 g, 2.00 mmol), and Hg (0.020 g, catalytic) were dissolved in py ca. 20 mL. After two days CS_2 (0.060 mL, 1.00 mmol) was added. After one week the yellow solution was filtered and layered yielding yellow crystals.

Entry MR-9-843 To an oven dried flask with magnetic stir bar Cd (0.112 g, 1.00 mmol), $(SPh)_2$ (0.436 g, 2.00 mmol), and I_2 (0.126 g, 0.500 mmol) were dissolved in py. The next day Th (0.232g, 1.0 mmol) was added and the reaction was stirred for four days. Reaction AK 277 which was a solution of (Th + $2(SPh)_2 \rightarrow$2Bipy) was filtered into the original reaction. After three days the orange solution was filtered and layered yielding yellow crystals.

Entry MR-9-844 To an oven dried flask with magnetic stir bar Hg (0.200 g, 1.00mmol) and $(SPh)_2$ (0.936 g, 3.0 mmol) were dissolved in pyridine. After four days Th (0.232 g, 1.00 mmol) was added and two days later 4,4'-bipyridine (0.039 g, 0.250 mmol) was added. After three days yellow solution was filtered from and was layered with hexane ca. 15 mL. Yielded white crystals.

Entry MR-4-365 to an oven dried flask with magnetic stir bar Th (0.232 g, 1.00mmol), $(SPh)_2$ (0.382 g, 1.75 mmol), $(SePh)_2$ (0.050g, catalytic), I_2 (0.032 g, 0.250 mmol), and Hg (0.025 g, catalytic) were dissolved in pyridine. The next day AgF (0.127 g, 1.00 mmol) was added to the greenish solution. After three days yellow solution was filtered from and was layered with hexane ca. 15 mL.

Entry MR-2-168

To an oven dried flask with magnetic stir bar Th (0.232g, 1.00 mmol), $(SPh)_2$ (0.655 g, 3.0 mmol), and Hg (1.00 g, 1.00 mmol) was added and dissolved in pyridine. After one day a green solution with grey precipitate and amalgam were present. After five days the solution was filtered and layered with hexanes.

Synthesis of $py_8Th_4Hg_2Se_4SePh_8$ entry MR-1-88

To an oven dried flask with magnetic stir bar Th (0.232g, 1.00mmol), $(SePh)_2$ (0.624 g, 2.0 mmol), and Hg (0.060 g, 0.30 mmol) were added and dissolved in a 1:1 mixture of pyridine and toluene ca. 20 mL. After one day elemental Se was added (0.079 g, 1.0 mmol). A clear yellow solution was filtered from green grey precipitate, was concentrated slightly and layered with hexane ca. 5 mL. Small plates formed. (Hg complex with 2 Hg 1 with uncertainty)

Entry MR-8-677 To an oven dried flask with magnetic stir bar Hg (0.200 g, 1.00mmol), $(SePh)_2$ (1.56 g, 5.0 mmol) were dissolved in pyridine ca. 20 mL. Two days later Th (0.464 g, 2.0 mmol) was added. Three days later elemental Se (0.158 g, 2.00 mmol) was added and stirred for about 2.5 hours. The solution was filtered, and the orange solution was layered with hexanes ca 20 mL. The crystals formed had no partial occupancy and a polar asymmetric coordination. The PXRD did not match though.

Reproduced in entry MR-8-65;

Synthesis of $Th(SePh)_4[(Me)_2N(CH_2)_2N^+(Me)_2CH_2CHO^-]_2$ entry MR-2-97

To an oven dried flask with magnetic stir bar Th (0.232g, 1.00mmol), $(SePh)_2$ (0.624 g, 2.0 mmol), TMEDA (0.3 mL, 2.0 mmol) and Hg (0.03 g, catalytic) were added and tetrahydrofuran ca. 25 mL. After one week a clear yellow solution was filtered from brick red precipitate, was concentrated slightly and layered with hexane ca. 15 mL. Small colorless cubes formed. TMEDA ring opened THF

Tried again in MR-4-316 yielded yellow oil, Tried again in MR-4-317 Th and SePh in py then TMEDA in second step with THF yellow oil again, MR-5-465 with SPh instead of SePh made oil in THF, MR-5-471 SePh cold in THF orange oil, MR-6-488 oil, MR-6-546 orange oil, MR-7-605 with tol, yellow oil

Synthesis of $bipy_5Th_5O_4(SePh)_{10}$ entry MR-2-112

To an oven dried flask with magnetic stir bar 2,2'-bipyridine was dissolved in tetrahydrofuran ca. 15 mL. The next day Th (0.232g, 1.00mmol), $(SePh)_2$ (0.624 g, 2.0

mmol), and Hg (0.060 g, 0.30 mmol) were added. After three days elemental S was added (0.019 g, 0.6 mmol). A red orange solution was filtered from yellow precipitate, was concentrated slightly and layered with hexane ca. 5 mL. Small opaque clusters formed. Th sq. planar with Se capping case of pyramid, SePh bridging, 1 bipy per metal and O bridging to Th MP:248 decomp at 297

Attempted synthesis: $Th+1.5(SePh)_2 \rightarrow 2Se+1SeO_2$ with hg in py entry MR-2-119

To an oven dried flask with magnetic stir bar Th (0.232g, 1.00mmol), $(SePh)_2$ (0.624 g, 2.0 mmol), and Hg (0.060 g, 0.30 mmol), and pyridine (3.1640 g, 40 mmol) were added and dissolved in toluene ca. 20 mL. After two days elemental Se (0.158 g, 2.00 mmol) and SeO2 (0.111 g, 1.00 mmol were added. After six days the solution was filtered, and the yellow solution was layered with hexanes ca 5 mL. Small thin plates formed. X-ray data not collected.

Synthesis of $py_8Th_4[Hg(SePh)_2]_{3.5}S_4SePh_8$ with hg in py entry MR-2-132

To an oven dried flask with magnetic stir bar Th (0.232g, 1.00mmol), (SePh)2 (0.624 g, 2.0 mmol), and Hg (0.025 g, catalytic) were added and dissolved in pyridine ca. 10 mL. In a separate flask was added Hg (0.200 g, 1.00 mmol) and) and (SePh)2 (0.624 g, 2.0 mmol) dissolved in pyridine ca. 10 mL. After one day the first reaction (green with black precipitate) was filtered into the second. After 1-day elemental S (0.042 g, 1.3 mmol) was added. After 10 days an orange solution was filtered, concentrated slightly and layered with hexane ca. 15 mL. Tiny crystals formed. Thermolysis and QTI

Synthesis of $py_3Tm(SeC_6F_5)_3$ and $[py_9Tm_3Se(SeC_6F_5)_6]^+[Hg(SeC_6F_5)_3]^- \cdot 5Tol$ entry Mr-2-135

To an oven dried flask with magnetic stir bar Tm (0.169g, 1.00mmol), (SeC6F5)2 (0.7380 g, 1.5 mmol), and Hg (0.025 g, catalytic), and pyridine (0.356 g, 4.5 mmol) were added and dissolved in toluene ca. 15 mL. After 8 days yellow solution was filtered from green grey precipitate and concentrated by half volume. After one week, cubes (trimer salt) and needles (monomer) were formed.

Attempted synthesis: 2Bipy→1Th+2(SePh)2 with hg in THF entry MR-2-138

To an oven dried flask with magnetic stir bar Bipy (0.312g, 2.00mmol) was dissolved in tetrahydrofuran ca. 15 mL. After two days to a clear colorless solution was added Th (0.232 g, 1.00 mmol),), $(SePh)_2$ (0.624 g, 2.0 mmol), and Hg (0.03 g, catalytic). After five days an orange solution was filtered from black precipitate. After 2 weeks crystals were analyzed, were not viable for analysis.

Synthesis of $py_8U_4Se_4SePh_8 \cdot 4Py$ entry MR-3-209

To an oven dried flask with magnetic stir bar U (0.232g, 1.00mmol), $(SePh)_2$ (0.645 g, 2.0 mmol), Hg (0.250 g, catalytic), and I_2 (0.010 g, catalytic) were dissolved in pyridine ca. 20 mL. The next day the solution was heated to about 60 °C. After one day elemental Se was added (0.158 g, 2.0 mmol) with toluene. A red black solution was filtered from black precipitate, was concentrated slightly, and was layered with hexane ca. 11 mL. Rods formed.

Attempted synthesis: 1Hg+3$(SPh)_2$→Th→S with hg in py entry MR-3-213

To an oven dried flask with magnetic stir bar Hg (0.200 g, 1.00mmol) and $(SPh)_2$ (0.936 g, 3.0 mmol) were dissolved in pyridine. After three days Th (0.232 g, 1.00 mmol) was added to the pale-yellow solution. After five days elemental S was added (0.032 g, 1.0

mmol). A greyish solution was filtered from grey precipitate, was concentrated slightly, and was layered with hexane ca. 11 mL. Crystals were impossibly twinned, and no unit cell was collected.

Attempted synthesis: U+2(SePh)2+1 2,2':6'2" terpyridine with I_2 in py entry MR-3-223

To an oven dried flask with magnetic stir bar U (0.238 g, 1.00mmol), $(SePh)_2$ (0.645 g, 2.0 mmol), and terpyridine (0.233 g, 1.00 mmol), and iodine (0.010 g, catalytic) were dissolved in pyridine. The next day the solution was heated to about 60 °C overnight. After 19 days the resulting black red solution was settled before filtration. The solution was filtered from precipitate, was concentrated slightly, and was layered with hexane ca. 11 mL. Crystals present were too small for x-ray determination.

Attempted synthesis: Th+2$(SePh)_2$→Se→0.5S with hg in py entry MR-4-286

To an oven dried flask with magnetic stir bar Th (0.232g, 1.00mmol), $(SePh)_2$ (0.624 g, 2.0 mmol) and Hg (0.03 g, catalytic) were added and dissolved pyridine ca. 20 mL. After four days elemental Se was added (0.079 g, 1.00 mmol) and stirred for 1 hour before adding S (.0160 g, 0.50 mmol) and stirring for 1.5 hours. A cloudy yellow solution was filtered, was concentrated slightly and layered with hexane ca. 11 mL. Lumpy off-white powder formed.

Attempted synthesis: Th+2$(SePh)_2$→Se +0.5 SeO_2 with hg in py entry MR-4-287

To an oven dried flask with magnetic stir bar Th (0.232g, 1.00mmol), $(SePh)_2$ (0.624 g, 2.0 mmol) and Hg (0.03 g, catalytic) were added and dissolved pyridine ca. 20 mL. After four days elemental Se (0.079 g, 1.00 mmol) and SeO_2 (.056 g, 0.50 mmol) were added.

The next day a yellow solution was filtered from black powder, was concentrated slightly and layered with hexane ca. 11 mL. Pale yellow powder formed.

Reproduced as entry MR-8-657, same results of significant yellow powder.

Attempted synthesis: Th + 2$(SePh)_2$ + 2Bipy→Se with hg and py entry MR-4-289

To an oven dried flask with magnetic stir bar Th (0.232g, 1.00mmol), $(SePh)_2$ (0.624 g, 2.0 mmol), and 2,2'-bipyridine (0.312 g, 2.00 mmol), and Hg (0.03 g, catalytic) were added and dissolved pyridine ca. 20 mL. The next day elemental Se (0.079 g, 1.00 mmol) and toluene were added. A orange yellow solution was filtered from black powder, was concentrated slightly and layered with hexane ca. 11 mL. Pale orange powder formed.

Reproduced as entryMR-8-661 first in step py than dried and dissolved in DME, resulted in powder,

Attempted synthesis: Th + 2$(SePh)_2$ + 1Cd→Se with hg and py entry MR-4-290

To an oven dried flask with magnetic stir bar Th (0.232g, 1.00mmol), $(SePh)_2$ (0.624 g, 2.0 mmol), and cadmium (0.112 g, 1.00 mmol), and Hg (0.03 g, catalytic) were added and dissolved pyridine ca. 20 mL. After 8 days the solution was heated at 40 °C for two days before stirring again at RT. Three days later elemental Se (0.079 g, 1.00 mmol) was added. A orange solution was filtered from black powder, was concentrated slightly and layered with hexane ca. 11 mL. Pale orange powder formed.

Reproduced as entry MR-4-333 Cd and $(SePh)_2$ in first step, Th in second, Se in third, resulted in orange oil. Entry MR-8-678 Cd 5$(SePh)_2$ in first step, 2 Th in second, Se in third again yielded orange oil.

Attempted synthesis: Th+2$(SePh)_2$+Zn→Se entry MR-4-295

To an oven dried flask with magnetic stir bar Th (0.232g, 1.00mmol), $(SePh)_2$ (0.624 g, 2.0 mmol), and zinc (0.065 g, 1.00 mmol), and Hg (0.03 g, catalytic) were added and dissolved pyridine ca. 20 mL. After two days the solution was heated at 40 °C for two days before stirring again at RT. Three days later elemental Se (0.079 g, 1.00 mmol) was added. A orange solution was filtered from black powder, was concentrated slightly and layered with hexane ca. 11 mL. Yellow and black powder formed.

Reproduced as entry MR-8-694 Zn and 5 $(SePh)_2$ in first step 2 Th in second, dried and dissolved in THF with Se addition resulted in oil.

Attempted synthesis: Th+2$(SePh)_2$→4,4'-bipyridine with hg in py and THF entry MR-4-306

To an oven dried flask with magnetic stir bar Th (0.232g, 1.00mmol), $(SePh)_2$ (0.624 g, 2.0 mmol), and Hg (0.03 g, catalytic) were added and dissolved pyridine ca. 20 mL. The next day the solution was dried, then 4,4'-bipyridine (0.039 g, 0.25 mmol) was added and dissolved in tetrahydrofuran ca 20 mL. Four days later orange brown solution was filtered was concentrated slightly and layered with hexane ca. 3 mL. Red oil formed.

Attempted synthesis: Th + 2(SePh)2 + 2Bipy→Se with hg and py entry MR-4-310

To an oven dried flask with magnetic stir bar Th (0.232g, 1.00mmol), $(SePh)_2$ (0.624 g, 2.0 mmol), and 2,2'-bipyridine (0.312 g, 2.00 mmol), and Hg (0.03 g, catalytic) were added and dissolved tetrahydrofuran ca. 20 mL. Six days later the reaction was dried and dissolved in pyridine ca 25 mL. After three days elemental Se (0.079 g, 1.00 mmol) and more pyridine was added. A red solution was filtered, was concentrated slightly and

layered with hexane ca. 10 mL. Small crystals formed but were encased in some solid or polymer.

Attempted synthesis: Th+ cat. $(SePh)_2$+2$(SPh)_2$+2BIpy with hg in py entry MR-4-337

To an oven dried flask with magnetic stir bar Th (0.232g, 1.00mmol), $(SePh)_2$ (0.050 g, catalytic), $(SPh)_2$ (0.437 g, 2.00 mmol), 2,2'-bipyridine (0.312 g, 2.00 mmol) and Hg (0.030 g, catalytic) were added and dissolved tetrahydrofuran ca. 20 mL. After six days an orange solution was filtered from green precipitate. Crystals formed, very unstable melted/decomposed before they could be analyzed.

Attempted synthesis: Th+ cat $(SePh)_2$+2$(SPh)_2$→2AgF with hg in py entry MR-4-342

To an oven dried flask with magnetic stir bar Th (0.232g, 1.00mmol), $(SePh)_2$ (0.050 g, catalytic), $(SPh)_2$ (0.437 g, 2.00 mmol) and Hg (0.030 g, catalytic) were added and dissolved in pyridine ca. 20 mL. The next day AgF was added. After three days a green solution was filtered. Oil formed.

Attempted synthesis: Th+ 2 $(SePh)_2$→2AgF with hg in py entry MR-4-351

To an oven dried flask with magnetic stir bar Th (0.232g, 1.00mmol), $(SePh)_2$ (0.624 g, 2.00 mmol), and Hg (0.030 g, catalytic) were added and dissolved in pyridine ca. 20 mL. The next day AgF was added. After four days a yellow solution was filtered yielding an orange oil.

Attempted synthesis: Th+ 1.75$(SePh)_2$+0.25I_2→1AgF with hg in py entry MR-4-364

To an oven dried flask with magnetic stir bar Th (0.232g, 1.00mmol), $(SePh)_2$ (0.546 g, 1.75 mmol), I_2 (0.032 g, 0.25 mmol), and Hg (0.030 g, catalytic) were added and

dissolved in pyridine ca. 20 mL. The next day AgF was added. After three days a green solution was filtered yielding orange blocks that were not crystalline.

Attempted synthesis: Th+ cat $(SePh)_2$+1.5$(SPh)_2$+0.5I_2→1AgF with hg in py entry MR-4-370

To an oven dried flask with magnetic stir bar Th (0.232g, 1.00mmol), $(SePh)_2$ (0.050 g, catalytic), $(SPh)_2$ (0.328 g, 1.50 mmol), I_2 (0.064 g, 0.5 mmol), and Hg (0.030 g, catalytic) were added and dissolved in pyridine ca. 20 mL. The next day AgF was added and the solution was heated to about 60 °C overnight. After three days an orange solution was filtered yielding orange oil.

Attempted synthesis: Th+ 2 $(SePh)_2$+2(Bipy)→2AgCl with hg in THF entry MR-4-380

To an oven dried flask with magnetic stir bar Th (0.232g, 1.00mmol), $(SePh)_2$ (0.624 g, 2.00 mmol), 2,2'-bipyridine (0.312 g, 2.00 mmol), and Hg (0.030 g, catalytic) were added and dissolved in tetrahydrofuran ca. 20 mL. Five days later AgF was added, and then two days later a red orange solution was filtered but the crystals formed did not diffract well.

Attempted synthesis: Th+ 2 $(SePh)_2$→1AgF with hg in py entry MR-4-391

To an oven dried flask with magnetic stir bar Th (0.232g, 1.00mmol), $(SePh)_2$ (0.624 g, 2.00 mmol), and Hg (0.030 g, catalytic) were added and dissolved in pyridine ca. 20 mL. The next day AgF was added. After three days a yellow solution was filtered yielding orange oil.

Synthesis of $py_7Th_2F_5(SC_6F_5)_3$ entry MR-4-392

To an oven dried flask with magnetic stir bar Th (0.232g, 1.00mmol), $(SC_6F_5)_2$ (0.199 g, 0.5 mmol), $(SePh)_2$ (0.468 g, 1.50 mmol), and Hg (0.030 g, catalytic) were added and dissolved in pyridine ca. 20 mL. The next day AgF_2, then the following day the solution was filtered small orange crystals.

Attempted synthesis: Th+2$(SePh)_2$→[Cd+$(SePh)_2$]→Se with hg in py entry MR-395

To an oven dried flask with magnetic stir bar Th (0.232g, 1.00mmol), $(SePh)_2$ (0.624 g, 2.00 mmol), and Hg (0.030 g, catalytic) were added and dissolved in pyridine ca. 20 mL. In a separate oven dried flask with magnetic stir bar Cd (0.112 g, 1.00 mmol) and $(SePh)_2$ (0.312 g, 1.00 mmol) were dissolved in pyridine. Three days later another 0.5 mmol of Cd was added to the later reaction. After five days the Th solution was filtered into the Cd solution. The next day elemental Se (0.118 g, 1.50 mmol) was added. The following day an orange solution was filtered yielding light orange powder.

Reproduced as entry MR-5-424 with 2 Se and MR-5-425 with 2$(SePh)_2$ in both flasks, results unchanged.

Attempted synthesis: Th+2$(SePh)_2$→[Zn+$(SePh)_2$]→Se with hg in py entry MR-396

To an oven dried flask with magnetic stir bar Th (0.232g, 1.00mmol), $(SePh)_2$ (0.624 g, 2.00 mmol), and Hg (0.030 g, catalytic) were added and dissolved in pyridine ca. 20 mL. In a separate oven dried flask with magnetic stir bar Zn (0.065 g, 1.00 mmol) and $(SePh)_2$ (0.312 g, 1.00 mmol) were dissolved in pyridine. Three days later another 0.5 mmol of $(SePh)_2$ was added to the later reaction. After five days the Th solution was filtered into the Zn solution. The next day elemental Se (0.118 g, 1.50 mmol) was added and stirred

for about 1 hour. Two days later the solution was heated to about 60 °C for a hot filtration. The yellow orange solution was filtered yielding light-yellow powder.

Attempted synthesis: Th+2,2':6'2" terpyridine+2($SeC_6F_5)_2$with hg in py entry MR-5-422

To an oven dried flask with magnetic stir bar Th (0.232g, 1.00mmol), ($SeC_6F_5)_2$ (0.984 g, 2.00 mmol), 2,2':6',2" terpyridine (0.233 g, 2.00 mmol), and Hg (0.030 g, catalytic) were added and dissolved in pyridine ca. 20 mL. After three days the Th solution heated for an hour before pyridine was added. The next day the solution was hot filtered. Two days later the solution put in a -16 °C fridge. The orange solution yielded dark red orange powder.

Synthesis of $py_6Th_2I_4(Se_2)_2$ entry MR-435

To an oven dried flask with magnetic stir bar I_2 (0.252g, 1.00mmol), $(SePh)_2$ (0.468 g, 1.50 mmol), and Hg (0.100 g, 0.5 mmol) were added and dissolved in pyridine ca. 20 mL. After two days Th (0.23 g, 1.00 mmol) was added. Three days later elemental Se (0.158 g, 2.00 mmol) were add with some pyridine. Six days later the orange solution was filtered and layered with hexanes.

Synthesis of $Th_6I_6Se_9$ entry MR-436

To an oven dried flask with magnetic stir bar Zn (0.033g, 0.50mmol), $(SePh)_2$ (0.624 g, 2.00 mmol), and I_2 (0.126 g, 0.50 mmol) were added and dissolved in pyridine ca. 20 mL. After three days Th (0.23 g, 1.00 mmol) was added after two days of the metal not going into solution catalytic Hg was added. Six days later the orange solution was filtered and layered with hexanes.

Attempted synthesis: Th+2$(SePh)_2$+2,2'Bipyridine→Se entry MR-5-443

To an oven dried flask with magnetic stir bar Th (0.232g, 1.00mmol), $(SePh)_2$ (0.624 g, 2.0 mmol), and Bipyridine (0.156 g, 1.00 mmol), and Hg (0.03 g, catalytic) were added and dissolved pyridine ca. 20 mL. After four days elemental Se (0.079 g, 1.00 mmol) was added. Three days later a red solution was filtered and layered with hexane ca. 11 mL. These tiny crystals yielded a new unit cell but were not suitable for a full analysis. Triclinic V=3200, A=13.65, B=14.7, C=17.68

Synthesis of pyterpy$_2$ThI$_3$I$^-$ entry MR-6-507

To an oven dried flask with magnetic stir bar Th (0.232g, 1.00mmol), $(SePh)_2$ (0.312 g, 1.0 mmol), and I_2 (0.252 g, 1.00 mmol), and Hg (0.03 g, catalytic) were added and dissolved pyridine ca. 20 mL. After three days elemental S (0.032 g, 1.00 mmol) and 2,2':6',2" terpyridine (0.467 g, 2.00 mmol) was added. Two days later a red solution was filtered and layered with hexane ca. 20 mL yielding crystals.

Attempted synthesis: U+1.5I_2→2TMEDA entry MR-6-512

To an oven dried flask with magnetic stir bar U (0.238 g, 1.00mmol) and I_2 (0.378 g, 1.50 mmol were added and dissolved ether ca. 20 mL. After six days the red-brown solution was dried, dissolved in toluene ca. 25 mL, and TMEDA (0.030 mL, 2.00 mmol) was added. The next day an orange solution was filtered and layered with hexane ca. 10 mL yielding solid that was amorphous glass not crystalline.

Attempted synthesis: U+2$(SePh)_2$→4(2,2'-bipyridine)→H_2O entry MR-6-520

To an oven dried flask with magnetic stir bar U (0.238 g, 1.00mmol) and $(SePh)_2$ (0.624 g, 2.00 mmol were added and dissolved pyridine ca. 20 mL. After three days solution was dried, dissolved in THF ca. 25 mL, and bipyridine (0.625 mL, 4.00 mmol) was added. After three days, 1-2 drops of distilled H_2O were added. Three days later the solution was hot filtered and slowly cooled before layering with hexanes ca. 15 mL. The dark brown plates appear to be 8-coordinate, U_4O_4 cubane with one bipy per each U and 4 bridging SePh. The U have terminal SePh and 2 of the U don't have a terminal ligand, but instead have a link to an unknown bridging species, which is a tetrahedral dianion having electron density and geometry that so far best fits dimethyl-silane-diolato, but that Si could be anything within a couple of protons of Si. Furthermore, the C and O can be C, N, or O, I guess, as in H2PO4. The data are not that good. Each of the bipy engages a nearby SePh for pi…pi, and the 2 other SePh engage an adjacent molecule for pi…pi. Also, there appears to be little or no lattice solvent.

Attempted synthesis: $U+2(SePh)_2 \rightarrow 1Hg+1Se$ entry MR-6-522

To an oven dried flask with magnetic stir bar U (0.238 g, 1.00mmol) and $(SePh)_2$ (0.624 g, 2.00 mmol) were added and dissolved in pyridine ca. 20 mL. After three days mercury (0.200 mL, 1.00 mmol) and elemental Se (0.079 g, 1.00 mmol) was added. After five days, the dark was filtered and layered with hexanes. The resulting crystals did not diffract past 1.2 angstroms.

Attempted synthesis: $U+I_2 \rightarrow 0.5(SC_6F_5)_2+2$(2,2'-Bipyridine) entry MR-6-523

To an oven dried flask with magnetic stir bar U (0.238 g, 1.00mmol) and I_2 (0.378 g, 1.50 mmol) were added and dissolved in THF ca. 20 mL before stirring in -2 °C. The next day

$(SC_6F_5)_2$ (0.199 g, 0.5 mmol) and 2,2'-Bipyridine (0.312 g, 2.00 mmol) were added. After three days the dark red solution was filtered and layered with hexanes. The resulting orange crystals were covered in a black coating and not suitable for analysis.

Attempted synthesis: U+2$(SPy)_2$→1.5S entry MR-6-526

To an oven dried flask with magnetic stir bar U (0.238 g, 1.00mmol) and $(SPy)_2$ (0.431 g, 2.00 mmol) were added and dissolved THF ca. 20 mL before stirring at 65 °C for about 2 weeks. Elemental S (0.048 g, 1.50 mmol) was added. After five days, the brown-orange solution was filtered and layered with hexanes. The resulting crystals did not diffract sufficiently.

Attempted synthesis: Th+2$(SePh)_2$→2(2,2'-bipyridine)→H_2O entry MR-6-541

To an oven dried flask with magnetic stir bar Th (0.232 g, 1.00mmol), $(SePh)_2$ (0.624 g, 2.00 mmol), and Hg (0.025 g, catalytic) were added and dissolved pyridine ca. 20 mL. After two days solution was dried, dissolved in THF ca. 25 mL, and bipyridine (0.625 mL, 4.00 mmol) was added and stirred for about 3 hrs. until water 1-2 drops of distilled water were added. After three days, the solution was hot filtered and slowly cooled before layering with hexanes ca. 15 mL. The precipitate was preserved and dissolved in py before being filtered and layered. This precipitate yielded crystals too small for analysis.

Reproduced as entry MR-6-544, 1.5 bipy used but the crystals did not diffract enough.

Attempted synthesis: Th+2$(SPy)_2$→1S entry MR-6-549

To an oven dried flask with magnetic stir bar Th (0.232 g, 1.00mmol) and $(SPy)_2$ (0.431 g, 2.00 mmol) were added and dissolved THF ca. 20 mL. The solution was stirred for

five days at RT before heating at 65 °C for four days. Elemental S (0.032 g, 1.00 mmol) was added. After 1.5 weeks, the light green solution was filtered and layered with hexanes yielding lots of white powder.

Attempted as entry MR-6-566 no S added, still powder and some solids that did not diffract, entry Mr-7-576 1$(Spy)_2$ and 1$(SPh)_2$ yielded lots of white powder, entry MR-7-577 1$(Spy)_2$ and 1$(SPh)_2$ with Se, cubic solid that did not polarize light.

Attempted synthesis: Th+1I_2+1$(SePh)_2$→2(2,2'-bipyridine) entry MR-6-557

To an oven dried flask with magnetic stir bar Th (0.232g, 1.00mmol), $(SePh)_2$ (0.312 g, 1.00 mmol), I_2 (0.252 g, 1.00 mmol), and Hg (0.030 g, catalytic) were added and dissolved in pyridine ca. 20 mL. The next day Bipy (0.324 g, 2.00 mmol) was added. After five days a deep red-orange solution was filtered and layered yielding red oil.

Attempted synthesis: Th+1.5I_2+0.5$(SePh)_2$→2(2,2':6',2"-terpyridine) entry MR-6-558

To an oven dried flask with magnetic stir bar Th (0.232g, 1.00mmol), $(SePh)_2$ (0.156 g, 0.50 mmol), I_2 (0.378 g, 1.50 mmol), and Hg (0.030 g, catalytic) were added and dissolved in pyridine ca. 20 mL. The next day terpy (0.467 g, 2.00 mmol) was added. After three days a deep red-orange solution was filtered and layered yielding red oil.

Attempted synthesis: Th+1.5$(SePh)_2$+2,2'-bipyridine→ with hg in THF entry MR-7-575

To an oven dried flask with magnetic stir bar Th (0.232g, 1.00mmol), $(SePh)_2$ (0.468 g, 1.5 mmol), 2;2'-bipyridine (0.156 g, 1.00 mmol), and Hg (0.060 g, 0.30 mmol) were added and dissolved in THF ca. 20 mL. After 10 days the solution was filtered, and the

red solution was layered with hexanes ca 5 mL. Small crystals formed along with powder and oil, the material was sticky and not crystalline. X-ray data not collected.

Attempted synthesis: Th+1I_2+1$(SePh)_2$→2(2,2':6',2"-terpyridine)+S entry MR-7-584

To an oven dried flask with magnetic stir bar Th (0.232g, 1.00mmol), $(SePh)_2$ (0.312 g, 1.00 mmol), I_2 (0.252 g, 1.00 mmol), and Hg (0.030 g, catalytic) were added and dissolved in pyridine ca. 20 mL. After four days terpy(0.467 g, 2.00 mmol) and elemental S(0.032 g, 1.00 mmol) was added. After three days a deep red-orange solution was hot filtered and slowly cooled before layering with hexane. The resulting solid was not crystalline.

Attempted as entry MR-7-609 used $(SPh)_2$ instead yielded deep amber oil.

Attempted synthesis: Th+1I_2+0.5$(SePh)_2$+0.5$(SC_6F_5)_2$+2(2,2'-Bipyridine) →Se entry MR-7-613

To an oven dried flask with magnetic stir bar Th (0.232g, 1.00mmol), $(SePh)_2$ (0.156 g, 0500 mmol), I_2 (0.252 g, 1.00 mmol), $(SC_6F_5)_2$ (0.199 g, 0.5 mmol), 2,2'-bipyridine (0.312 g, 2.00 mmol), and Hg (0.030 g, catalytic) were added and dissolved in pyridine ca. 20 mL. After two days elemental Se (0.079 g, 1.00 mmol) was added. After three days a dark orange solution was filtered and layered with hexanes. The solid was not crystalline.

Attempted synthesis: Th+2$(SePh)_2$→Se with bipy entry MR-7-632

To an oven dried flask with magnetic stir bar Th (0.232g, 1.00mmol), $(SePh)_2$ (0.624 g, 2.00 mmol), and Hg (0.030 g, catalytic) were added and dissolved in pyridine ca. 20 mL.

The next day elemental Se (0.79 g, 1.00 mmol) was added. In a separate flask 2,2'-bipyridine (0.156 g, 1.00 mmol) was dissolved in pyridine before. The next day the Th solution was filtered and layered with the bipy solution and let settle for 10 days before layering with hexanes. Solid formed, but the material amorphous and not crystalline. -ray data not collected.

Attempted synthesis: $Th+2(SePh)_2 \rightarrow Se$ with bipy entry MR-7-632

To an oven dried flask with magnetic stir bar Th (0.232g, 1.00mmol), $(SePh)_2$ (0.624 g, 2.00 mmol), and Hg (0.030 g, catalytic) were added and dissolved in pyridine ca. 20 mL. The next day elemental Se (0.79 g, 1.00 mmol) was added. In a separate flask 2,2'-bipyridine (0.156 g, 1.00 mmol) was dissolved in pyridine before. The next day the Th solution was filtered and layered with the bipy solution and let settle for 10 days before layering with hexanes. Solid formed, but the material amorphous and not crystalline. X-ray data not collected.

Attempted synthesis: $Th+ +1.5(SePh)_2+0.5I_2 \rightarrow$ Bipy with hg in py entry MR-7-642

To an oven dried flask with magnetic stir bar Th (0.232g, 1.00mmol), $(SePh)_2$ (0.468 g, 1.50 mmol), I_2 (0.064 g, 0.5 mmol), and Hg (0.030 g, catalytic) were added and dissolved in pyridine ca. 20 mL. In a separate flask 2,2'-bipyridine (0.156 g, 1.00 mmol) was dissolved in THF. After three days the Th solution was filtered and layered with the bipy solution before stirring in -2 °C fridge overnight. After settling, the red solution was filtered and layered with hexanes yielding red oil.

Attempted synthesis: $3Cu+3(SePh)_2 \rightarrow Th+1.5(SePh)_2+0.5(SC_6F_5)_2+2Bipy \rightarrow AgF_2$ entry MR-8-659

To an oven dried flask with magnetic stir bar Cu (0.191 g, 3.00 mmol), $(SePh)_2$ (0.936 g, 3.00 mmol) and Hg (0.025 g, catalytic) was added and dissolved in py. After four days Th (0.232 g, 1.00 mmol), $(SePh)_2$ (0.468 g, 1.50 mmol), $(SC_6F_5)_2$ (0.199 g, 0.50 mmol), and bipy (0.312 g, 2.00 mmol) was added to the orange solution. The next day AgF_2 (0.073 g, 0.500 mmol) was added to the dark red solution. The next day the solution was stopped and settled overnight before filtration. The filtrate was layered with hexanes yielding dark red oil.

Attempted as entry MR-8-660 Cu and Th in first step with 5 mmol $(SePh)_2$ and AgF_2 in second step, resulted in dark red oil.

Attempted synthesis: $Th+2(SePh)_2 \rightarrow 1Se+0.25SeO_2$ with hg and py entry MR-8-664

To an oven dried flask with magnetic stir bar Th (0.232g, 1.00mmol), $(SePh)_2$ (0.624 g, 2.0 mmol), and Hg (0.016 g, catalytic) dissolved in pyridine ca. 20 mL. After two days elemental Se (0.158 g, 2.00 mmol) and SeO_2 (0.028 g, 0.25 mmol were added and the solution was heated to about 90 °C. After six days the solution was hot filtered, and the light orange solution was cooled before being layered with hexanes ca 20 mL. A brown fudge like substance formed in the botted of the flask.

Attempted synthesis: $Th+Hg+4(SePh)_2$ + 2,2'-bipyridine$\rightarrow$1Se with hg and py entry MR-8-666

To an oven dried flask with magnetic stir bar Th (0.232g, 1.00mmol), $(SePh)_2$ (1.25 g, 4.0 mmol), 2,2'-bipyridine (0.156 g, 1.00 mmol), and Hg (0.200 g, 1.00 mmol) dissolved in pyridine ca. 20 mL. The next day elemental Se (0.079 g, 1.00 mmol) was added. After

three days the solution was filtered, and the deep orange solution was layered with hexanes ca 20 mL. A dark red oil formed.

Synthesis of $py_3AgSiF_6 \cdot py_3Ag$ entry MR-8-681

To an oven dried flask with magnetic stir bar Th (0.232g, 1.00mmol), $(SC_6F_5)_2$ (0.199 g, 0.5 mmol), $(SePh)_2$ (0.468 g, 1.50 mmol), 2,2'-bipyridine (0.324 g, 2.00 mmol), and Hg (0.030 g, catalytic) were added and dissolved in pyridine ca. 20 mL. The next day AgF_2 (0.146 g, 1.00 mmol) then after three days the orange solution was filtered and layered yielding crystals.

Attempted synthesis: $Th+3(SeC_6F_5)_2+0.5Hg \rightarrow Se$ entry MR-8-683

To an oven dried flask with magnetic stir bar Th (0.232g, 1.00mmol), $(SC_6F_5)_2$ (1.48 g, 3.0 mmol), and Hg (0.100 g, 0.5 mmol) were added and dissolved in pyridine ca. 20 mL. Three days later elemental Se (0.079 g, 1.00 mmol) was added and stirred overnight. After three days the bright red orange solution was filtered and layered yielding crystals. A unit cell was collected, but the sample was not good enough for a full data set.

Attempted synthesis: $1Hg+5(SePh)_2 \rightarrow 2Th+2(2,2'=bipyridine) \rightarrow Se$ with hg in py entry MR-8-711

To an oven dried flask with magnetic stir bar Hg (0.200 g, 1.00mmol) and $(SePh)_2$ (1.56 g, 5.0 mmol) were dissolved in pyridine. The next day Th (0.464 g, 2.00 mmol) and 2,2'-bipyridine (0.324 g, 2.00 mmol) were added to the pale-yellow solution. After three days elemental Se was added (0.079 g, 1.0 mmol). A red orange was filtered from black precipitate, was concentrated slightly, and was layered with hexane ca. 11 mL. Red oil formed.

Synthesis of bipy$_2$ThSPh$_2$(SC$_6$F$_5$)$_2$ entry MR-8-717

To an oven dried flask with magnetic stir bar Th (0.232g, 1.00mmol), $(SPh)_2$ (0.437 g, 2.00 mmol), $(SC_6F_5)_2$ (0.199 g, 0.50 mmol), 2,2'-bipyridine(0.312 g, 2.00 mmol) and Hg (0.100 g, 0.5 mmol) were added and dissolved in pyridine ca. 20 mL. After 10 days a deep red-orange solution was filtered and layered. IR and MP done around 140

Attempted synthesis: Th+2ClSePh→2NaBipy entry MR-9-759

To an oven dried flask with magnetic stir bar Th (0.232g, 1.00mmol), ClSePh (0.383 g, 2.00 mmol and Hg (0.025 g, catalytic) were added and dissolved in pyridine ca. 20 mL. In a separate flask metallic Na (0.023 g, 1.00 mmol) and 2,2'-bipyridine (0.156 g, 1.00 mmol) were dissolved in toluene ca. 20 mL. After four days a red-orange Th solution was filtered into the dark purple Nabipy solution and stirred overnight. The final black solution was filtered and layered yielding black amorphous material.

Attempted synthesis: Cu+3$(SePh)_2$→Th→Se entry MR-9-783

To an oven dried flask with magnetic stir bar Cu (0.064g, 1.00mmol), $(SePh)_2$ (0.936 g, 3.00 mmol) were dissolved in pyridine ca. 20 mL. After three days Th(0.232 g, 1.00 mmol) and Hg (0.025 g, catalytic) were added. After two days, elemental Se (0.079 g, 1.00 mmol) and toluene ca. 10 mL were added and stirred for two days. The resulting yellow solution was filtered and layered yielding orange oil.

Attempted synthesis: Th+3Cu+4.5$(SePh)_2$+0.5$(SC_6F_5)_2$→1.5AgF entry MR-9-785

To an oven dried flask with magnetic stir bar Th (0.232 g, 1.00 mmol), Cu (0.191 g, 3.00mmol), $(SePh)_2$ (1.40 g, 4.50 mmol), $(SC_6F_5)_2$ (0.199 g, 0.50 mmol), and Hg (0.100

g, 0.5 mmol) were dissolved in pyridine ca. 20 mL. After two days AgF (0.190 g, 1.50 mmol) was added. After two days, the resulting solution was filtered and layered yielding orange oil.

Reproduced with entry MR-9-809 dried after first step, dissolved in THF with AgF addition, orange oil

Synthesis of $Th_2F_5(SC_6F_5)_3$ entry MR-9-791

To an oven dried flask with magnetic stir bar Th (0.232 g, 1.00 mmol), Cu (0.032 g, 0.50mmol), $(SePh)_2$ (1.25 g, 4.00 mmol), $(SC_6F_5)_2$ (0.199 g, 0.50 mmol), and Hg (0.100 g, 0.5 mmol) were dissolved in pyridine ca. 20 mL. After three days AgF (0.190 g, 1.50 mmol) was added. After two days, the resulting orange-brown solution was filtered and layered.

Attempted synthesis: $Cu+(SePh)_2 \rightarrow [Th+2(SePh)_2] \rightarrow 1.5Se$ entry MR-9-792

To an oven dried flask with magnetic stir bar Th (0.232g, 1.00mmol), $(SePh)_2$ (0.624 g, 2.0 mmol), and Hg (0.060 g, 0.30 mmol) were added and dissolved in pyridine ca. 10 mL. In a separate flask was added Cu (0.064 g, 1.00 mmol), Hg (0.0.25 g, catalytic), and $(SePh)_2$ (0.312 g, 1.0 mmol) dissolved in pyridine ca. 10 mL. After six days the Cu solution was filtered into the Th solution. The mixture was then dried and dissolved in THF before adding Se (0.118 g, 1.50 mmol). After 6 a yellow solution was filtered, concentrated slightly and layered with hexane ca. 15 mL. Orange oil formed.

Attempted synthesis: $Th+2(SePh)_2 \rightarrow 1CS_2$ entry MR-9-795

To an oven dried flask with magnetic stir bar Th (0.232g, 1.00mmol), $(SePh)_2$ (0.624 g, 2.0 mmol), and Hg (0.060 g, 0.30 mmol) were added and dissolved in pyridine ca. 20 mL. The next day CS_2 (0.060 mL, 1.00 mmol) and stirred in about 2 °C. After one day an orange-brown solution was filtered, concentrated slightly and layered with hexane ca. 15 mL. Dark red oil formed.

Attempted synthesis: $Th+2(SePh)_2 \rightarrow 1CS_2$ entry MR-9-810

To an oven dried flask with magnetic stir bar Th (0.232g, 1.00mmol), $(SePh)_2$ (0.624 g, 2.0 mmol), and Hg (0.060 g, 0.30 mmol) were added and dissolved in pyridine ca. 20 mL. The next day the solution was dried and dissolved in THF before CuF_2 (0.102 g, 1.00 mmol) was added and stirred in about 2 °C. After 1 a yellow solution was filtered, concentrated slightly and layered with hexane ca. 15 mL before putting in the freezer, -30 °C. Yellow oil formed

Attempted synthesis: $1Cd+3(SPh)_2 \rightarrow Th \rightarrow S$ with hg in py entry MR-9-842

To an oven dried flask with magnetic stir bar Cd (0.112 g, 1.00mmol), Hg (0.025 g, catalytic), and $(SePh)_2$ (0.936 g, 3.0 mmol) were dissolved in pyridine. The next day the solution was heated to about 65 °C for three days. The pale-yellow solution was cooled before Th (0.232 g, 1.00 mmol) and Hg (0.025 g, catalytic) were added and heated at the previous temperature overnight. After two days elemental S was added (0.048 g, 1.50 mmol) and stirred for 30 min. A pale-yellow solution was filtered and layered with hexane ca. 20 mL. A significant amount of white powder was generated, and a solid pudding-like blob filled the bottom of the flask with a volume of about 15 mL.

Synthesis of py_4CdI_2 entry MR-9-848

To an oven dried flask with magnetic stir bar Cd (0.112 g, 1.00mmol), I_2 (0.126 g, 0.50 mmol), Hg (0.013 g, catalytic), and $(SePh)_2$ (0.624 g, 2.0 mmol) were dissolved in pyridine. The next day Th (0.232 g, 1.00 mmol) was added and stirred overnight. After 1-day elemental Se was added (0.118 g, 1.50 mmol) was added. After three days bright yellow solution was filtered and layered with hexane ca. 20 mL.

Attempted synthesis: $Th + 2(SePh)_2 \rightarrow Se \rightarrow CuF_2$ entry MR856

To an oven dried flask with magnetic stir bar Th (0.232 g, 1.00 mmol), $(SePh)_2$ (1.40 g, 4.50 mmol), and Hg (0.025 g, catalytic) were dissolved in pyridine ca. 20 mL. The next day elemental Se (0.079 g, 1.00 mmol). Three days later CuF_2 (.101 g, 1.00 mmol) was added. After two days, the resulting solution was filtered and layered yielding orange powder.

Synthesis of $py_8U_3O_2I_8$ entry MR859

To an oven dried flask with magnetic stir bar U (0.238 g, 1.00 mmol), and I_2 (0.380 g, 1.50 mmol) were dissolved in ether ca. 20 mL and stirred at 2 °C. After two days the red solution and precipitate were dried and dissolved in py. The solution was heated and CuS (0.096 g, 1.00 mmol) was added. After four days the solution was settled overnight and then hot filtered. The reaction was slowly cooled over a two-day period. After four days the solution was concentrated slightly and layered with hexanes ca. 14 mL. Large brown crystals were recovered.

Synthesis of $py_6U_2I_4S_4$ entry MR861

To an oven dried flask with magnetic stir bar U (0.238 g, 1.00 mmol), and I_2 (0.380 g, 1.50 mmol) were dissolved in ether ca. 20 mL and stirred at 2 °C. After five days the

solution was dried and dissolved in py after S (0.096 g, 3.00 mmol) was added. After four days the solution was filtered and layered with hexanes yielding black cubes. IR: 2922 (w), 2360 (bs), 1597 (s), 1462 (b), 1377 (s), 1261 (s), 1219 (s), 1151 (bs), 1098 (bs), 1066 (s), 1037 (s), 1000 (s), 752 (s), 697 (s), 621 (s), 523 (s) cm^{-1}. PXRD

Attempted synthesis: $U + 1.5I_2 \rightarrow 3Te$ entry MR862

To an oven dried flask with magnetic stir bar U (0.238 g, 1.00 mmol), and I_2 (0.380 g, 1.50 mmol) were dissolved in ether ca. 20 mL and stirred at 2 °C. After two days the solution was dried and dissolved in py after Te (0.383 g, 3.00 mmol) was added. After one week the solution was filtered and layered with hexanes. Two large dark crystals were formed, but they did not diffract past 1.1 Å.

Attempted synthesis: $Th + I_2 + (SePh)_2 \rightarrow 1.5Te$ entry MR 868

To an oven dried flask with magnetic stir bar Th (0.232 g, 1.00 mmol), $(SePh)_2$ (0.312 g, 1.00 mmol), I_2 (0.252 g, 1.00 mmol), and Hg (0.020 g, catalytic) were dissolved in pyridine ca. 20 mL. The next day elemental Te (0.191 g, 1.50 mmol) was added. After four days, the resulting solution was filtered and layered yielding chunky dark orange powder.

Synthesis of py_4ThI_4 entry MR 893

To an oven dried flask with magnetic stir bar Hg (0.200 g, 1.00 mmol) and $TePh_2$ (1.23g 3.00 mmol) were dissolved in py, wrapped in foil, and stirred in 2 °C. The next day Th (0.232 g, 1.00 mmol) was added. After ten days one half mmol of both I_2 and $TePh_2$ were added. After one week the solution was filtered and layered.

Attempted synthesis: U + 2$(SPh)_2$→1Pz + 1S entry MR895

To an oven dried flask with magnetic stir bar U (0.238 g, 1.00 mmol), $(SPh)_2$ (0.436 g, 2.00 mmol), and I (0.010 g, catalytic) were dissolved in pyridine ca. 20 mL. After two days the solution was heated to about 65 °C for two days. After three days I_2 (0.126 g, 0.500 mmol) was added and 8 days after that $(SPh)_2$ (0.109 g, 0.500 mmol) was added. Three days later Pyrazole (Pz) (0.068 g, 1.00 mmol) and elemental S (0.032 g, 1.00 mmol) was added. The next day the solution was settled and after six days the dark solution was filtered and layered. An amorphous material was yielded that polarized light slightly but did not diffract.

Synthesis of $Th_6I_6Se_9$ entry MR897

To an oven dried flask with magnetic stir bar Th (0.232 g, 1.00 mmol), $(SePh)_2$ (0.312 g, 1.00 mmol), I_2 (0.252 g, 1.00 mmol), and Hg (0.200 g, 1.00 mmol) were dissolved in pyridine ca. 20 mL. The next day elemental Se (0.118 g, 1.50 mmol) was added. After one week, the resulting yellow solution was filtered and layered yielding yellow crystals.

Reproduced as entry MR899 To an oven dried flask with magnetic stir bar Th (0.232 g, 1.00 mmol), $(SePh)_2$ (0.624 g, 2.00 mmol), and Hg (0.020 g, catalytic) were dissolved in pyridine ca. 20 mL. In a separate oven dried flask with magnetic stir bar Cu (0.063 g, 1.00 mmol), $(SePh)_2$ (0.156 g, 0.500 mmol), and I_2 (0.126 g, 0.500 mmol) were dissolved in pyridine ca. 20 mL. After four days the Th solution was cannulaed into the Cu solution and stirred for three days before elemental Se (0.158 g, 2.00 mmol) was added. After three days the resulting orange solution was filtered and layered yielding yellow crystals.

Synthesis of $bipy_6Fe_2I_4$ entry MR906

To an oven dried flask with magnetic stir bar Th (0.232 g, 1.00 mmol), $(SePh)_2$ (0.468 g, 1.50 mmol), $(SC_6F_5)_2$ (0.199 g, 0.500 mmol), Bipy (0.312 g, mmol), and Hg (0.020 g, catalytic) were dissolved in pyridine ca. 20 mL. After two days FeI_2 (0.310 g, 1.00 mmol) was added. After one week the resulting raspberry-colored solution was filtered and layered yielding red crystals.